Neurochemical Measurements in Rodents that Model

Huntington's Disease and Oxidative Stress

by

Andrea N. Ortiz

University of Kansas, April 26, 2011

Submitted to the graduate degree program in Chemistry and the Graduate Faculty of the University of Kansas in partial fulfillment of the requirements for the degree of Doctor of Philosophy

Dissertation Committee:_____

Michael A. Johnson, Ph.D.

_____

James A. Orr, Ph.D.

_____

Richard S. Givens, Ph.D.

_____

Susan M. Lunte, Ph.D.

_____

Heather Desaire Ph.D.

The Dissertation Committee for Andrea N. Ortiz certifies that this is the approved version of the following dissertation:

Neurochemical measurements in rodents that model

Huntington's disease and oxidative stress

Andrea N. Ortiz

_____

Michael A. Johnson

Date Approved: April 27, 2011

Abstract

Huntington's disease (HD) is a fatal, neurodegenerative movement disorder caused by a CAG repeat expansion on the gene encoding the huntinin protein. HD is characterized by preferential and extensive striatal degeneration. We used fast-scan cyclic voltammetry to measure dopamine release and reserve pool dopamine in genetically and chemically altered rodents that model HD. Genetic HD model mice and rats (R6/1 mice, R/2 mice, and HDtg rats) showed an age-dependent decrease in dopamine release in the dorsolateral caudate putamen. A similar decrease is not seen in 3-nitropropionic (3NP)-treated rats. In the case of R6/2 mice, stimulation at increasing frequencies showed a decrease in dopamine at the highest frequencies of 50 Hz and 60 Hz. The number of reserve pool vesicles was found to decrease in the R6/2 mice while it increased in the 3NP treated rats.

In a separate study, methionine sulfoxide reductase A (MsrA) mice, which model oxidative stress, have been reported to have chronically high dopamine levels relative to control mice. Additionally, these high levels parallel an increased presynaptic dopamine release when stimulated *in vitro* without drug treatments. Here we show evidence in striatal tissue for an increase in dopaminergic reserve pools that correlates to the increased dopamine levels of this knockout mouse. The results suggest that dopamine in reserve pool vesicles accumulates in the MrsA knockout mouse. This evidence supports previous reports that suggest the amount of dopamine in reserve pools is dependent on the overall dopamine levels, including readily releasable dopamine vesicles.

Acknowledgements

I would like to thank my advisor Michael A. Johnson for all of his support and encouragement. He trusted me to explore my own interest while keeping me focused and motivated. I would also like to acknowledge my committee James Orr, Richard Givens, Susan Lunte, and Heather Desaire for their guidance. I would also like to express my dearest thanks to my lab mates Gregory L. Osterhaus, Sam V. Kaplan, Todd Coffey, Ben J. Kurth, Sean Bonanni, and Patrick Selley. For all of their collaborations and help with the MsrA project I would like to thank Jakob Moskovitz, Derek B. Oien, and Heather Menchen.

None of this would have been possible without the undying love and support of my family including my parents Tony and Janice Ortiz, my sisters Tina Barrera and Amy Bodily and of course my little brother Daniel Ortiz. The love of my family in both Kansas and California has been so important to me during this journey and I will forever be in debt to you all. Most importantly I would like to thank my daughter Gabriella for being my inspiration to finish my doctorate.

Chapter 1: Introduction

Using electrochemical methods allows for the detection of electro-active chemicals. In our studies we are most interested in measuring dopamine in brain slices of rats and mice. Using cyclic voltammetry we have a method that allows for good spatial and temporal resolution and will cause very little harm to brain tissue allowing us measure dopamine in vivo.

A. Fast Scan Cyclic Voltammetry

Fast-scan cyclic voltammetry (FSCV) at carbon-fiber microelectrodes is an analytical technique that has often been used to measure electro-active neurochemicals, such as dopamine, serotonin, norepinephrine, and epinephrine (Wightman et al., 1988, Wightman et al., 1991, Robinson et al., 2003, John et al., 2006). The use of FSCV provides several advantages, including: low (nM) limits of detection, excellent (sub-s to near ms) temporal resolution, good (μm) spatial resolution, and reasonable chemical selectivity for the analyte of interest (a characteristic cyclic voltammogram is generated) (Robinson et al., 2003). Moreover, measurements using carbon-fiber microelectrodes are particularly well-suited for obtaining chemical measurements in biological tissues, neuronal tissues in particular, because damage to the tissue is minimized.

When conducting measurements using FSCV in neuronal tissue a triangular waveform if often applied in which a holding potential of -0.4 V (versus Ag/AgCl reference electrode) is applied to the carbon-fiber microelectrode. The potential is then linearly increased to +1.0 V and then decreased back down to -0.4 V. A scan rate often used in conjunction with this waveform, at least when measuring dopamine, is 300 V/s. The waveform application frequency is typically

10 scans/s, allowing for the collection of 10 cyclic voltammograms (CVs) per second. When using this waveform, the oxidation and reduction of DA is a two electron process.

A.

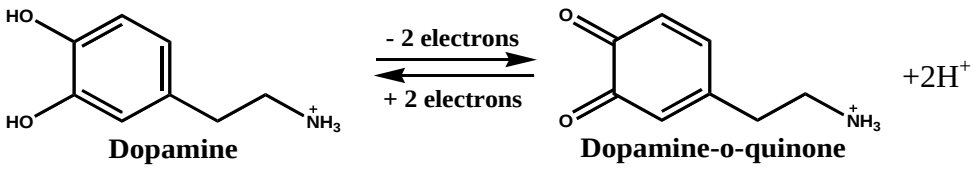

B

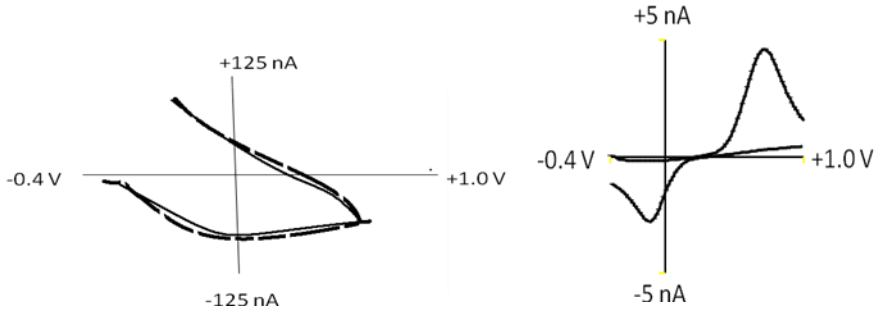

Figure 1. The oxidation and reduction of DA is a two electron process as shown in 1A. Using FSCV the current is plotted against applied voltage as shown in 1B. The solid line represents the background current and the dotted line represents the current that is present in the presence of DA. By subtracting out the background a characteristic CV of DA is given as shown as in 1C.

DA is oxidized at about +0.6 V, forming the DA ortho-quinone. Scanning back down to -0.4 V, the DA ortho-quinone is reduced to DA at about -0.2 V. These oxidation and reduction peaks are plotted versus applied potential to give a CV (see Figure 1). Due to the high scan rate, however, a large charging current, which may be several orders of magnitude larger than the faradaic current, is formed. To remove this charging current, a background CV, obtained when dopamine is not present, is subtracted from the CV collected in the presence of DA. This background subtraction operation gives a characteristic CV that serves as a "signature" for DA. This background subtraction operation is summarized in Figure 1.

The concentration of DA is calculated using the average of a pre and post calibration of the electrode. The concentration of DA is proportional the the current calculated for each electrode.

B. Dopamine System

Dopamine is a catecholamine neurotransmitter associated with many aspects of brain function, including behavior, cognition, addiction, and movement, to name just a few (Cooper et al., 2003). Therefore, it is not surprising that alterations the regulation of extracellular DA levels are associated with a variety of neurological disorders, including Huntington's Disease (HD), Parkinson's disease (PD), and Tourette's syndrome (Barbeau and Ando, 1975, Hornykiewicz, 2008, Steeves et al., 2010). Careful study of the DA system, using selected analytical techniques, such as FSCV, may allow for a better understanding of how brain function is impacted in selected areas of the diseased brain. In this sub-section, aspects of mammalian CNS anatomy that are relevant to these studies are summarized. Additionally, the dopamine release process is reviewed. Finally, animal models used to study Huntington's disease and oxidative stress are described.

1. Anatomy

Dopaminergic neurons originate in the substantia nigra pars compacta, ventral tegmental areas (VTA), and hypothalmas forming four major dopaminergic pathways. The four main pathways responsible for domainergic intervention to specific areas of the brain; these pathways are mesocortical, mesolimbic, tuberoinfundibular, and nigrostriatal pathways. The mesocortical and mesolimbic pathways are used in order to transfer DA from the VTA to the nucleus accumbens and the frontal cortex, respectively. The tuberoinfundibular pathway is involved in the transportation of DA from the hypothalamus to the pituitary gland. The nigrostriatal pathway which is involved in the control of motor function transports DA from the substantia nigra to the striatum.

The striatum is the largest integrative part of the basil ganglia, it is here that gluatamatergic and dopaminergic inputs converge. The striatum is located on the interior of the forebrain and consists of about 96% medium spiny neurons. The other types of neurons also present in the striatum include Deiters' neurons, cholinergic interneurons, GABAergic parvalbumin, GABAergic calretinin, and GABAergic somatosstatin. Medium spiny neurons play a key role in controlling motor function by either activating D1 receptors or by inhibiting the activation of D2 receptors (DeLong et al., 1984, Alexander et al., 1990). There are two types of medium spiny neurons found in the striatum; one expressing D1 receptors and one expressing D2 receptors. The medium spiny neurons which contain D2 receptors provide an indirect pathway to control motor function while the medium spiny neurons containing D1 receptors allow for a direct pathway (DeLong et al., 1984, Alexander et al., 1990, Tang et al., 2005, Tang et al., 2007, Charvin et al., 2008).

The substantia nigra pars compacta (SnC) plays a major role in motor function. The substantia nigra itself cannot control motor function but it is (Yin et al., 2009, Yin, 2010) in charge of supplying DA to the striatum leading to fine tuning of motor control. Dopaminergic neurons project from the SnC to the dorsal caudate putamen. Various behaviors are then generated based on the subarea of the striatum that is activated. The dorsal lateral, dorsal medial, and ventral striatum are all associated with learning and behaviors associated with rewards. The dorsal lateral striatum is more specifically associated with behaviors that are learned by a stimulus or out of habit while the dorsal medial striatum is associated with behaviors that are a response to reward (Wickens et al., 2007, Horvitz, 2009, Yin et al., 2009, Ashby et al., 2010, Yin, 2010). Lesions caused in this area of the brain are present in Parkinson's disease and that is why it is thought that the there is a loss of motor control in patients with Parkinson's disease.

2. Dopamine

Dopamine is synthesized in the presynaptic terminals and in the soma starting with the hydroxylation of L-tyrosine to L-Dihydroxyphenylamine (L-DOPA). This is the rate limiting step for DA synthesis and is controlled by tyrosine hydroxylase. L-DOPA is then converted to DA via DOPA decarboxylase. Once DA is synthesized in can then be packaged into vesicles through the vesicular monoamine transporter (VMAT). Vesicles can then stored for later use of be released into the synapse where DA can react with autoreceptors or be taken back into the presynaptic terminal by the DA transporter (DAT).

One mode of the release of DA is through exocytosis, which occurs when the vesicle membrane fuses with the neuronal membrane. Exocytosis is a calcium-dependent process. When the membrane is depolarized, the voltage-gated calcium channels open, allowing extracellular Ca^{2+} to enter. These Ca^{2+} ions associate with the SNARE protein complex, which

then causes the vesicle membrane to fuse with the neuronal membrane, and allows the vesicle contents to exit into the extracellular space (Becherer and Rettig, 2006). It is currently thought that exocytosis happens in one of two ways: either classical exocytosis (just described) or in a "kiss and run" type action. In the kiss and run method a fusion pore transiently opens up allowing for the release of neurotransmitters. In the kiss and run method endocytosis of the vesicles can happen as fast as a sub-second (Rizzoli and Betz, 2005).

After DA is released into the synaptic cleft through exocytosis, it may either interacts with the D1 or D2 autoreceptors, diffuse out the synaptic cleft, or may be taken back up into the presynapitc terminal. In order to be taken back up into the synaptic cleft it has to be transported through the DA transporter (DAT) (Garris and Wightman, 1994). The DAT is an 80 kDA protein found on the plasma membrane and contains 12 transmembrane regions as shown in table 1 (Schenk et al., 2005). It is a sodium and calcium dependent transporter with the first five transmembrane regions being involved in the ion dependence transport. The transmembrane regions six through eight are thought to be target sites for DAT inhibitors such as AMPH and COC (Kitayama et al., 1992). The regions nine through twelve are used to determine substrate affinity and stereoselectivity (Giros and Caron, 1993, Buck and Amara, 1994, Buck et al., 1996). The DAT is important in dopaminergic signaling and alterations can lead to signaling problems affecting downstream pathways.

Transmembrane Region of DAT	Function
1 through 5	Ion dependent transport
6 through 8	Target site for DAT inhibitors
9 through 12	Determines substrate affinity and stereoselectivity

Table 1. The DAT is made up of 12 transmembrane regions. The 12 regions are broken down into 3 subgroups that each play an important role. Regions 1-5 are important for ion dependent transport. Regions 6-8 are target sites for DAT inhibitors such as AMPH, COC, and METH. Regions 9-12 are important in determining the affinity and stereoselectivity of various substrates.

Synaptic vesicles in the presynaptic terminal are thought to reside in distinct pools. Catecholamines are commonly classified into three distinct vesicle pools (as shown in Figure 3), although some studies support a four pool system (Rizzoli and Betz, 2005). The readily releasable pool (RRP) which consists of 0.1%-2% of the total vesicles. The recycling pool, which is used to replenish the RRP vesicles, consists of 5%-20% of all vesicles found in the presynaptic terminal. The third and largest vesicle pool (80%-95% of the vesicles) is the reserve pool (Neves and Lagnado, 1999, Zucker and Regehr, 2002, Rizzoli and Betz, 2005).

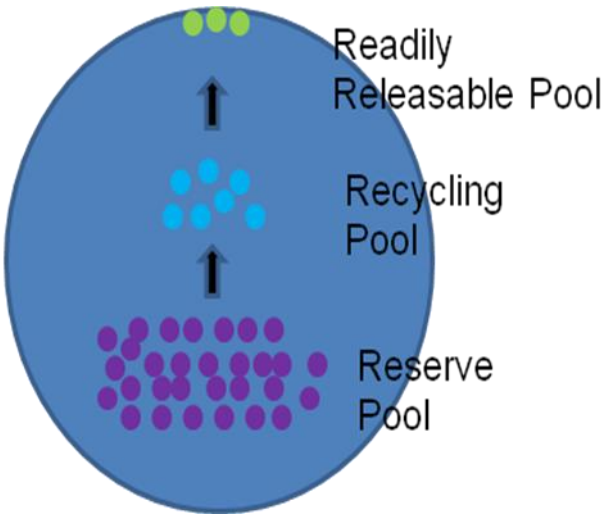

Figure 3. The three pool system consists of the readily releasable pool, recycling pool, and reserve pool. Readily Releasable Pool makes up ~1% of total vesicle pool and is available upon stimulation. The Recycling Pool makes up ~10-15% of the total vesicle pool and is released upon moderate stimulation. The Reserve Pool makes up ~80-90% of total vesicles and is released after intense stimulation and is thought to be mobilized after the depletion of Recycling Pool

The RRP are a group of vesicles that are primed and docked at the active zone in the presynaptic terminal. They are the easiest and quickest vesicles to mobilize. The mobilization of the RRP is activated upon mild stimulation where the axon terminal is depolarized by an action potential (Wu and Borst, 1999). The stimulation needed in order for the release of the RRP can come in the form of electrical stimulation, depolarization lasting a few milliseconds, and hypertonic shock (Elmqvist and Quastel, 1965, Rosenmund and Stevens, 1996, Schneggenburger et al., 1999, Delgado et al., 2000, Richards et al., 2003). The RRP is rapidly replenished (~1 sec) by vesicles in the recycling pool (Wu and Borst, 1999, Sakaba and Neher, 2001).

The recycling pool is the second largest pool accounting for 5-20% of all vesicles in the terminal (Richards et al., 2003, Rizzoli and Betz, 2005). The recycling pool is an intermediate stage between the RRP and the reserve pool vesicles. The recycling pool vesicles are mobilized under moderate stimulation and are thought to only mobilize once the RRP vesicles are diminished. The recycling pool vesicles can rapidly be docked and released if needed (a few seconds) (Rizzoli and Betz, 2005). The recycling pool is replenished with vesicles from the reserve pool.

The largest pool of vesicles making up 80-90% of all vesicles is the reserve pool (Rizzoli and Betz, 2005). This pool of vesicles is only released upon intense stimulation and is thought to only mobilize once the recycling pool vesicles have diminished. Using a stimulation frequency of 50 Hz with train pulses of 2 and 4 seconds an increase in DA release is found due to the mobilization of the reserve pool vesicles (Yavich, 1996, Yavich and MacDonald, 2000). The reserve pool vesicles can also be mobilized through pharmacological means; cocaine has been shown to mobilize the synapsin dependent reserve pool vesicles (Venton et al., 2006).

C. Huntington's Disease

HD is an autosomal dominant neurodegenerative disorder caused by an expanded CAG repeat which codes for a polyglutamine stretch on the *huntingtin* gene (htt) (The Huntington's Disease Collaborative Research Group, 1993). The mutated gene is located on chromosome 4 (The Huntington's Disease Collaborative Research Group, 1993). The expanded CAG repeat causes degeneration of the medium spiny neurons resulting in mood disturbances, choreic movement, and cognitive dysfunction(Bates et al., 2002).

On average the age of onset varies between 35-50 years of age. The variation in age of onset is in part due to the number of CAG repeats a person has. There is a correlation between the number of CAG repeats a person has and the age of onset; where a larger number of CAG repeats results in an earlier onset. Individuals who have less than 28 CAG repeats will not develop physical or psychological deficits associated with HD, individuals with ≥40 CAG repeats will typically develop the HD syndrome some time during a normal life time. Individuals with more than 60 CAG repeats may develop HD symptoms as juveniles (The Huntington's Disease Collaborative Research Group, 1993).

1. Disease Progression

As HD progresses it causes movement, cognitive, and psychiatric dysfunction. Psychiatric dysfunction, most commonly in the form of depression, usually occur before the onset of other more noticeable characteristics such as choriec involuntary movement, impaired coordination, dementia, and personality changes (The Huntington's Disease Collaborative Research Group, 1993). The age of onset varies from 35-50 years old, depending on the length of the CAG repeat with a typical duration of 15-20 years.

One of the main characteristics of HD is the neurodegeneration of the medium spiny neurons. GABAergic neurons make up 85-90% of the striatal neurons and are the main target for destruction by HD (Vonsattel et al., 1985, Ross et al., 1997, Vonsattel and DiFiglia, 1998). Though the striatal cells are targeted for apoptosis, the reason by which cell death is induced is uncertain. One possible explanation is that mitochondrial dysfunction leads to apoptosis. It has previously been shown in lymphoblasts from HD patients and in various genetic models of HD that a reduction in mitochondrial membrane potential is present (Sawa et al., 1999, Panov et al., 2002, Bae et al., 2005). HD patients also have been found to have a decrease in the activity of mitochondrial complex II (mCII) due to the reduced expression of mCII subunits (Benchoua et al., 2006, Benchoua et al., 2008). The mCII plays a role in oxidative energy metabolism and its down regulation has been shown to cause an increase in the vulnerability of striatal neurons to the mutant htt toxicity (Benchoua et al., 2008).

Another possible explanation for the cell death of the medium spiny neurons could be due to the formation of reactive oxidative species (ROS). The main source for ROS is mitochondrial dysfunction and impairments in the electron chain. Lipid peroxides are a proposed biomarker to measure oxidative stress in vivo for neurological diseases. When measured blood plasma of HD patients, plasma lipid peroxide and lactate concentrations were shown to be elevated, indicating the patient was under oxidative stress (Duran et al., , Sayre et al., 2008). The plasma activity of aminopeptidases for aspartate and glutamate were also measured in blood plasma for HD patients and it was found to decrease, in both symptomatic and nonsymptomatic patients, indicating that there is a decrease in plasma activity before the symptoms of HD can be seen in patients (Duran et al.). Signs of oxidative stress have also been shown to be present in post

mortem brains of HD brains including: cytoplasmic lipoofuscin, DNA strand breaks, and oxidative markers in DNA bases (Tellez-Nagel et al., 1974, Browne et al., 1999).

It has also been shown that caspase-1, an enzyme in controlling cellular death is activated in both patients and mouse models of HD. Caspase-1 is activated early on in HD progression and it is the earliest caspase activated in HD rodent models (Zhang et al., 2003, Wang et al., 2005). The levels of Caspase-1 increase along with disease progression possibly explaining the increase in cellular death that also occurs (Chen et al., 2000, Zhang et al., 2003).

Neurological and behavioral disturbances of HD can be attributed to the selective pattern of cell loss in the brain and the pathways that are affected. Studies using R6/2 mice have shown behavior deterioration that resembles that found in HD patients (Carter et al., 1999). Using FSCV our group has previously shown that there is an age dependent DA inhibition in both R6/2 and R6/1 mice and the reserve pool DA in R6/2 mice is diminished (Johnson et al., 2006, Johnson et al., 2007, Ortiz et al., 2010, 2011a). The behavioral impairments found in HD could possibly be partially explained by an impairment in the DA release that has been shown in R6/1 and R6/2 mice models of HD.

2. Rodents That Model Huntington's Disease

In order to study the dynamics of HD, the use of an animal model, in which the disease progression is quicker, is often entailed. The most common rodent models are transgenic mouse models. Until the recent generation of the HD transgenic rat model, rats were treated with neurotoxins to create a chemically induced HD rat model.

a. Mice

Various mouse models are available for the study of HD. There are two main types of mouse models, those that have a full length mutant htt gene and those that use a truncated version of the gene. The full length HD model is a yeast artificial chromosome (YAC) transgenic mouse model. The truncated version is the more common mouse models used and are generated using the R6 mouse germ line.

The YAC mouse model uses a full-length human gene that codes for the htt protein. The two mouse models contain CAG repeats similar to that of found in humans with adult onset and juvenile onset. YAC_{46} contains 46 CAG repeats and represents the adult onset model and the YAC_{72} contains 72 CAG repeats and represents the juvenile onset. Both the YAC_{46} and YAC_{72} models show early electrophysiological abnormalities. The YAC_{46} model though it shows signs of electrophysiogical abnormalities at 12 months of age, behavior abnormalities are not present until about 20 months. Behavioral abnormalities are seen in the YAC_{72} that correlate to the amount of htt protein present, mice with higher levels of protein present show an early behavioral onset, aggregates, and neruodegeneration of the striatum at about six weeks of age The YAC_{72} model with lower levels htt protein present show electrophysiological abnormalities at 4 to 6 months with signs of neurodegeneration at 12 months of age.

A second type of mouse model that is used to study HD uses a truncated version of the human HD gene. In these models exon 1 of the human HD gene is introduced into the mouse germ line using a 2kb fragment that spans the 5' end of the human gene (Mangiarini et al., 1996, Sathasivam et al., 1999). To date there are six lines that have been established all with varying lengths of CAG repeats. Four of the models have CAG repeats that are representative of those of juvenile HD; R6/1 has 113 CAG repeats, R6/2 with 144 CAG repeats, R6/5 has 128-156 CAG repeats, and R6/0 has 142 CAG repeats (Bates et al., 1998, Sathasivam et al., 1999). The

remaining two models HDex6 and HDex27 both are controls with 18 CAG repeats. Of the six HD models from the R6 germ line the R6/1 and R6/2 are the most extensively studied. Both the R6/1 and R6/2 mice show signs of abnormal behavior such as irregular gait, shudders, tremors, hindleg clasping, and stereotypic behaviors (Sathasivam et al., 1999). The typical age of onset is 8 weeks for the R6/2 mice with death occurring at about 12 weeks and between 4-5 months for the R6/1 mice with an early death of about one year. The brains of 12 week old R6/2 mice have been shown to be 20% smaller then age-matched WT control mice and neurogeneration occurring at about 14 weeks of age. R6/1 mice show similar signs of HD as those found in R6/2 mice accept on a slower time scale.

b. Rats

Using rat models of HD allows for a mammalian model that more closely related to humans. Rat models allow for the study of HD over a longer time frame, which will give a better idea of the disease progression as it occurs in an adult opposed to in children. Until recently the only rat models for HD came from the use of mitochondrial toxins to create similar characteristics to those of HD patients, now there is transgenic rat model available made with the a portion of the human htt gene.

The HDtg rat is the first transgenic rat model for a neurodegenerative brain disorder. The HDtg rat model is similar to the R6/2 mouse model in that is uses a truncated version of the htt gene. It contains a strand of cDNA that corresponds to a 51 CAG repeat. The length of the repeat corresponds to an adult onset of HD (von Hörsten et al., 2003). The HDtg rats show signs of HD similar to those found in humans. These rats have shown an age dependent impaired striatal function including enlarged striatal ventricles and atrophy (Kantor et al., 2006).

The HDtg rats also show an age dependent, genotype dependent decrease in behavior including signs of choriec movements (Cao et al., 2006).

Several chemically-induced models of HD have been developed to mimic the neurological and behavioral features of human HD. Glutamate analogues such as kainate and quinolinate and mitochondrial toxins such as amino-oxyacetate, rotenone, MPP+, malonate, 3-acetylpyridine and 3-nitropropionic acid (3NP) are among some of the compounds used with 3NP being the most extensively used (McGeer and McGeer, 1976, Beal et al., 1986, Beal et al., 1993a, Beal et al., 1993b, Brouillet et al., 1993, Schulz and Beal, 1994). 3NP is an irreversible inhibitor of the tricarboylic acid cycle which leads to the inhibition of the mitochondrial respiratory chain complex II (Alston et al., 1977, Coles et al., 1979). The administration of 3NP causes degeneration of putamen and caudate nucleus which causes severe neurological behaviors like those found in HD (Brouillet et al., 2005).

Rats treated with 3NP show symptoms similar to those found in HD patients. Chronic 3NP treatment causes a lesion in the striatum when administered to rats and mice. 3NP-treated rats have also been shown to have a decrease in DA release in vivo and a diminished locomoter activity, characteristics that are present in R6/1 and R6/2 mice (Johnson et al., 2006, Johnson et al., 2007, Kraft et al., 2009, Ortiz et al., 2011a).

D. Oxidative Stress and Methione Sulfoxide Reductase Mice($MsrA^{-/-}$)

Many neurological diseases, such as Parkinson's disease, HD, and Lou Gehrig's disease have been linked with an increase in reactive oxidative species which causes an increase in the degree of cell oxidative stress found in the brain (Cohen, 1983, Perez-Severiano et al., 2004, Patten et al., 2010). Reactive oxygen species can cause post-translational modifications that alter

protein functions and in most cases these modifications cannot be reversed. Methionine sulfoxide (MetO) modifications though are an exception and can be reversed by the methionine sulfoxide reductase (Msr) system. The Msr system consists of two parts MsrA which reduces S-MetO and MsrB which reduces R-MetO (Moskovitz, 2005). The Msr system has a role in antioxidant defense, may prevent irreversible protein damage, and regulate protein function (Moskovitz et al., 1995, Moskovitz et al., 1997, Moskovitz et al., 2001). An over-expression of MsrA has been shown to provide protection from oxidative stress toxicity (Moskovitz et al., 1998). The MrsA $^{-/-}$ knockout mouse is hypersensitive to oxidative stress and expresses brain pathologies associated with neurodegenerative diseases (Moskovitz et al., 2001).

The MrsA$^{-/-}$ mice show characteristics that would suggest dysfunction of the dopaminergic pathway. Using FSCV it has been shown that MsrA mice have an increase in DA release when compared to age-matched wild-type mice, increased reserve pool DA and the DA content is higher in MsrA$^{-/-}$ mice (Oien et al., 2008, Ortiz et al., 2011b). MrsA$^{-/-}$ also show a lack of locomotor activity, abnormal gait, and are less responsive to AMPH (Oien et al., 2008).

The oxidative stress mouse model and the various HD rodent models allow for the further study of the dopaminergic pathway and the affects that is has on neurodegenerative disease pathways. By getting a better understanding of the dysfunction in these animal models could potentially allow for future pharmalogical intervention.

E. References

Alston TA, Mela L, Bright HJ (3-Nitropropionate, the toxic substance of Indigofera, is a suicide inactivator of succinate dehydrogenase. Proc Natl Acad Sci U S A 74:3767-3771.1977).

Bae BI, Xu H, Igarashi S, Fujimuro M, Agrawal N, Taya Y, Hayward SD, Moran TH, Montell C, Ross CA, Snyder SH, Sawa A (p53 mediates cellular dysfunction and behavioral abnormalities in Huntington's disease. Neuron 47:29-41.2005).

Bates GP, Harper PS, Jones L (2002) Huntington's Disease. Oxford: Oxford University Press.

Bates GP, Mangiarini L, Davies SW (Transgenic mice in the study of polyglutamine repeat expansion diseases. Brain Pathol 8:699-714.1998).

Beal MF, Brouillet E, Jenkins B, Henshaw R, Rosen B, Hyman BT (Age-dependent striatal excitotoxic lesions produced by the endogenous mitochondrial inhibitor malonate. J Neurochem 61:1147-1150.1993a).

Beal MF, Brouillet E, Jenkins BG, Ferrante RJ, Kowall NW, Miller JM, Storey E, Srivastava R, Rosen BR, Hyman BT (Neurochemical and histologic characterization of striatal excitotoxic lesions produced by the mitochondrial toxin 3-nitropropionic acid. J Neurosci 13:4181-4192.1993b).

Beal MF, Kowall NW, Ellison DW, Mazurek MF, Swartz KJ, Martin JB (Replication of the neurochemical characteristics of Huntington's disease by quinolinic acid. Nature 321:168-171.1986).

Becherer U, Rettig J (Vesicle pools, docking, priming, and release. Cell Tissue Res 326:393-407.2006).

Benchoua A, Trioulier Y, Diguet E, Malgorn C, Gaillard MC, Dufour N, Elalouf JM, Krajewski S, Hantraye P, Deglon N, Brouillet E (Dopamine determines the vulnerability of striatal

neurons to the N-terminal fragment of mutant huntingtin through the regulation of mitochondrial complex II. Hum Mol Genet 17:1446-1456.2008).

Benchoua A, Trioulier Y, Zala D, Gaillard MC, Lefort N, Dufour N, Saudou F, Elalouf JM, Hirsch E, Hantraye P, Deglon N, Brouillet E (Involvement of mitochondrial complex II defects in neuronal death produced by N-terminus fragment of mutated huntingtin. Mol Biol Cell 17:1652-1663.2006).

Brouillet E, Jacquard C, Bizat N, Blum D (3-Nitropropionic acid: a mitochondrial toxin to uncover physiopathological mechanisms underlying striatal degeneration in Huntington's disease. J Neurochem 95:1521-1540.2005).

Brouillet E, Jenkins BG, Hyman BT, Ferrante RJ, Kowall NW, Srivastava R, Roy DS, Rosen BR, Beal MF (Age-dependent vulnerability of the striatum to the mitochondrial toxin 3-nitropropionic acid. J Neurochem 60:356-359.1993).

Browne SE, Ferrante RJ, Beal MF (Oxidative stress in Huntington's disease. Brain Pathol 9:147-163.1999).

Buck KJ, Amara SG (Chimeric dopamine-norepinephrine transporters delineate structural domains influencing selectivity for catecholamines and 1-methyl-4-phenylpyridinium. Proc Natl Acad Sci U S A 91:12584-12588.1994).

Buck KJ, Lorang D, Amara SG (Discrete structural domains and cell-specific expression determine functional selectivity of the dopamine and norepinephrine transporters. NIDA Res Monogr 161:154-175.1996).

Cao C, Temel Y, Blokland A, Ozen H, Steinbusch HW, Vlamings R, Nguyen HP, von Horsten S, Schmitz C, Visser-Vandewalle V (Progressive deterioration of reaction time

performance and choreiform symptoms in a new Huntington's disease transgenic ratmodel. Behav Brain Res 170:257-261.2006).

Carter RJ, Lione LA, Humby T, Mangiarini L, Mahal A, Bates GP, Dunnett SB, Morton AJ (Characterization of progressive motor deficits in mice transgenic for the human Huntington's disease mutation. J Neurosci 19:3248-3257.1999).

Chen M, Ona VO, Li M, Ferrante RJ, Fink KB, Zhu S, Bian J, Guo L, Farrell LA, Hersch SM, Hobbs W, Vonsattel JP, Cha JH, Friedlander RM (Minocycline inhibits caspase-1 and caspase-3 expression and delays mortality in a transgenic mouse model of Huntington disease. Nat Med 6:797-801.2000).

Cohen G (The pathobiology of Parkinson's disease: biochemical aspects of dopamine neuron senescence. J Neural Transm Suppl 19:89-103.1983).

Coles CJ, Edmondson DE, Singer TP (Inactivation of succinate dehydrogenase by 3-nitropropionate. J Biol Chem 254:5161-5167.1979).

Delgado R, Maureira C, Oliva C, Kidokoro Y, Labarca P (Size of vesicle pools, rates of mobilization, and recycling at neuromuscular synapses of a Drosophila mutant, shibire. Neuron 28:941-953.2000).

Duran R, Barrero FJ, Morales B, Luna JD, Ramirez M, Vives F (Oxidative stress and plasma aminopeptidase activity in Huntington's disease. J Neural Transm 117:325-332).

Elmqvist D, Quastel DM (A quantitative study of end-plate potentials in isolated human muscle. The Journal of physiology 178:505-529.1965).

Garris PA, Wightman RM (Different kinetics govern dopaminergic transmission in the amygdala, prefrontal cortex, and striatum: an in vivo voltammetric study. J Neurosci 14:442-450.1994).

Giros B, Caron MG (Molecular characterization of the dopamine transporter. Trends Pharmacol Sci 14:43-49.1993).

Johnson MA, Rajan V, Miller CE, Wightman RM (Dopamine release is severely compromised in the R6/2 mouse model of Huntington's disease. J Neurochem 97:737-746.2006).

Johnson MA, Villanueva M, Haynes CL, Seipel AT, Buhler LA, Wightman RM (Catecholamine exocytosis is diminished in R6/2 Huntington's disease model mice. J Neurochem 103:2102-2110.2007).

Kantor O, Temel Y, Holzmann C, Raber K, Nguyen HP, Cao C, Turkoglu HO, Rutten BP, Visser-Vandewalle V, Steinbusch HW, Blokland A, Korr H, Riess O, von Horsten S, Schmitz C (Selective striatal neuron loss and alterations in behavior correlate with impaired striatal function in Huntington's disease transgenic rats. Neurobiol Dis 22:538-547.2006).

Kitayama S, Shimada S, Xu H, Markham L, Donovan DM, Uhl GR (Dopamine transporter site-directed mutations differentially alter substrate transport and cocaine binding. Proc Natl Acad Sci U S A 89:7782-7785.1992).

Kraft JC, Osterhaus GL, Ortiz AN, Garris PA, Johnson MA (In vivo dopamine release and uptake impairments in rats treated with 3-nitropropionic acid. Neuroscience 161:940-949.2009).

Mangiarini L, Sathasivam K, Seller M, Cozens B, Harper A, Hetherington C, Lawton M, Trottier Y, Lehrach H, Davies SW, Bates GP (Exon 1 of the HD gene with an expanded CAG repeat is sufficient to cause a progressive neurological phenotype in transgenic mice. Cell 87:493-506.1996).

McGeer EG, McGeer PL (Duplication of biochemical changes of Huntington's chorea by intrastriatal injections of glutamic and kainic acids. Nature 263:517-519.1976).

Moskovitz J (Methionine sulfoxide reductases: ubiquitous enzymes involved in antioxidant defense, protein regulation, and prevention of aging-associated diseases. Biochim Biophys Acta 1703:213-219.2005).

Moskovitz J, Bar-Noy S, Williams WM, Requena J, Berlett BS, Stadtman ER (Methionine sulfoxide reductase (MsrA) is a regulator of antioxidant defense and lifespan in mammals. Proc Natl Acad Sci U S A 98:12920-12925.2001).

Moskovitz J, Berlett BS, Poston JM, Stadtman ER (The yeast peptide-methionine sulfoxide reductase functions as an antioxidant in vivo. Proc Natl Acad Sci U S A 94:9585-9589.1997).

Moskovitz J, Flescher E, Berlett BS, Azare J, Poston JM, Stadtman ER (Overexpression of peptide-methionine sulfoxide reductase in Saccharomyces cerevisiae and human T cells provides them with high resistance to oxidative stress. Proc Natl Acad Sci U S A 95:14071-14075.1998).

Moskovitz J, Rahman MA, Strassman J, Yancey SO, Kushner SR, Brot N, Weissbach H (Escherichia coli peptide methionine sulfoxide reductase gene: regulation of expression and role in protecting against oxidative damage. J Bacteriol 177:502-507.1995).

Neves G, Lagnado L (The kinetics of exocytosis and endocytosis in the synaptic terminal of goldfish retinal bipolar cells. The Journal of physiology 515 (Pt 1):181-202.1999).

Oien DB, Osterhaus GL, Latif SA, Pinkston JW, Fulks J, Johnson M, Fowler SC, Moskovitz J (MsrA knockout mouse exhibits abnormal behavior and brain dopamine levels. Free radical biology & medicine 45:193-200.2008).

Ortiz AN, Kurth BJ, Osterhaus GL, Johnson MA (Dysregulation of intracellular dopamine stores revealed in the R6/2 mouse striatum. J Neurochem 112:755-761.2010).

Ortiz AN, Kurth BJ, Osterhaus GL, Johnson MA (Impaired dopamine release and uptake in R6/1 Huntington's disease model mice. Neurosci Lett.2011a).

Ortiz AN, Oien DB, Moskovitz J, Johnson MA (Quantification of reserve pool dopamine in methionine sulfoxide reductase A null mice. Neuroscience 177:223-229.2011b).

Panov AV, Gutekunst CA, Leavitt BR, Hayden MR, Burke JR, Strittmatter WJ, Greenamyre JT (Early mitochondrial calcium defects in Huntington's disease are a direct effect of polyglutamines. Nat Neurosci 5:731-736.2002).

Patten DA, Germain M, Kelly MA, Slack RS (Reactive oxygen species: stuck in the middle of neurodegeneration. J Alzheimers Dis 20 Suppl 2:S357-367.2010).

Perez-Severiano F, Santamaria A, Pedraza-Chaverri J, Medina-Campos ON, Rios C, Segovia J (Increased formation of reactive oxygen species, but no changes in glutathione peroxidase activity, in striata of mice transgenic for the Huntington's disease mutation. Neurochem Res 29:729-733.2004).

Richards DA, Guatimosim C, Rizzoli SO, Betz WJ (Synaptic vesicle pools at the frog neuromuscular junction. Neuron 39:529-541.2003).

Rizzoli SO, Betz WJ (Synaptic vesicle pools. Nat Rev Neurosci 6:57-69.2005).

Rosenmund C, Stevens CF (Definition of the readily releasable pool of vesicles at hippocampal synapses. Neuron 16:1197-1207.1996).

Ross CA, Margolis RL, Rosenblatt A, Ranen NG, Becher MW, Aylward E (Huntington's disease and the related disorder, dentatorubral-pallidolusian atrophy (DRPLA). Medicine (Baltimore) 76:305-338.1997).

Sakaba T, Neher E (Calmodulin mediates rapid recruitment of fast-releasing synaptic vesicles at a calyx-type synapse. Neuron 32:1119-1131.2001).

Sathasivam K, Hobbs C, Mangiarini L, Mahal A, Turmaine M, Doherty P, Davies SW, Bates GP (Transgenic models of Huntington's disease. Philos Trans R Soc Lond B Biol Sci 354:963-969.1999).

Sawa A, Wiegand GW, Cooper J, Margolis RL, Sharp AH, Lawler JF, Jr., Greenamyre JT, Snyder SH, Ross CA (Increased apoptosis of Huntington disease lymphoblasts associated with repeat length-dependent mitochondrial depolarization. Nat Med 5:1194-1198.1999).

Sayre LM, Perry G, Smith MA (Oxidative stress and neurotoxicity. Chem Res Toxicol 21:172-188.2008).

Schenk JO, Wright C, Bjorklund N (Unraveling neuronal dopamine transporter mechanisms with rotating disk electrode voltammetry. J Neurosci Methods 143:41-47.2005).

Schneggenburger R, Meyer AC, Neher E (Released fraction and total size of a pool of immediately available transmitter quanta at a calyx synapse. Neuron 23:399-409.1999).

Schulz JB, Beal MF (Mitochondrial dysfunction in movement disorders. Curr Opin Neurol 7:333-339.1994).

Tellez-Nagel I, Johnson AB, Terry RD (Studies on brain biopsies of patients with Huntington's chorea. J Neuropathol Exp Neurol 33:308-332.1974).

The Huntington's Disease Collaborative Research Group (A novel gene containing a trinucleotide repeat that is expanded and unstable on Huntington's disease chromosomes Cell 72:971-983.1993).

Venton BJ, Seipel AT, Phillips PE, Wetsel WC, Gitler D, Greengard P, Augustine GJ, Wightman RM (Cocaine increases dopamine release by mobilization of a synapsin-dependent reserve pool. J Neurosci 26:3206-3209.2006).

von Hörsten S, Schmitt I, Nguyen HP, Holzmann C, Schmidt T, Walther T, Bader M, Pabst R, Kobbe P, Krotova J, Stiller D, Kask A, Vaarmann A, Rathke-Hartlieb S, Schulz JB, Grasshoff U, Bauer I, Vieira-Saecker AM, Paul M, Jones L, Lindenberg KS, Landwehrmeyer B, Bauer A, Li XJ, Riess O (Transgenic rat model of Huntington's disease. Hum Mol Genet 12:617-624.2003).

Vonsattel JP, DiFiglia M (Huntington's Disease. J Neuropathol Exp Neurol 57:369-384.1998).

Vonsattel JP, Myers RH, Stevens TJ, Ferrante RJ, Bird ED, Richardson EP, Jr. (Neuropathological classification of Huntington's disease. J Neuropathol Exp Neurol 44:559-577.1985).

Wang X, Wang H, Figueroa BE, Zhang WH, Huo C, Guan Y, Zhang Y, Bruey JM, Reed JC, Friedlander RM (Dysregulation of receptor interacting protein-2 and caspase recruitment domain only protein mediates aberrant caspase-1 activation in Huntington's disease. J Neurosci 25:11645-11654.2005).

Wu LG, Borst JG (The reduced release probability of releasable vesicles during recovery from short-term synaptic depression. Neuron 23:821-832.1999).

Yavich L (Two simultaneously working storage pools of dopamine in mouse caudate and nucleus accumbens. British journal of pharmacology 119:869-876.1996).

Yavich L, MacDonald E (Dopamine release from pharmacologically distinct storage pools in rat striatum following stimulation at frequency of neuronal bursting. Brain Res 870:73-79.2000).

Zhang Y, Ona VO, Li M, Drozda M, Dubois-Dauphin M, Przedborski S, Ferrante RJ, Friedlander RM (Sequential activation of individual caspases, and of alterations in Bcl-2 proapoptotic signals in a mouse model of Huntington's disease. J Neurochem 87:1184-1192.2003).

Zucker RS, Regehr WG (Short-term synaptic plasticity. Annu Rev Physiol 64:355-405.2002).

Chapter 2: DA Release and Uptake in HD

The DA release and uptake has been shown to be inhibited in the R6/2 mouse model. Using FSCV an age dependent study showed that as the age progresses an inhibition in the DA release was shown. At six weeks of age there was not a significant decrease in DA release but at 12 weeks of age the DA release was inhibited. Microdialysis studies also showed a decrease in DA release in R6/1 mice. The following three papers published from our lab look at the DA release in R6/1 mice, HDtg rats, and in 3NP treated rats.

A. Impaired Dopamine Release and Uptake in Huntington's Disease Model Mice

Huntington's disease (HD) is a progressive, neurodegenerative movement disorder. Here, we used fast-scan cyclic voltammetry to measure dopamine release and uptake in striatal brain slices from R6/1 HD model mice. Peak dopamine release ($[DA]_{max}$) was significantly diminished in R6/1 mice compared to age-matched wild-type control mice at 24 weeks of age (52.2% of wild-type), but not at 10 or 16 weeks of age. Similarly, dopamine released per locally applied electrical stimulus pulse ($[DA]_p$), which is $[DA]_{max}$ corrected for uptake and electrode performance, was also diminished in R6/1 mice at this age (43.1% of wild-type). Moreover, V_{max}, the maximum rate of dopamine uptake, obtained by modeling the stimulated release plots, was decreased at 16 and 24 weeks of age in R6/1 mice (51.0 and 48.0% of wild-type, respectively). Thus, impairments in both dopamine release and uptake appear to progress in an age-dependent manner in R6/1 mice.

Introduction

Huntington's disease (HD) is an autosomal dominant neurodegenerative disorder caused by an expanded CAG repeat on the gene that encodes the *huntingtin (htt)* protein (The

Huntington's Disease Collaborative Research Group, 1993). This expansion results in the expression of an extended polyglutamine segment which ultimately causes striatal degeneration, mood disturbances, choreic movements, and cognitive dysfunction (Bates et al., 2002). Dopaminergic innervation projecting from the substantia nigra pars compacta to the striatum exerts influence over the control of intentional movement (Kandel et al., 2000). Therefore, it has been suggested that impairments in dopamine release may contribute to the progressive motor phenotype that is characteristic of HD (Johnson et al., 2006, Kraft et al., 2009, Ortiz et al., 2010).

Several genetically engineered mouse strains that model HD have been used to investigate dopaminergic system alterations. Of these, the R6/2 mouse, which possesses exon 1 of the human huntingtin (htt) protein with about 144 CAG repeats (Mangiarini et al., 1996, Davies et al., 1997), has been the most extensively studied. R6/2 mice express a progressive, overt behavioral phenotype that starts between 9 to 11 weeks of age and typically die at 10 to 13 weeks of age (Mangiarini et al., 1996, Davies et al., 1997). In contrast, R6/1 mice, which also express a truncated version of the human htt, have a shorter CAG repeat length of about 116 repeats. Thus, overt phenotype onset begins later in life at 15 to 21 weeks of age with death occurring between 32 and 40 weeks of age (Mangiarini et al., 1996).

Studies in which exocytotic DA release was directly measured in R6/1 mice have not been published to our knowledge; however, recent evidence raises that possibility that dopamine system function is indeed altered. Increases in extracellular DA induced by ip injection of malonate, an excitotoxin, are less in R6/1 mice compared to WT control mice even though DA content, measured in striatal lysates, is unchanged (Petersén et al., 2002, Pineda et al., 2005)

Moreover, R6/1 mice exhibit a blunted locomotor response to amphetamine, but not apomorphine, indicating that presynaptic dysfunction of the dopaminergic system is responsible for these behavioral alterations (Pineda et al., 2005). Nevertheless, it is not known if DA release and uptake are altered. A clear assessment of DA release and uptake dynamics in R6/1 mice and other HD model rodents is important because underlying genetic differences, such as CAG repeat length, may alter nervous system function differently between strains.

In this work, we used FSCV to investigate DA release and uptake in striatal brain slices harvested from R6/1 mice. FSCV is useful in this case because its good temporal resolution (10 measurements/s as applied in this work) allows for DA release and uptake to be measured as separate processes.

Methods

Animals. R6/1 [CBy.Cg-Tg(HDexon1)61b] and wild-type mice were purchased from Jackson Laboratories (Bar Harbor, Maine) and were housed at the University of Kansas animal care unit prior to use. Food and water were provided ad libitum and a 12-hour light-dark cycle was used. All animal procedures were approved by the University of Kansas Institutional Animal Care and Use Committee.

Brain Slice Preparation. Brain slices were prepared, as previously described, from R6/1 and WT mice at 10, 16, and 24 weeks of age (Johnson et al., 2006). Mice were anesthetized by isoflurane inhalation and then decapitated. The brain was immediately removed and placed in ice cold artificial cerebrospinal fluid (aCSF) consisting of 126 mM NaCl, 2.5 mM KCl, 1.2 mM NaH_2PO_4, 2.4 mM $CaCl_2$, 1.2 mM $MgCl_2$, 25 mM $NaHCO_3$, 20 mM HEPES, and 11 mM D-Glucose with a pH of 7.4. The aCSF was oxygenated by bubbling 95% O_2/5% CO_2 gas into the

aCSF throughout the experiment. After the brain was removed from the skull, the cerebellum was sliced off and the brain was mounted on an aluminum block. Coronal slices, 300 μm thick, were made using a vibratome slicer (Leica, Wetzlar, Germany). A single brain slice was placed in the superfusion chamber, which was maintained at 34°C and had a continuous flow of aCSF at a rate of 2 mL/min. Each brain slice was equilibrated in the superfusion chamber for 60 minutes prior to obtaining measurements.

DA release in brain slices. Carbon-fiber microelectrodes were fabricated as previously described (Kraft et al., 2009). Briefly, a single 7 μm diameter carbon-fiber (Goodfellow Cambridge Ltd, Huntingdon, U.K.) was aspirated through a glass capillary tube (1.2 mm outer diameter, 0.68 mm inner diameter, 4 inches long, A-M Systems, Inc. Carlsborg, WA, USA), and then the capillary tube was pulled using a heated coil puller (Narishige International USA, Inc., East Meadow, NY). After the electrodes were trimmed to about 25 μm from the glass seal they were further insulated with epoxy resin (EPON resin 815C, EPIKURE 3234 curing agent, Miller-Stephenson, Danbury, CT, USA), and then cured at 100°C for 1 h. The electrodes were backfilled with 0.5 M potassium acetate in order to provide an electrical connection between the carbon fiber and an inserted silver wire.

A triangular waveform was applied to the carbon-fiber working electrode. The potential was held -0.4 V, increased to +1.0 V, and then scanned back to -0.4 V at a scan rate of 300 V/s and an update rate of 60 Hz. A headstage amplifier (UNC Chemistry Department Electronics Design Facility, Chapel Hill, NC) was interfaced with a computer via a breakout box and custom software provided by R.M. Wightman and M.L.A.V. Heien, University of North Carolina, Chapel Hill. A chlorided silver wire was used as an Ag/AgCl reference electrode. The carbon fiber microelectrode was inserted to a depth of 100 μm in the dorsolateral caudate-putamen

region of the striatum between the prongs of a bipolar stimulation electrode (Plastics One, Roanoke, VA), which was separated by a distance of 200 μm. A single electrical stimulus pulse at 60Hz was applied to the brain slice and the current was then measured at the peak oxidation potential for dopamine (about +0.6V versus Ag/AgCl reference electrode). Working electrodes were calibrated with dopamine standards of known concentration in a flow cell before and after each use. The average of the pre- and post-calibration measurements was used as the calibration factor.

DA release measurements were collected in four locations of the dorsal lateral striatum in each brain slice. Each release plot was then modeled based on Michaelis-Menten kinetics, as previously described in Johnson et al., 2006 (Johnson et al., 2006) to determine $[DA]_p$, the peak DA release per electrical stimulus pulse, and V_{max}, the maximum uptake rate of DA by the dopamine transporter. $[DA]_p$ is distinguished from $[DA]_{max}$, the peak DA release amplitude, because it is corrected for uptake and electrode performance. Values obtained from the four sampling points were used to obtain an average value for each slice.

Statistics. All values are represented as the average ± SEM, where *N* = the number of brain slices. Comparisons were made using a Student's t test.

Results

DA release was measured using a single pulse stimulation and FSCV at carbon fiber microelectrodes in brain slices harvested from R6/1 and WT mice at 10, 16, and 24 weeks old (Fig. 1A). Cyclic voltammograms (CVs) obtained at the highest point of stimulated release were used to verify that the analyte detected was DA. The average values of $[DA]_{max}$ (Fig. 1B) were: 10 weeks of age, 0.82 ± 0.17 μM (R6/1; n = 9) and 0.89 ± 0.14 μM (WT; n = 8); 16 weeks of

age, 1.03 ± 0.17 µM (R6/1, n = 16) and 1.50 ± 0.23 µM (WT, n = 8); and 24 weeks of age, 0.48 ± 0.13 µM (R6/1, n = 8) and 0.92 ± 0.14 µM (WT, n = 15). Peak stimulated DA release ($[DA]_{max}$) was less in R6/1 mice than WT control mice at 24 weeks of age ($p < 0.05$).

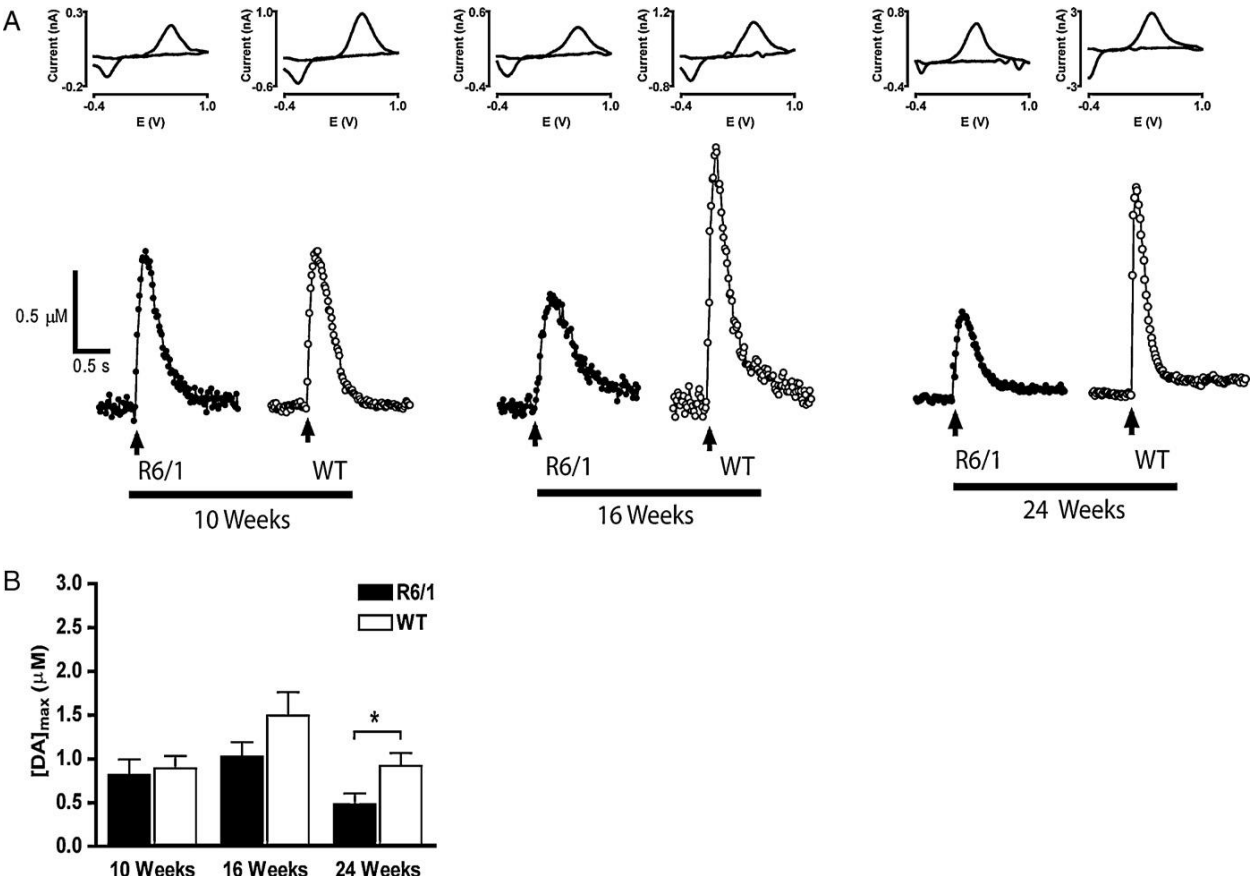

Fig 1. Stimulated DA release is diminished in older R6/1 mice compared to age-matched WT mice. (A) Representative plots of stimulated DA release in R6/1 and WT striatal brain slices. The time of stimulated release is indicated by the arrow. (B) Bar graph of average $[DA]_{max}$ measured in striatal slices from R6/1 and WT control mice at 10, 16, and 24 weeks of age. $[DA]_{max}$ was significantly diminished in R6/1 mice at 24 weeks of age (*$p<0.05$, n= 8 R6/1 and 15 WT slices).

The stimulated release plots were modeled, using a simplex-based computer program, to determine $[DA]_p$, the peak extracellular DA concentration (per stimulus pulse) corrected for uptake and electrode performance (Fig. 2A). Similar to the trend observed with $[DA]_{max}$, $[DA]_p$ was found to decrease as the age of the mice increased (Fig. 2B). The average values of $[DA]_p$ were: 10 weeks of age, 1.58 ± 0.44 µM (R6/1; n = 9) and 1.67 ± 0.30 µM (WT; n = 8); 16 weeks of age, 1.45 ± 0.21 µM (R6/1, n = 16) and 2.13 ± 0.36 µM (WT, n = 8); and 24 weeks of age, 0.66 ± 0.14 µM (R6/1, n = 8) and 1.53 ± 0.27 µM (WT, n = 15). By 16 weeks of age, $[DA]_p$, although not significant, appeared to be less in R6/1 mice than in WT mice. At 24 weeks of age, the R6/1 mice released significantly less ($p < 0.05$) DA than age-matched WT control mice. Additionally, R6/1 mice released less DA at 10 weeks of age than R6/1 mice at 24 weeks of age ($p < 0.005$).

The data obtained from the aforementioned modeling operation also provided us with V_{max}, which describes the maximum rate of uptake by the DAT and is directly proportional to the number of functioning DAT protein molecules. The average values of V_{max} were: 10 weeks of age, 10.5 ± 4.3 µM/s (R6/1; n = 9) and 9.0 ± 2.3 µM/s (WT; n = 8); 16 weeks of age, 4.12 ± 0.55 µM/s (R6/1, n = 16) and 8.08 ± 1.99 µM/s (WT, n = 8); and 24 weeks of age, 3.13 ± 0.98 µM/s (R6/1, n = 8) and 6.52 ± 1.74 µM/s (WT, n = 15). Compared to age-matched WT controls, V_{max} was significantly decreased ($p < 0.05$) in slices from R6/1 mice at 16 and 24 weeks of age (Fig. 2C).

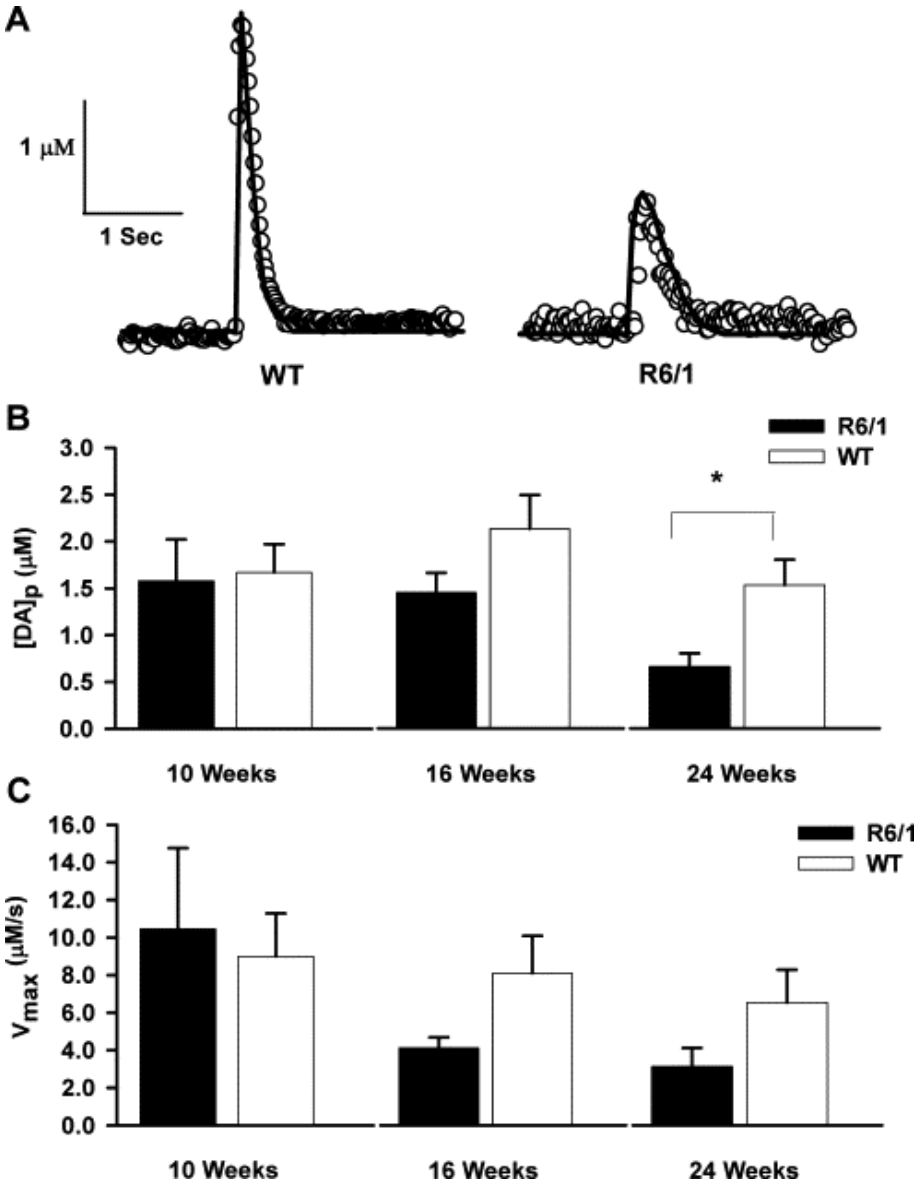

Fig. 2. DA release per pulse $[DA]_p$ and V_{max} are decreased in older R6/1 mice compared to age-matched WT mice. (A) Representative plots and modeled curves of stimulated DA release in an R6/1 slice and a WT slice. (B) The $[DA]_p$ is inhibited in 24 week old R6/1 mice when compared to WT mice of the same age (*$p<0.05$, n= 8 R6/1 and 15 WT slices) but not in 10 and 16 week old mice. (C) V_{max} is inhibited in 16 and 24 week old R6/1 mice when compared to age-matched WT mice (*$p<0.05$; 16 weeks: n= 16 R6/1 and 8 WT slices, 24 weeks: n= 8 R6/1 and 15 WT slices).

Discussion

In this study, we examined the DA release and uptake in R6/1 mice at 10, 16, and 24 weeks of age. $[DA]_p$ and V_{max} were determined from the best-fit parameters that were used in modeling the stimulated release plots. These results show that $[DA]_{max}$, $[DA]_p$, and V_{max} decrease progressively over time compared to age-matched WT mice.

Our initial results indicated that $[DA]_{max}$, the peak concentration of evoked DA detected at the electrode, progressively decreased in R6/1 mice as they aged. Therefore, we modeled the plots to determine $[DA]_p$ and V_{max}. $[DA]_p$ may be considered a more reliable measure of how much DA is released per electrical stimulus pulse because it takes into account DA uptake and electrode performance. $[DA]_p$ was significantly diminished by 24 weeks of age. Complimentary to our results are previous microdialysis studies which show that basal DA levels and malonate-induced DA efflux are diminished in the R6/1 striatum (Petersén et al., 2001) even though striatal DA content is unchanged at either 16 weeks (Petersén et al., 2001) or 30 weeks of age (Pineda et al., 2005). Therefore, the $[DA]_p$ values obtained using FSCV allow us to make the more specific interpretation that the ability of dopaminergic terminals to release DA by exocytosis is progressively impaired in R6/1 mice. These findings are similar to those found in R6/2 mice (Johnson et al., 2006); however, consistent with having a shorter CAG repeat length, this impairment progresses more slowly with age.

In addition to DA release, values of V_{max} were decreased in R6/1 mice compared to WT control mice at 16 and 24 weeks of age. Previous labeling experiments indicate that striatal DAT expression is similar in R6/1 and WT mice. Thus, decreased uptake is likely not related to a decrease in the number of DAT protein molecules. This determination is important because DA

uptake by the DAT is known to follow Michaelis-Menten uptake kinetics and, therefore, the equation $V_{max} = k_{cat}[E]_t$ is obeyed, where k_{cat} is a rate constant and $[E]_t$ represents the total enzyme concentration (Mathews and van Holde, 1996), in this case DAT. Thus, since $[E]_t$ is likely unchanged, the difference in uptake may represent a modification of the transporter. It is also important to note that these findings differ from those obtained in R6/2 mice, in which V_{max} was unchanged throughout the entire course of phenotype progression. Therefore, age, coupled with the HD mutation, apparently also plays an important role in the changes in V_{max}.

In conclusion, this report reveals key malfunctions in DA release in R6/1 mice, and also shows that the DA uptake kinetics of R6/1 differ from those of R6/2 mice, a popularly used genetic HD model. These findings reveal potentially important considerations for researchers studying DA system function in these HD models.

B. Enhanced Striatal Dopamine Stores in Rats Treated with 3-Nitropropionic Acid

Fast-scan cyclic voltammetry at carbon-fiber microelectrodes was used to measure electrically-evoked dopamine release and uptake in the dorsolateral caudate of striatal brain slices harvested from rats treated with 3-nitropropionic acid. Both release and uptake in this brain region were unchanged in 3-nitropropionic acid-treated rats, compared to sham controls. However, further investigation indicated that reserve pool dopamine content was enhanced ~112% by 3-nitropropionic acid treatment, suggesting that a compensatory effect, in which the dopamine reserve pool is augmented, occurs in this brain region.

Introduction

Huntington's disease (HD) is a familial neurodegenerative disorder caused by an expanded CAG repeat sequence on the gene that encodes the huntingtin protein (Huntington's Disease Collaborative Research Group, 1993). HD is characterized by cognitive dysfunction, choreic movements, and striatal degeneration (Bates et al., 2002). Previous evidence suggests that impaired striatal dopamine (DA) release in transgenic HD mice contributes to the progressive motor phenotype. (Abercrombie and Russo, 2002, Hickey et al., 2002, Petersén et al., 2002, Johnson et al., 2006, Johnson et al., 2007).

A number of chemical compounds, administered locally and systemically, have been applied to various strains of rat in attempts to replicate neurological and behavioral features of human HD. These compounds include kainate (McGeer and McGeer, 1976), malonate (Beal et al., 1993), 3-acetylpyridine (Schulz and Beal, 1994), and 3-nitropropionic acid (3NP) (Beal et al., 1993, Brouillet et al., 1993), to name a few. Of these and other chemical treatments, the application of 3NP is among the most extensively used to model HD. Previous work has suggested that DA release, evoked by stimulation of the medial forebrain bundle (mfb) and measured in the dorsomedial caudate putamen with fast scan cyclic voltammetry (FSCV), is diminished in the dorsomedial striatum of 3NP treated rats. The subsequent finding that DA content in striatal lysates was unaffected by 3NP treatment prompted us to probe further the amount of striatal DA stored in the reserve pool (Kraft et al., 2009).

In this work, we used FSCV to measure locally-stimulated DA release in striatal brain slices from 3NP-treated rats. Interestingly, DA release in 3NP-treated rats was unchanged compared to sham controls. Moreover, DA uptake appeared to be unaffected by 3NP treatment.

However, measurements of DA efflux, induced by amphetamine (AMPH) and obtained after inhibiting DA synthesis, suggest that an increased number of DA molecules are held in reserve in 3NP rats compared to sham-treated rats.

Materials and Methods

Animal Procedures

The 3NP experiments were carried out on 12 week old male Lewis rats (300-350 g), obtained from Charles River Laboratories, Inc. (Wilmington, MA). Rats were anesthetized with a mixture containing ketamine hydrochloride (56.25 mg/kg), xylazine hydrochloride (2.85 mg/kg), and acepromazine maleate (0.56 mg/kg), injected im. An incision was made between the shoulder blades and a 2 mL Alzet osmotic pump (2ML1; delivering 10 uL/hr for up to 7 days; Durect Corporation, Cupertino, CA) containing 3NP was positioned subcutaneously. The final concentration of 3NP in the pump was adjusted according to the weight of the rat on the day of surgery, so that 54 mg/kg day was delivered. Rats were continuously infused with 3NP for 5 days. Sham controls rats underwent the same surgical procedure without the implantation of the Alzet pump. All rats were provided with food and water *ad libitum* in a temperature/humidity-controlled environment on a 12-h light/dark cycle. All animal procedures were approved by the University of Kansas Institutional Animal Care and Use Committee.

Brain Slice Preparation

Rats were anesthetized by isoflurane inhalation and decapitated. The brain was immediately removed and placed in ice cold artificial cerebrospinal fluid (aCSF). The aCSF consisted of 126 mM NaCl, 2.5 mM KCl, 1.2 mM NaH_2PO_4, 2.4 mM $CaCl_2$, 1.2 mM $MgCl_2$, 25 mM $NaHCO_3$, 20 mM HEPES, and 11 mM D-Glucose. The pH was adjusted to 7.4 using 5 M

HCl and was continuously saturated with 95% O_2/5% CO_2. The cerebellum was sliced off with a razor blade and then the brain was glued onto an aluminum block. Coronal slices, 300 μm thick, were made using a vibratome. Brain slices containing the striatum were stored in ice cold aCSF. A single slice was placed in a superfusion chamber that was maintained at 34°C and had a continuous flow of aCSF (2 mL/min). Each brain slice was equilibrated for 60 minutes prior to obtaining measurements. To apply αMPT and AMPH, aCSF containing the drugs was maintained in a separate reservoir and introduced through a three-way valve.

DA Release in Brain Slices

For a typical experiment, a triangular waveform, starting at -0.4 V, increasing to +1.0 V, and then scanning back down to -0.4 V, was applied to a carbon fiber microelectrode. A scan rate of 300 V/s and a cyclic voltammogram (CV) collection rate of 10 CVs/s was used. DA was evoked by application of either a single electrical stimulus pulse or a series of 120 pulses, with each pulse having a duration of 4 ms and a current of 350 μA. A headstage amplifier (UNC chemistry department electronics design facility, Chapel Hill, NC) was interfaced with a computer via a breakout box and custom software provided by R.M. Wightman and M.L.A.V. Heien, University of North Carolina, Chapel Hill. An Ag/AgCl reference electrode was used. The carbon fiber was inserted 100 μm into the dorsolateral caudate-putamen region of the striatum between the prongs of a bipolar stimulation electrode (Plastics One, Roanoke, VA). DA release was measured at four locations in the dorsal lateral striatum and averaged to obtain a single value for each slice. The values obtained for each slice were then combined to obtain an average value for each animal. Working electrodes were calibrated with DA standards of known concentrations in a flow cell before and after each use. The average of the pre- and post-calibration values was used as the calibration factor.

Reserve pool DA was measured using previously established procedures (Ortiz et al., 2010). Briefly, a single pulse stimulus was applied every five minutes until peak stimulated DA release remained constant between stimulations. Next, 50 µM aMPT was added to the aCSF, while continuing to stimulate the brain slice every 5 minutes, until DA release disappeared. The aMPT/aCSF solution was then changed to also contain 20 µM AMPH and the peak amplitude of AMPH-induced DA efflux ($[DA]_{AMPH}$), which occurred after about 25 minutes, was measured.

Data Analysis

Single pulse measurements taken in slices from the 3NP-treated rats and sham controls were modeled using software, designed by P. A. Garris, Illinois State University, that incorporates a simplex algorhythm in order to determine $[DA]_p$ and V_{max}. $[DA]_p$ is the peak DA release per electrical stimulus pulse corrected for uptake and electrode performance. V_{max} corresponds to the maximum rate of DA uptake and is directly proportional to the number of functioning membrane-bound DAT protein molecules. The application of this software to data obtained in rodents that model HD has been described previously (Johnson et al., 2006, Kraft et al., 2009).

For statistical comparisons, GraphPad Prism (version 4.03) statistical software was used. Data are expressed as mean +/- SEM. Comparisons were assessed by Student's t-test (unpaired). A probability level of 5% ($p < 0.05$) was considered significant.

Results and Discussion

Striatal Dopamine Release and Uptake

Voltammetric measurements of DA release in brain slices were obtained during local electrical stimulation (120-pulses applied over a 2-s period); thus, differences in release should be attributed to changes that have occurred to dopaminergic terminals as a result of 3NP treatment. However, peak DA release (Figure 1) did not significantly differ between the 3NP-treated and sham rats ($p > 0.05$, 3NP-treated, 3.71 ± 0.46 µM, $n = 5$ rats; sham, 3.33 ± 0.42 µM, $n = 5$ rats), suggesting that treatment did not alter the ability of dopaminergic terminals in the dorsolateral caudate to release DA. Moreover, these results suggest that the motor syndrome associated with the 3NP model may also be caused by neurological dysfunction in other brain regions. It is important to note that the dorsomedial caudate lacked structural integrity (fell apart upon slicing) in these experiments, making FSCV measurements in this brain region impractical.

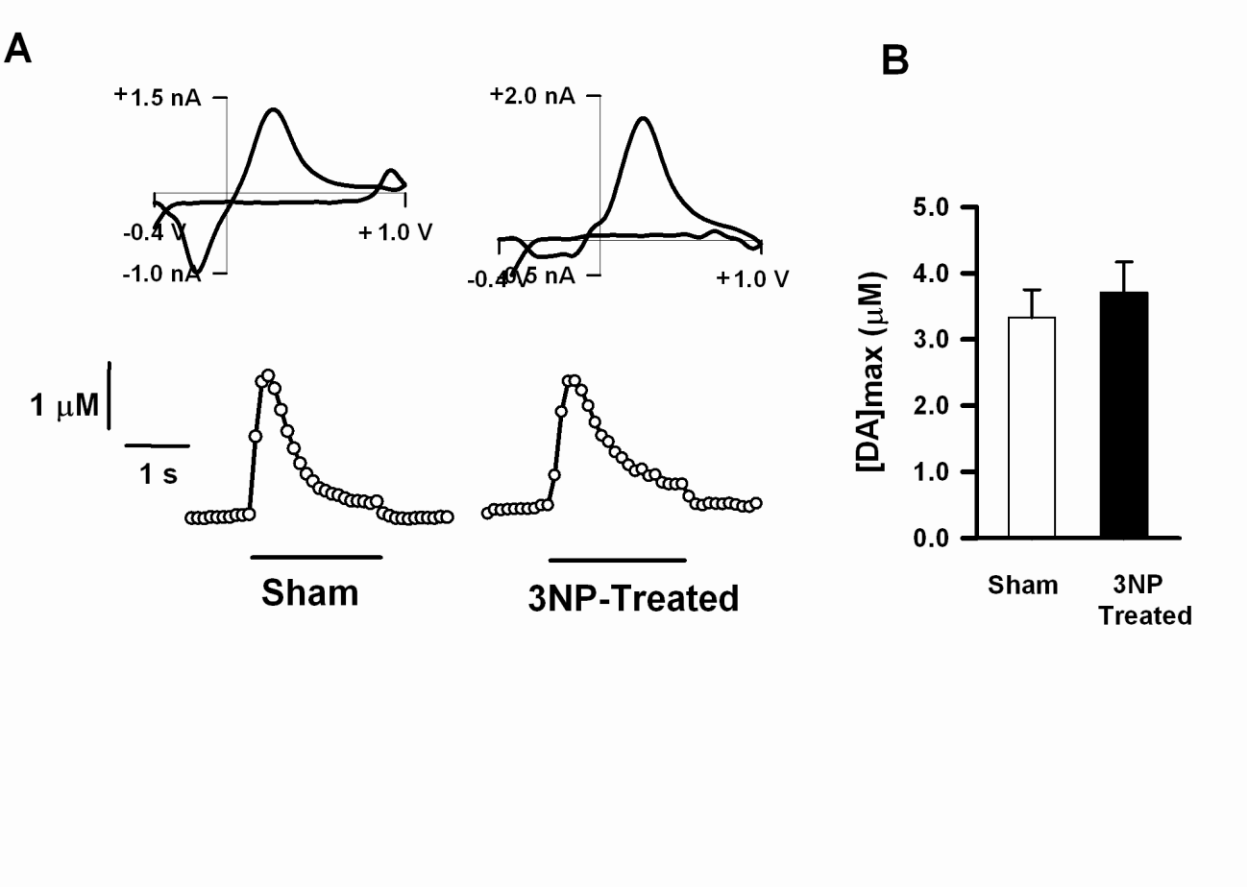

Figure 1.

Striatal DA release is unchanged in 3NP-treated rats compared to sham control rats. DA release was evoked by local application of 120-pulse electrical stimuli, indicated by bars under the release plots. (A) Representative plots and CVs obtained by FSCV at carbon-fiber microelectrodes are shown for 3NP-treated and sham rats. (B) Stimulated DA release was unchanged between the 3NP-treated and sham control rats. The average DA release values for the 3NP-treated was 3.71 ± 0.46 μM, (n = 5 rats); and the sham rats had an average release of 3.33 ± 0.42 μM (n = 5 rats).

To determine if DA uptake is altered in brain slices from 3NP rats, plots of DA release, evoked by single stimulus pulses, were obtained. These plots were modeled, based on Michaelis-Menten kinetics, to determine V_{max} and $[DA]_p$. This modeling operation has been described previously (Johnson et al., 2006). V_{max} is directly proportional to the total number of functioning DAT protein molecules and $[DA]_p$ is DA released per stimulus pulse, corrected for uptake and electrode performance. V_{max} and $[DA]_p$ were both unchanged between the 3NP-treated and sham rats, indicating that both release and uptake are unaffected by 3NP treatment (Figure 2).

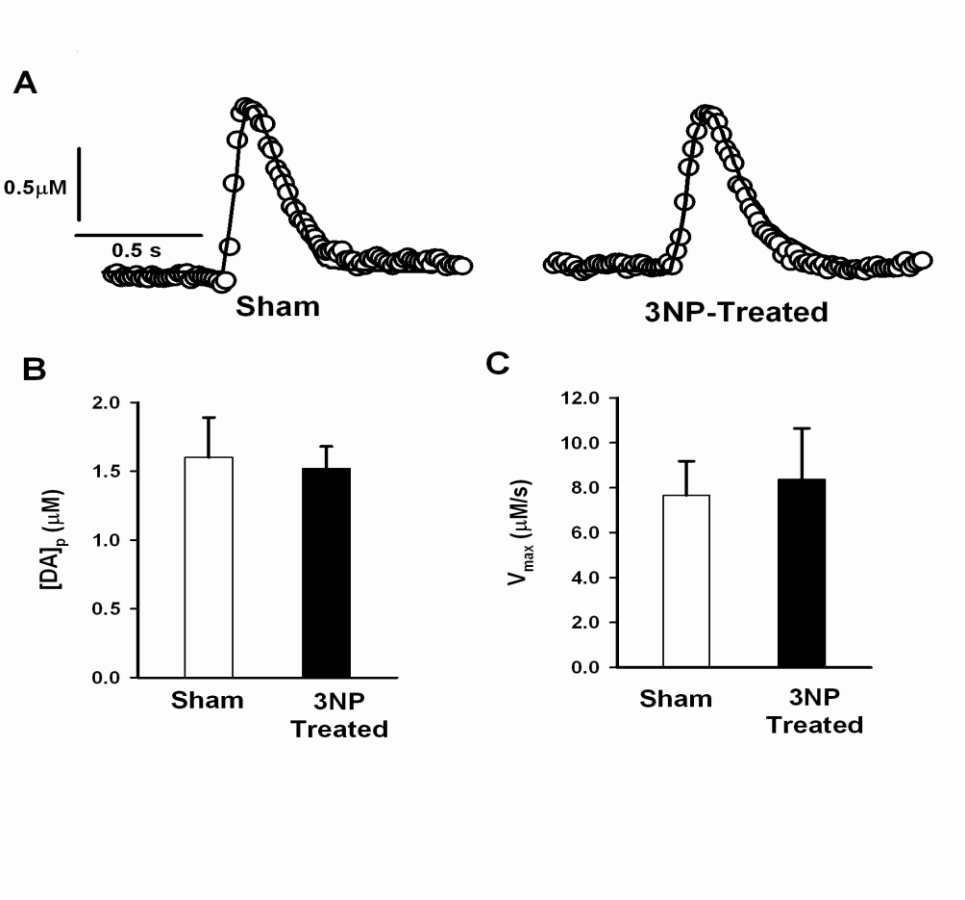

Figure 2.

DA release plots obtained by application of a single electrical stimulus pulse were modeled to determine $[DA]_p$ and V_{max} in 3NP-treated and sham-treated control rats. (A) The experimental data (open circles) for the Sham and 3NP-treated rats in comparison with the modeled curves (solid line). (B) $[DA]_p$ was unchanged between the sham and 3NP-treated rats ($p > 0.05$; n = 5 sham and 3NP-treated rats). The average $[DA]_p$ for the sham rats is 1.60 ± 0.29 µM and 1.52 ± 0.16 µM. (C) V_{max} was unchanged between the 3NP-treated rats and the sham-treated control rats ($p > 0.05$). The average V_{max} for the sham rats was 7.66 ± 2.28 µM/s (n = 5 rats) and the 3NP-treated rats was 8.36 ± 1.52 µM/s (n = 5 rats).

These results also indicate that the number of functioning DAT protein molecules was unchanged, and that the vesicular release machinery was functioning normally. It is interesting that in vivo DA release, evoked in anesthetized 3NP-treated rats by stimulation of the dopaminergic pathway at the medial forebrain bundle (mfb) and measured in the dorsomedial striatum with FSCV (Kraft et al., 2009), was diminished. Thus, it is possible that a mechanism is in place in this brain region that could help preserve normal levels of DA release in the dorsolateral region.

The sub-second temporal resolution of FSCV allows for the measurement and analyses of specific DA release events, whereas microdialysis can show only slower changes in extracellular DA levels. Thus, the FSCV measurements in this work provide a more direct measure of how well presynaptic terminals release dopamine by exocytosis and take it back up through the DAT. To our knowledge, this work and Kraft et al. (2009) are the only studies in which DA release and uptake were measured at high temporal resolutions in 3NP-treated animals.

Reserve Pool DA Levels in 3NP Rats

The DA reserve pool is thought to mobilize during periods of prolonged synaptic activity (Neves and Lagnado, 1999, Zucker and Regehr, 2002, Rizzoli and Betz, 2005). To identify the impact of 3NP treatment on reserve pool DA, brain slices were exposed to 50 μM αMPT, which inhibits tyrosine hydroxylase, the rate limiting enzyme in DA synthesis (Figure 3A). A single electrical stimulus pulse was then applied every five minutes until there was no longer DA release. At this point, DA in the extracellular space and in releasable vesicles was depleted, leaving only DA stored in the reserve pool. After release disappeared, 20 μM AMPH was added to the aCSF perfusion solution and the resulting DA efflux was measured over the course of 25

minutes to determine $[DA]_{AMPH}$. AMPH is a competitive DAT inhibitor that empties vesicles and induces reverse transport from terminals, allowing for the quantitative measurement of internal DA stores. Thus, upon the addition of AMPH both cytosolic and vesicular DA exit the terminals by reverse transport through the DAT into the extracellular space (Sulzer et al., 1995, Floor and Meng, 1996, Jones et al., 1998). $[DA]_{AMPH}$ in 3NP-treated rats was greater than that of the sham control rats (Figure 3B; $p < 0.05$; 3NP-treated, 16.7 ± 2.5 µM, n = 3 rats; sham, 7.86 ± 1.79 µM, n = 5 rats).

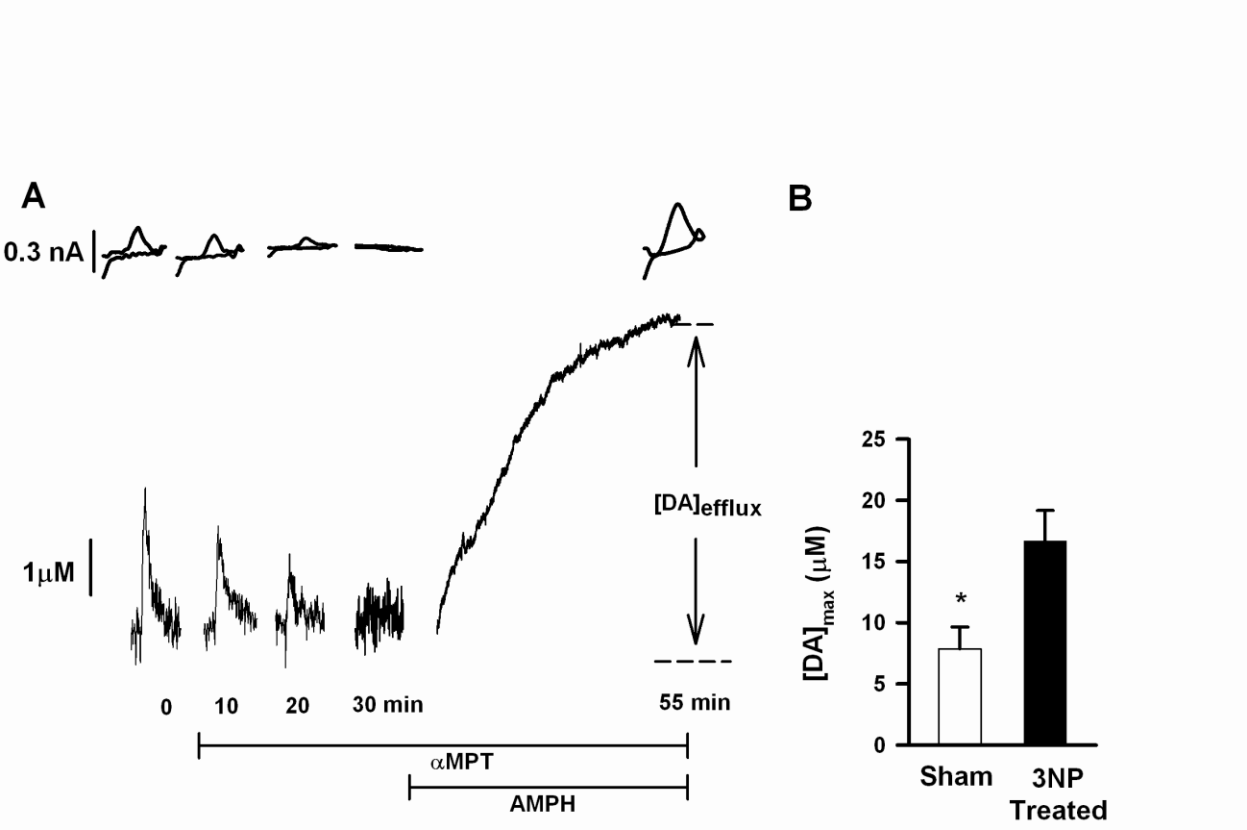

Figure 3.

AMPH-induced efflux after treatment with αMPT is greater in 3NP-treated rats than in WT rats. (A) Slices were treated with αMPT until the stimulated DA release peak disappeared. Slices were then treated with AMPH and $[DA]_{AMPH}$ was measured. (B) $[DA]_{AMPH}$ was significantly increased in slices from 3NP-treated rats compared to those from age-matched sham control mice (*$p < 0.05$). The average $[DA]_{AMPH}$ in 3NP-treated rats was 16.68 ± 2.49 μM (n = 3 rats) and 7.86 ± 1.79 μM (n = 5 rats) in sham control rats.

Our recent evidence suggests that the 120-pulse stimulation regimen evokes the release of DA from multiple stores within presynaptic terminals in striatal brain slices (Ortiz et al., 2010). Therefore, speculate that 3NP treatment induced the occurrence of a compensatory effect, in which the amount of DA within the reserve pool was boosted. One of the more common models of vesicle distribution within presynaptic terminals identifies vesicles as belonging to one of three groups (Rizzoli et al., 2005): the readily releasable pool (RRP), the recycling pool, and the reserve pool. The RRP undergoes exocytosis upon mild stimulation, and is then replenished by the recycling pool (Neves and Lagnado, 1999). Reserve pool vesicles, which make up ~80-90% of total vesicles (Zucker et al., 2002; Rizzoli et al., 2005), are thought to aid in neurotransmission during periods of prolonged synaptic activity. Therefore, striatal dysfunction in HD could potentially arise from impairments in the mobilization or storage of reserve pool DA. We have previously shown that R6/2 mice have fewer vesicles in the reserve pool then wild type control mice (Ortiz et al., 2010).

These DA efflux measurements reveal that 3NP-treated rats had an increased amount of reserve pool DA. Although the underlying causes of this increase have not been identified, a possible mechanism could be the uptake of DA released by the degeneration of surrounding neurons caused by 3NP treatment (Ouary et al., 2000, El Massioui et al., 2001, Brouillet et al., 2005). This enhanced reserve pool may help supply the dopaminergic terminals with sufficient DA-filled vesicles for a normal level of release. Alternatively, these enhanced DA levels may also increase oxidative stress by increased production of hydroxyl radicals (Pandey et al., 2009).

In conclusion, our studies reveal an inherent difference in DA storage in the dorsolateral caudate of 3NP-treated rats compared with sham-treated rats. These differences may arise from an enhancement of the DA reserve pool in 3NP-treated rats, and should be considered when using chemically-induced animal models to study DA-related mechanisms.

C. References

Abercrombie ED, Russo ML (2002) *Neurochemistry in the R6/2 Transgenic Mouse Model of Huntington's Disease*. In: *Program Number 19512* in *Society for Neuroscience* 2002 Orlando, FL.

Bates GP, Harper PS, Jones L (2002) Huntington's Disease. Oxford: Oxford University Press.

Beal MF, Brouillet E, Jenkins BG, Ferrante RJ, Kowall NW, Miller JM, Storey E, Srivastava R, Rosen BR, Hyman BT (Neurochemical and histologic characterization of striatal excitotoxic lesions produced by the mitochondrial toxin 3-nitropropionic acid. J Neurosci 13:4181-4192.1993).

Brouillet E, Jacquard C, Bizat N, Blum D (3-Nitropropionic acid: a mitochondrial toxin to uncover physiopathological mechanisms underlying striatal degeneration in Huntington's disease. J Neurochem 95:1521-1540.2005).

Brouillet E, Jenkins BG, Hyman BT, Ferrante RJ, Kowall NW, Srivastava R, Roy DS, Rosen BR, Beal MF (Age-dependent vulnerability of the striatum to the mitochondrial toxin 3-nitropropionic acid. J Neurochem 60:356-359.1993).

Davies SW, Turmaine M, Cozens BA, DiFiglia M, Sharp AH, Ross CA, Scherzinger E, Wanker EE, Mangiarini L, Bates GP (Formation of neuronal intranuclear inclusions underlies the neurological dysfunction in mice transgenic for the HD mutation. Cell 90:537-548.1997).

El Massioui N, Ouary S, Cheruel F, Hantraye P, Brouillet E (Perseverative behavior underlying attentional set-shifting deficits in rats chronically treated with the neurotoxin 3-nitropropionic acid. Exp Neurol 172:172-181.2001).

Floor E, Meng L (Amphetamine releases dopamine from synaptic vesicles by dual mechanisms. Neurosci Lett 215:53-56.1996).

Hickey MA, Reynolds GP, Morton AJ (The role of dopamine in motor symptoms in the R6/2 transgenic mouse model of Huntington's disease. J Neurochem 81:46-59.2002).

Johnson MA, Rajan V, Miller CE, Wightman RM (Dopamine release is severely compromised in the R6/2 mouse model of Huntington's disease. J Neurochem 97:737-746.2006).

Johnson MA, Villanueva M, Haynes CL, Seipel AT, Buhler LA, Wightman RM (Catecholamine exocytosis is diminished in R6/2 Huntington's disease model mice. J Neurochem 103:2102-2110.2007).

Jones SR, Gainetdinov RR, Wightman RM, Caron MG (Mechanisms of amphetamine action revealed in mice lacking the dopamine transporter. J Neurosci 18:1979-1986.1998).

Kandel ER, Schwartz JH, Jessell TM (2000) Principles of Neural Science. New York: McGraw-Hill.

Kraft JC, Osterhaus GL, Ortiz AN, Garris PA, Johnson MA (In vivo dopamine release and uptake impairments in rats treated with 3-nitropropionic acid. Neuroscience 161:940-949.2009).

Mangiarini L, Sathasivam K, Seller M, Cozens B, Harper A, Hetherington C, Lawton M, Trottier Y, Lehrach H, Davies SW, Bates GP (Exon 1 of the HD gene with an expanded CAG repeat is sufficient to cause a progressive neurological phenotype in transgenic mice. Cell 87:493-506.1996).

Mathews CK, van Holde KE (1996) Biochemistry. Menlo Park, CA: Benjamin/Cummings.

McGeer EG, McGeer PL (Duplication of biochemical changes of Huntington's chorea by intrastriatal injections of glutamic and kainic acids. Nature 263:517-519.1976).

Neves G, Lagnado L (The kinetics of exocytosis and endocytosis in the synaptic terminal of goldfish retinal bipolar cells. The Journal of physiology 515 (Pt 1):181-202.1999).

Ortiz AN, Kurth BJ, Osterhaus GL, Johnson MA (Dysregulation of intracellular dopamine stores revealed in the R6/2 mouse striatum. J Neurochem 112:755-761.2010).

Ouary S, Bizat N, Altairac S, Menetrat H, Mittoux V, Conde F, Hantraye P, Brouillet E (Major strain differences in response to chronic systemic administration of the mitochondrial toxin 3-nitropropionic acid in rats: implications for neuroprotection studies. Neuroscience 97:521-530.2000).

Pandey M, Borah A, Varghese M, Barman PK, Mohanakumar KP, Usha R (Striatal dopamine level contributes to hydroxyl radical generation and subsequent neurodegeneration in the striatum in 3-nitropropionic acid-induced Huntington's disease in rats. Neurochemistry international 55:431-437.2009).

Petersén A, Hansson O, Puschban Z, Sapp E, Romero N, Castilho RF, Sulzer D, Rice M, DiFiglia M, Przedborski S, Brundin P (Mice transgenic for exon 1 of the Huntington's disease gene display reduced striatal sensitivity to neurotoxicity induced by dopamine and 6-hydroxydopamine. Eur J Neurosci 14:1425-1435.2001).

Petersén A, Puschban Z, Lotharius J, NicNiocaill B, Wiekop P, O'Connor WT, Brundin P (Evidence for dysfunction of the nigrostriatal pathway in the R6/1 line of transgenic Huntington's disease mice. Neurobiol Dis 11:134-146.2002).

Pineda JR, Canals JM, Bosch M, Adell A, Mengod G, Artigas F, Ernfors P, Alberch J (Brain-derived neurotrophic factor modulates dopaminergic deficits in a transgenic mouse model of Huntington's disease. J Neurochem 93:1057-1068.2005).

Rizzoli SO, Betz WJ (Synaptic vesicle pools. Nat Rev Neurosci 6:57-69.2005).

Schulz JB, Beal MF (Mitochondrial dysfunction in movement disorders. Curr Opin Neurol 7:333-339.1994).

Sulzer D, Chen TK, Lau YY, Kristensen H, Rayport S, Ewing A (Amphetamine redistributes dopamine from synaptic vesicles to the cytosol and promotes reverse transport. J Neurosci 15:4102-4108.1995).

The Huntington's Disease Collaborative Research Group (A novel gene containing a trinucleotide repeat that is expanded and unstable on Huntington's disease chromosomes Cell 72:971-983.1993).

Zucker RS, Regehr WG (Short-term synaptic plasticity. Annu Rev Physiol 64:355-405.2002).

Chapter 3: Dopamine Reserve Pools in Huntington's Disease

Using FSCV it has previously been shown that there is a decrease in DA release in rodent models of Huntington's disease including R6/1 mice, R6/2 mice and 3NP treated rats. This chapter explores the DA reserve pools in the most extensively studied HD mouse model the R6/2 mice.

A. Dysregulation of intracellular dopamine stores revealed in the R6/2 mouse striatum

Huntington's disease is a fatal, neurodegenerative movement disorder characterized by preferential and extensive striatal degeneration. Here, we used fast-scan cyclic voltammetry to study the mobilization and efflux of reserve pool dopamine in striatal brain slices from Huntington's disease model R6/2 mice. When applying stimulus trains of 120 pulses, evoked dopamine release in wild-type slices was greater than that in R6/2 slices at the higher frequencies (50 and 60 Hz). To quantify cytosolic and reserve pool dopamine levels, amphetamine-induced dopamine efflux was measured after pre-treatment with either tetrabenazine or alpha-methyl-p-tyrosine. Slices from 12-week old R6/2 mice released less dopamine than slices from wild-type mice, while no difference was noted in slices from 6-week old mice. Dopamine efflux currents, normalized against stimulated release currents, suggest an enhancement of cytosolic dopamine levels in the R6/2 striatum. The vesicular release of reserve pool dopamine, mobilized by treatment with cocaine, was shorter lived in R6/2 slices compared to wild-type slices even though peak dopamine release was the same. Moreover, the number of dopamine reserve pool vesicles in R6/2 mice was less than half of that in wild-type. Therefore, our data suggest that

R6/2 mice have fewer dopamine reserve pool vesicles, but have enhanced cytosolic dopamine levels.

Introduction

Huntington's disease (HD) is an autosomal dominant neurodegenerative movement disorder caused by an expanded CAG repeat on the gene that encodes the huntingtin protein (htt). HD is characterized by mood disturbances, choreic movements, cognitive dysfunction, and degeneration of the striatum (Bates et al., 2002). Recent evidence indicates that impaired striatal dopamine (DA) release in HD rodent models contributes to the progressive motor phenotype. This evidence includes: in vivo microdialysis studies in which DA levels in R6/1 and R6/2 mice were lower than that of wild type (WT) controls (Abercrombie and Russo, 2002; Petersén et al., 2002); locomotor measurements in which R6/2 mice had a blunted response to cocaine (COC) and methamphetamine (METH; Hickey et al., 2002; Johnson et al., 2006); and stimulated DA release measurements taken using fast-scan cyclic voltammetry (FSCV) in which release in R6/2 brain slices was impaired (Johnson et al., 2006; Johnson et al., 2007). Furthermore, amperometry data collected from adrenal chromaffin cells suggest that quantal release of catecholamines is diminished in R6/2 mice (Johnson et al., 2007). Nevertheless, specific mechanisms underlying presynaptic DA release impairments in striatal brain tissue have not yet been thoroughly investigated.

One potential mechanism of striatal dysfunction in R6/2 mice involves the mobilization of reserve pool DA. Vesicles containing DA are believed to be partitioned into three distinct pools. These pools include the readily releasable pool (RRP), which undergoes exocytosis upon mild stimulation, the recycling pool, which is mobilized to replace RRP vesicles, and the reserve

pool, which is thought to be mobilized during periods of prolonged synaptic activity (Neves and Lagnado, 1999; Zucker and Regehr, 2002; Rizzoli and Betz, 2005). The reserve pool is the largest vesicle pool, consisting of ~80-90% of the total vesicles in the presynaptic terminal (Neves and Lagnado, 1999; Rizzoli and Betz, 2005). It has been shown previously that a synapsin-dependent DA reserve pool can be mobilized by treatment with COC (Venton et al., 2006). Thus, not only does this study suggest a possible mechanism for the attenuated psychostimulatory effect of COC in R6/2 mice, but it also identifies a mechanism by which DA reserve pools can be pharmacologically manipulated.

In this work, we investigated the neurochemical mechanisms that underlie striatal DA release impairments, which could potentially amplify phenotypical behavioral impairments observed in R6/2 mice (Carter *et al.* 1999). We hypothesized that reserve pool DA is depleted in R6/2 mice. To investigate this possibility, we used FSCV to measure amphetamine (AMPH) induced efflux and COC-induced vesicle mobilization of reserve pool DA in acute striatal slices from R6/2 and WT control mice. Our results suggest not only that the number of vesicles present in the DA reserve pool of R6/2 mice is diminished, but also that cytosolic dopamine levels may be enhanced.

Materials and Methods

Drugs. COC, αMPT, and AMPH were purchased from Sigma-Aldrich (St. Louis, MO). Tetrabenazine (TBZ) was a generous gift from Prof. Eric Floors, Department of Molecular Biosciences, University of Kansas.

Animals. R6/2 [B6CBA-Tg(HDexon1)62Gpb] and wild-type mice were purchased from Jackson Laboratories (Bar Harbor, Maine) and were housed at the University of Kansas animal care unit

prior to use. Food and water were provided ad libitum and a 12-hour light-dark cycle was used. All animal procedures were approved by the Institutional Animal Care and Use Committee.

Brain Slice Preparation. Brain slices were prepared as previously described (Johnson et al., 2006). Briefly, mice were anesthetized by isoflurane inhalation and then decapitated. The brain was immediately removed and placed in ice cold artificial cerebrospinal fluid (aCSF). The aCSF consisted of 126 mM NaCl, 2.5 mM KCl, 1.2 mM NaH_2PO_4, 2.4 mM $CaCl_2$, 1.2 mM $MgCl_2$, 25 mM $NaHCO_3$, 20 mM HEPES, and 11 mM D-Glucose. The pH was adjusted to 7.4. During the brain slice harvesting procedure and during experimentation, the aCSF was continuously saturated with 95% O_2/5% CO_2. The cerebellum was sliced off with a razor blade and then the brain was mounted on an aluminum block. Coronal slices, 300 μm thick, were made using a vibratome slicer (Leica, Wetzlar, Germany). Brain slices containing striata were stored in ice cold aCSF. A single slice was placed in the superfusion chamber, through which aCSF, maintained at 34° C, flowed at a continuous rate of 2 mL/min. Each brain slice was equilibrated in the superfusion chamber for 60 minutes prior to obtaining measurements. To apply αMPT, TBZ, AMPH, and COC, aCSF containing these drugs was maintained in a separate reservoir and introduced through a three-way valve.

DA release in brain slices. Carbon-fiber microelectrodes were fabricated as previously described (Kraft et al., 2009), with minor changes. Briefly, a single 7 μm diameter carbon-fiber (Goodfellow Cambridge Ltd, Huntingdon, U.K.) was aspirated through a glass capillary tube (1.2 mm outer diameter, 0.68 mm inner diameter, 4 inches long, A-M Systems, Inc. Carlsborg, WA, USA), which was pulled using a heated coil puller (Narishige International USA, Inc., East Meadow, NY). Electrodes were trimmed to 25 μm from the glass seal, further insulated with

epoxy resin (EPON resin 815C, EPIKURE 3234 curing agent, Miller-Stephenson, Danbury, CT, USA), and then cured at 100°C for 1 h. Prior to experimentation, electrodes were backfilled with 0.5 M potassium acetate in order to provide an electrical connection between the carbon fiber and an inserted silver wire. No further treatment of the electroactive surface was performed.

A triangular waveform, starting at -0.4 V, increasing to +1.0 V, and then scanning back to -0.4 V, was applied at the carbon-fiber working electrode. A scan rate of 300 V/s was used with an update rate of 60 Hz for single pulse stimulations and 10 Hz for 120-pulse stimulations. A headstage amplifier (UNC Chemistry Department Electronics Design Facility, Chapel Hill, NC) was interfaced with a computer via a breakout box and custom software provided by R.M. Wightman and M.L.A.V. Heien, University of North Carolina, Chapel Hill. A choridided silver wire was used as an Ag/AgCl reference electrode. The carbon fiber microelectrode was inserted 100 μm into the dorsolateral caudate-putamen region of the striatum between the prongs of a bipolar stimulation electrode (Plastics One, Roanoke, VA), which was separated by a distance of 200 μm. The current was then measured at the peak oxidation potential for dopamine (about +0.6V versus Ag/AgCl reference electrode). For the 120-pulse stimulations, DA release was measured using stimulation frequencies of 20, 30, 40, 50, and 60Hz at four locations in the dorsolateral striatum. At each location the DA release was measured going from the lowest frequency (20 Hz) to the highest frequency (60 Hz) with a 5 minute recovery time between each measurement. Working electrodes were calibrated with dopamine standards of known concentration in a flow cell before and after each use. The average of the pre and post calibration measurements was used as the calibration factor.

For DA efflux studies, single stimulus pulses were applied every five minutes until peak dopamine release was consistent over three consecutive measurements. Once the DA release

was consistent, either 50 μM αMPT or 10μM TBZ was added to the aCSF. The brain slice was stimulated every 5 minutes until the DA release peak disappeared. Next, 20 μM AMPH was introduced into the aCSF perfusion solution in addition to the αMPT or TBZ that was already present. AMPH-induced efflux was then measured without the use of electrical stimulation over the course of 25 minutes with an update rate of 5 Hz. This update rate was used in order to limit the size of the file. These data were also background-subtracted and collected at the same scan rate and potential limits as the stimulated release data. For studies using COC, the previous procedure for αMPT was followed except that once the DA release peak disappeared, 20μM COC was added to the αMPT solution and we continued to apply the single stimulus pulses every 5 minutes. Stimulus pulses were applied for up to 120 minutes in this case in order to capture the increase and eventual decrease in stimulated release.

Data Analysis. For statistical comparisons, GraphPad Prism (version 4.03) software was used. Data are expressed as a mean +/- SEM. Comparisons were assessed by Student's t-test (unpaired). A probability level of 5% ($p < 0.05$) was considered significant.

Results

Striatal DA Release

It has previously been shown using striatal brain slice preparations that upon single pulse electrical stimulation, 12-week old R6/2 mice release significantly less DA than their age-matched WT controls (Johnson et al., 2006). To investigate the impact of the HD mutation on DA reserve pool mobilization, slices from 12-week old R6/2 and WT mice were subjected to 120-pulse stimulations at 20, 30, 40, 50, and 60 Hz, and FSCV at carbon fiber microelectrodes was used to measure DA release (Fig. 1A). Cyclic voltammograms obtained at the highest point

of stimulated release ($[DA]_{stim}$) confirm that the analyte detected is dopamine. Although the DA release in WT slices appears to increase as frequency is increased, there was no statistically significant difference between stimulation frequencies (Fig. 1B; t-test, $p > 0.05$). Conversely, at 50 and 60 Hz stimulation frequencies, $[DA]_{stim}$ was significantly less in R6/2 slices than in WT slices ($p < 0.05$ at both frequencies). The average values for $[DA]_{stim}$ at 50 Hz were 1.20 ± 0.33 µM (R6/2; n = 5 mice) and 2.71 ± 0.47 µM (WT; n = 6 mice). At 60 Hz, the values were 1.31± 0.32 µM (R6/2; n = 5 mice) and 3.34 ± 0.76 µM (WT; n = 6 mice).

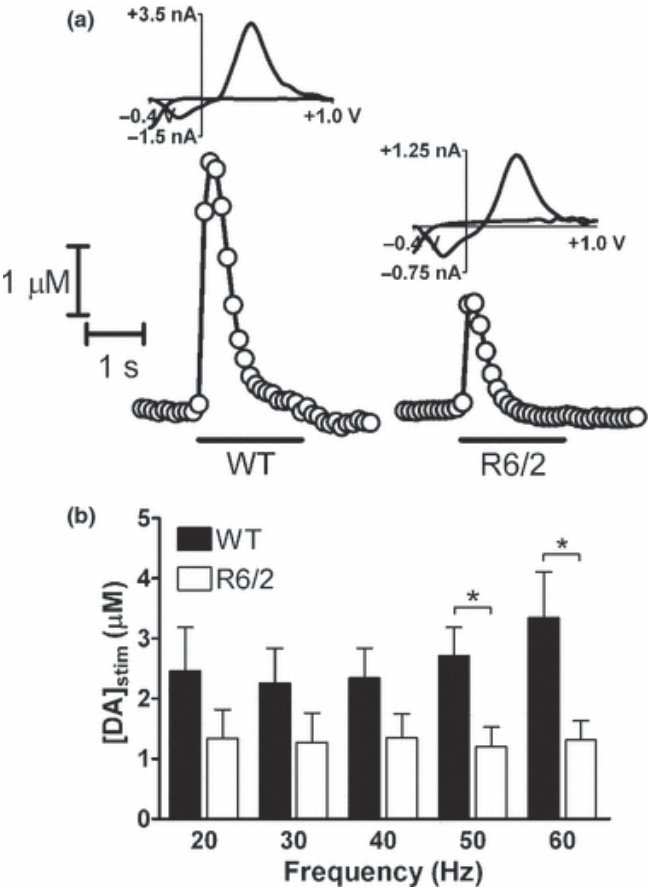

Figure 1. Striatal DA release, evoked by the application of 120-pulse stimulus pulse trains, is impaired in R6/2 brain slices compared with WT brain slices. (a) Representative plots and cyclic voltammograms obtained by FSCV at carbon-fiber microelectrodes for R6/2 and WT mice are shown. The representative plots where taken using a 60 Hz stimulation frequency. The duration of the stimulation is represented by the bar under each plot. The cyclic voltammograms confirm the presence of DA. (b) DA release was evoked by 20, 30, 40, 50, and 60 Hz 120-pulse stimulus trains. $[DA]_{stim}$ was significantly greater in WT brain slices compared with R6/2 brain slices when evoked using 50 and 60 Hz stimulus frequencies (*$p < 0.05$ at 50 and 60 Hz; $n = 5$ R6/2 mice and six WT mice). Although striatal DA release appears to increase with increasing frequency in WT slices, differences in release between application frequencies are not significant within either genotype (one-way anova).

Intracellular DA Levels

Next, we sought to determine the relative amounts of DA found in pharmacologically distinct pools. Amphetamine- induced DA efflux in brain slices of 6-week and 12-week R6/2 and WT mice was compared. Each slice was continuously treated with 10 µM TBZ, which blocks the loading of DA into vesicles by inhibiting VMAT (Kung *et al.* 1994). RRP dopamine was then depleted by applying single-pulse stimulations every five minutes until the stimulated release peak disappeared. At this point, the only dopamine remaining in the terminals is reserve pool and free cytosolic DA. Slices were then exposed to 20 µM AMPH, a competitive dopamine transporter (DAT) inhibitor that causes DA efflux from vesicles inside the presynaptic terminal. AMPH enters the presynaptic terminal either by lipophilic diffusion through the membrane or by passage through the DAT. AMPH that enters through the DAT causes allosteric translocation of the transporter and thereby induces reverse transport of DA from the cytoplasm (Liang & Rutledge 1982{Fischer, 1979 #698, Fischer & Cho 1979). AMPH also displaces vesicular DA into the cytoplasm where it can then be released by reverse transport (Chiueh & Moore 1975, Jones *et al.* 1998). The efflux of DA was measured over the course of 25 minutes. The amplitude of the peak ($[DA]_{AMPH}$) was used to determine the amount of DA released (Fig. 2A). In six-week old R6/2 and WT mice there was not a significant difference in the amount of AMPH induced efflux of DA (R6/2, 11.49 ± 2.36 µM, n= 6 mice; WT, 12.41 ± 2.26 µM, n = 7 mice). However, by 12 weeks of age, the R6/2 mice showed a significant decrease in AMPH-induced DA efflux after TBZ treatment (Fig. 2B; $p = 0.023$; R6/2, 5.41 ± 1.10 µM, n= 7 mice; WT, 10.44 ± 1.65 µM, n= 8 mice).

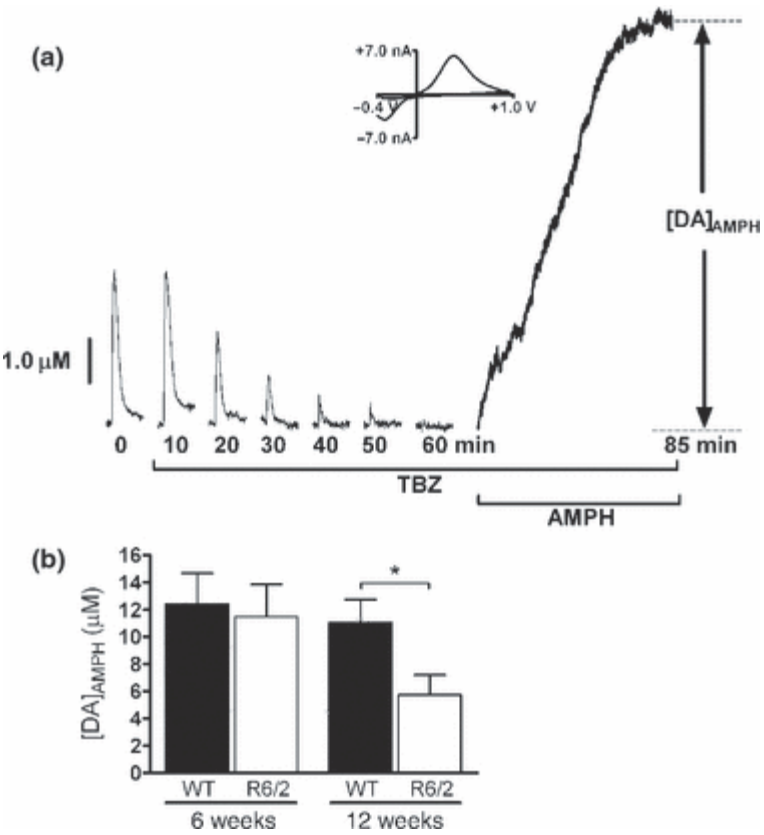

Figure 2. AMPH-induced DA efflux after TBZ treatment is impaired in 12-week-old R6/2 mice compared with WT mice. (a) Representative data from a 6-week-old WT mouse. The brain slice was exposed to 20 μM TBZ while applying single, 4 ms duration stimulus pulses (one pulse every 5 min) until DA release disappeared. The slice was then exposed to 20 μM AMPH for 25 min, and $[DA]_{AMPH}$ was measured. A CV is provided at peak release and confirms the presence of DA. Stimulated release plots were collected every 5 min, but are shown every 10 min for clarity. (b) In 12-week-old R6/2 mice, $[DA]_{AMPH}$ is significantly less than in WT mice (*$p < 0.05$; $n = 7$ R6/2 mice and 8 WT mice), but at 6-weeks of age there is not a significant difference between the two sets of mice ($p > 0.05$; $n = 6$ R6/2 and seven WT mice).

To measure reserve pool DA more selectively, a separate set of experiments were conducted in which slices were exposed to 50 µM αMPT rather than TBZ. The application of αMPT inhibits tyrosine hydroxylase, the rate limiting enzyme in DA synthesis. A stimulus pulse was applied every 5 minutes until the DA peak disappeared, and then AMPH was added to the aCSF perfusion solution at a final concentration of 20 µM. The peak amplitude of the efflux, $[DA]_{AMPH}$ in the presence of aMPT, was measured to quantify the amount of DA stored in reserve pool vesicles (Fig. 3). At 6 weeks of age, there was not a significant difference between R6/2 and WT mice (R6/2, 8.17 ± 1.96 µM, n= 5 mice; WT, 5.39 ± 0.88 µM, n= 3 mice). Conversely, $[DA]_{AMPH}$ was diminished in slices from 12-week old R6/2 mice compared to age-matched WT controls ($p < 0.05$; R6/2, 4.02 ± 0.74 µM, n= 5 mice; WT, 7.75 ± 1.48 µM, n= 4 mice).

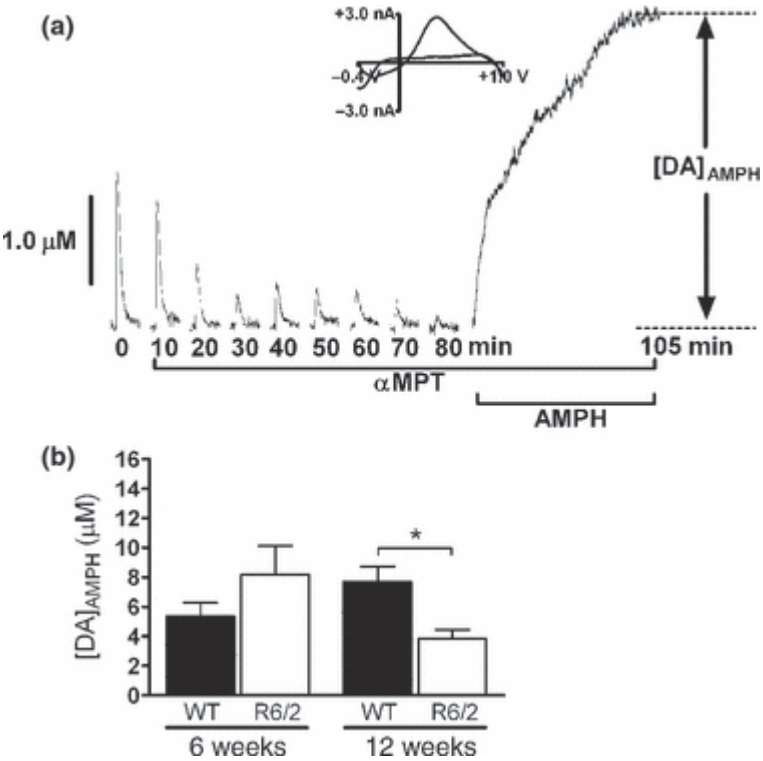

Figure 3. AMPH-induced DA efflux after αMPT treatment is diminished in older R6/2 mice. (a) Representative data from a 6-week old WT mouse. Slices were treated with 50 μM αMPT until the stimulated DA release peak disappeared. The slice was then exposed to 20 μM AMPH for 25 min and $[DA]_{AMPH}$ was measured. The last 20 min of AMPH treatment are shown in this particular plot. A CV is provided at peak release and confirms the presence of DA. Stimulated release plots collected every 10 min are shown for clarity. (b) AMPH-induced DA efflux was not significantly different between 6-week-old R6/2 and WT brain slices ($p > 0.05$; $n = 5$ R6/2 and three WT mice). $[DA]_{AMPH}$ was significantly decreased in slices from 12-week-old R6/2 mice compared with those from age-matched WT control mice (*$p < 0.05$; $n = 5$ R6/2 mice and 4 WT mice).

Mobilization of Reserve Pool DA

To determine if reserve pool DA is mobilized differently in older R6/2 mice compared to respective WT control mice, we used a combination of αMPT and COC, which has also been shown to mobilize DA reserve pools (Venton et al., 2006). DA release, evoked by the application of single stimulus pulses, was measured by FSCV in striatal brain slices. The stimulus pulses were applied prior to and throughout the pharmacological treatment of each slice. Slices from 12-week old R6/2 and WT mice were treated with 50 μM αMPT. Once the stimulated DA release peak disappeared, slices were treated with 20 μM COC in addition to the αMPT. The WT slices released DA for a longer period of time (90 min) after the addition of COC in comparison to R6/2 slices (30 min; Fig. 4A). The maximum COC-induced DA release was not significantly different between the R6/2 and WT mice (Fig. 4B). Area under the curve calculations suggest that the R6/2 slices released less vesicles of DA (41.6% of WT).

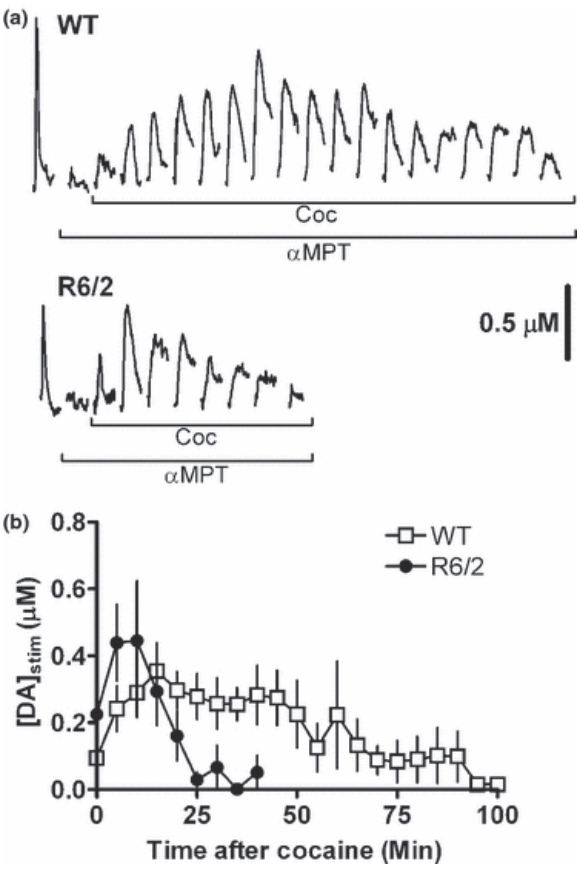

Figure 4. Reserve pool vesicles are depleted in 12-week-old R6/2 mice. Slices were treated with 50 μM αMPT while applying a 4 ms duration single-pulse electrical stimulus every 5 min. Once the stimulated DA release peak disappeared, 20 μM COC was added to the brain slice and the application of stimulus pulses continued. Stimulated DA release was measured by FSCV. (a) Representative data from R6/2 and WT slices. Reserve pool mobilization by COC resulted in measurable stimulated DA release. Stimulated release plots collected immediately after the addition of αMPT and the disappearance of the DA release peak have been omitted in this figure for clarity. (b) Pooled data from R6/2 and WT mice. Each data point represents the average value (± SEM) of $[DA]_{stim}$ obtained from five R6/2 mice and 6 WT mice. The maximum peak amplitudes obtained in R6/2 and WT slices were not significantly different.

Discussion

In this study, differences in DA reserve pool storage and mobilization in striatal brain slices from R6/2 and WT mice were examined. In R6/2 slices, electrically-induced release of dopamine was non-responsive to increasing stimulation frequencies. In contrast, release from WT slices was significantly greater than that in R6/2 slices at the higher stimulation frequencies. Moreover, AMPH-induced DA efflux was diminished in slices from R6/2 mice at 12 weeks of age, but not at 6 weeks of age. However, when efflux currents are normalized against stimulated release currents, the data are consistent with an enhancement of cytosolic DA in the striata of 12-week old R6/2 mice. Importantly, our data also suggest that after mobilization of the reserve pool DA, DA was released from fewer vesicles in slices from 12-week old R6/2 mice compared to slices from age-matched WT control mice; thus, fewer reserve pool vesicles are present in the R6/2 striatum.

Previous studies using R6/2 mice have shown that DA release, evoked using a single pulse stimulation, is impaired in brain slices from 12-week old R6/2 mice (Johnson et al., 2006). This single pulse application causes DA to be released from the RRP which makes up only 1 to 2% of vesicles in presynaptic terminals (Rizzoli and Betz, 2005). Similarly, electrically evoked release of DA using the 120-pulse stimulation regimen was diminished in R6/2 slices at the higher stimulation frequencies (50 and 60Hz) but not at the lower frequencies (20, 30, and 40 HZ). Even though peak dopamine levels were observed after the application of about 18 pulses at 60 Hz and 15 pulses at 50 Hz, a full 120 pulse regimen was applied in an attempt to reveal genotype-related differences. A difference in [DA] between R6/2 and WT at the end of this pulse regimen could potentially suggest a difference in the ability to sustain dopamine release during periods of excessive stimulation. However, there was not a significant difference

between the R6/2 and WT mice. Given that the reserve pool makes up 80 to 90% of vesicular DA stores (Neves and Lagnado, 1999; Rizzoli and Betz, 2005), it seems likely that, if these stores were mobilized, they would overwhelm and mask the release of RRP DA. Indeed, the average magnitude of DA release, evoked by the application of a 120-pulse train, was on the order of 3 to 4 μM from WT slices compared to about 1.5 μM evoked by application of a single stimulus pulse (Johnson et al., 2006). Thus, it is possible that the difference in DA release between the R6/2 and WT mice at high stimulation frequencies is driven by the mobilization of stored pool vesicles. According to the standard three pool model, the vesicles in the RRP are released first upon mild stimulation in which the axon terminal is depolarized by an action potential (Wu and Borst, 1999). As the RRP becomes depleted, the recycle pool vesicles mobilize (Harata et al., 2001; de Lange et al., 2003; Kuromi and Kidokoro, 2003; Richards et al., 2003). Upon frequent or more intense stimulation, the reserve pool vesicles mobilize (Richards et al., 2000; Richards et al., 2003; Heien and Wightman, 2006). It has been shown that, in anesthetized rats, reserve pool DA can be mobilized by stimulating the medial forebrain bundle at 5-second intervals using a stimulating frequency of 30 Hz (Yavich and MacDonald, 2000).

Phasic DA neuron firing is important for the expression of behavior (Heien and Wightman, 2006). However, it is also important to note that input from cortical glutamate afferents may exert control over behavior by driving striatal medium spiny neuron firing (Lape and Dani, 2004) and influencing DA release (Kulagina et al., 2001; Avshalumov et al., 2003). Tonic DA levels have been proposed to restrain the excitatory effects of glutamate input by acting primarily on dopaminergic D1 receptors (Kiyatkin and Rebec, 1999). The lower stimulation frequencies (20 or 30 Hz) are associated more with tonic DA levels in the striatum (Hyland et al., 2002; Heien and Wightman, 2006); therefore, because DA release was not

significantly different between R6/2 and WT at these frequencies, it appears unlikely that differences in tonic dopamine levels play a major role in the propagation of abnormal behaviors in these mice. Conversely, phasic bursts of DA may be associated with upper stimulation frequencies (50 and 60 Hz); therefore, it is possible that 12-week old R6/2 mice lack the ability to provide the needed phasic dopaminergic input required for normal motor control, thereby contributing to the abnormal behavioral phenotype.

The DA reserve pools were examined using various pharmacological agents. Treating the brain slices with TBZ coupled with electrical stimulation will deplete the releasable vesicles. Upon the addition of AMPH intracellular and vesicular DA will exit the terminals by reverse transport through the DAT into the extracellular space (Sulzer et al., 1995; Floor and Meng, 1996; Jones et al., 1998; Schwartz et al., 2005; Watanabe et al., 2005). The diminished DA efflux in 12-week old R6/2 mice indicates that DA, not released by stimulation with a single electrical pulse, becomes progressively depleted between 6 and 12 weeks of age. This DA is made up of reserve pool DA and free cytosolic DA. Similar results were obtained when reserve pool DA was selectively isolated by treatment of slices with αMPT, which, when combined with electrical stimulation, depletes releasable DA stores and free cytosolic DA. R6/2 mice typically develop the overt motor phenotype at 9 to 11 weeks of age; thus, the timescale of reserve pool depletion is consistent with the occurrence of motor symptoms.

A goal of this work was also to determine if cytosolic DA levels differ between R6/2 and WT mice. Presumably, the relative levels of cytosolic DA can be obtained by subtraction of $[DA]_{AMPH}$ obtained from αMPT-treated slices, from $[DA]_{AMPH}$ obtained from TBZ-treated slices. However, because the errors associated with this operation are additive, the calculated differences were not significant between R6/2 and WT. For this reason, we normalized efflux

current values against respective pre-drug stimulated release current values individually for each curve, which eliminated potential errors associated with electrode calibration and also corrected DA efflux for differences in stimulated DA release. No significant differences in normalized efflux current were present following treatment of slices from 6-week old mice with either TBZ or αMPT; however, the average normalized efflux current in αMPT-treated slices from 12-week old R6/2 mice was diminished compared to WT, while no difference was noted following TBZ pre-treatment. When combined with the application of single stimulus pulses, spaced 5 minutes apart, TBZ pre-treatment should result in the depletion of all DA except what is present in the cytosol and the DA reserve pool, while αMPT pre-treatment should result in the removal of all cytoplasmic DA except for that in the reserve pool. Therefore, our interpretation is that, at 12 weeks of age, an enhanced level of cytosolic DA is present in the R6/2 striatum compared to WT controls. This interpretation would be consistent with previous findings that vesicle loading by the vesicular monoamine transporter (VMAT) is impaired in adrenal chromaffin cells from R6/2 mice (Johnson et al., 2007), a phenomenon that may very well apply to vesicle loading in the striatum. This enhanced level of DA may also result in further intracellular damage, given the chemically reactive nature of DA.

More commonly known as a dopamine uptake inhibitor, COC has a similar affinity for DAT in R6/2 mice as compared to WT mice (Johnson et al, 2006). Thus, the differences seen after treating R6/2 and WT slices with COC following pre-treatment with αMPT most likely arise from differences in reserve pools release, not differences in uptake. Because the peak DA levels evoked by single pulse electrical stimulation are the same in R6/2 and WT control slices under these conditions, it is likely that R6/2 mice can mobilize reserve pool vesicles normally, and that the vesicles contain the same number of DA molecules. These results also imply that

there are similar densities of DA-releasing presynaptic terminals in the R6/2 and WT striata. However, the DA release lasted roughly three times as long in slices from WT mice compared to slices from R6/2 mice, suggesting that R6/2 mice suffer from a depletion of the number of DA reserve pool vesicles (approximately 41.6% of WT, according to area under the curve calculations). Although the normal intracellular functions of the endogenous Htt protein are not fully understood, recent studies have shown that the expanded CAG repeat, along with promoting the formation of aggregates in neurons of both HD model mice and people who have HD (Cooper et al., 1998; Hazeki et al., 1999; Meade et al., 2002), can also cause impairments in vesicular transport (Edwardson et al., 2003; Morton et al., 2001; Li et al., 2003). It is therefore possible that the R6/2 mice have fewer reserve pool vesicles because they are unable to transport vesicles or maintain vesicles in the reserve pool as well as WT mice.

Collectively, our data suggest that a progressive loss of DA reserve pool vesicles may contribute to the progressive behavioral phenotype of R6/2 mice. Moreover, our data are consistent with the concept that vesicle loading is impaired, resulting in enhanced intracellular DA levels. These findings may help guide the development of therapeutic interventions to treat chorea and other motor syndromes associated with HD. Additionally, future research efforts may be aimed at resolving the cellular mechanisms that are responsible for the depletion of the DA reserve pool.

B. References

Abercrombie, E. D. and Russo, M. L. (2002) *Neurochemistry in the R6/2 Transgenic Mouse Model of Huntington's Disease*. In: *Program Number 195.12. in Society for Neuroscience. 2002. Orlando, FL.*

Avshalumov, M. V., Chen, B. T., Marshall, S. P., Pena, D. M. and Rice, M. E. (2003) Glutamate-dependent inhibition of dopamine release in striatum is mediated by a new diffusible messenger, H2O2. *J Neurosci,* **23,** 2744-2750.

Bates, G. P., Harper, P. S. and Jones, L. (2002) *Huntington's Disease*. Oxford University Press, Oxford.

Cooper, J. K., Schilling, G., Peters, M. F. et al. (1998) Truncated N-terminal fragments of huntingtin with expanded glutamine repeats form nuclear and cytoplasmic aggregates in cell culture. *Hum Mol Genet,* **7,** 783-790.

Carter, R. J., Lione, L. A., Humby, T., Mangiarini, L., Mahal, A., Bates, G. P., Dunnett, S. B. and Morton, A. J. (1999) Characterization of progressive motor deficits in mice transgenic for the human Huntington's disease mutation. *J Neurosci,* **19,** 3248-3257.

Chiueh, C. C. and Moore, K. E. (1975) D-amphetamine-induced release of "newly synthesized" and "stored" dopamine from the caudate nucleus in vivo. *J Pharmacol Exp Ther,* **192,** 642-653.

de Lange, R. P., de Roos, A. D. and Borst, J. G. (2003) Two modes of vesicle recycling in the rat calyx of Held. *J Neurosci,* **23,** 10164-10173.

Edwardson J.M., Wang C.T., Gong B. et al. (2003) Expression of mutant huntingtin blocks exocytosis in PC12 cells by depletion of complexin II. *J Biol Chem,* **278**, 30849-30853.

Fischer, J. F. and Cho, A. K. (1979) Chemical release of dopamine from striatal homogenates: evidence for an exchange diffusion model. *J Pharmacol Exp Ther,* **208**, 203-209.

Floor, E. and Meng, L. (1996) Amphetamine releases dopamine from synaptic vesicles by dual mechanisms. *Neurosci Lett,* **215,** 53-56.

Harata, N., Ryan, T. A., Smith, S. J., Buchanan, J. and Tsien, R. W. (2001) Visualizing recycling synaptic vesicles in hippocampal neurons by FM 1-43 photoconversion. *Proc Natl Acad Sci U S A,* **98,** 12748-12753.

Hazeki, N., Nakamura, K., Goto, J. and Kanazawa, I. (1999) Rapid aggregate formation of the huntingtin N-terminal fragment carrying an expanded polyglutamine tract. *Biochem Biophys Res Commun,* **256,** 361-366.

Heien, M. L. and Wightman, R. M. (2006) Phasic dopamine signaling during behavior, reward, and disease states. *CNS Neurol Disord Drug Targets,* **5,** 99-108.

Hickey, M. A., Reynolds, G. P. and Morton, A. J. (2002) The role of dopamine in motor symptoms in the R6/2 transgenic mouse model of Huntington's disease. *J Neurochem,* **81,** 46-59.

Hyland, B. I., Reynolds, J. N., Hay, J., Perk, C. G. and Miller, R. (2002) Firing modes of midbrain dopamine cells in the freely moving rat. *Neuroscience,* **114,** 475-492.

Johnson, M. A., Rajan, V., Miller, C. E. and Wightman, R. M. (2006) Dopamine release is severely compromised in the R6/2 mouse model of Huntington's disease. *J Neurochem,* **97,** 737-746.

Johnson, M. A., Villanueva, M., Haynes, C. L., Seipel, A. T., Buhler, L. A. and Wightman, R. M. (2007) Catecholamine exocytosis is diminished in R6/2 Huntington's disease model mice. *J Neurochem,* **103,** 2102-2110.

Jones, S. R., Gainetdinov, R. R., Wightman, R. M. and Caron, M. G. (1998) Mechanisms of amphetamine action revealed in mice lacking the dopamine transporter. *J Neurosci,* **18,** 1979-1986.

Kiyatkin, E. A. and Rebec, G. V. (1999) Striatal neuronal activity and responsiveness to dopamine and glutamate after selective blockade of D1 and D2 dopamine receptors in freely moving rats. *J Neurosci,* **19,** 3594-3609.

Kulagina, N.V., Zigmond, M.J., Michael, A.C. (2001) Glutamate Regulates the Spontaneous and Evoked Release of Dopamine in the Rat Striatum. *Neuroscience*,**102**,121-128.

Kung, M. P., Canney, D. J., Frederick, D., Zhuang, Z., Billings, J. J. and Kung, H. F. (1994) Binding of 125I-iodovinyltetrabenazine to CNS vesicular monoamine transport sites. *Synapse,* **18,** 225-232.

Kraft, J. C., Osterhaus, G. L., Ortiz, A. N., Garris, P. A. and Johnson, M. A. (2009) In vivo dopamine release and uptake impairments in rats treated with 3-nitropropionic acid. *Neuroscience,* **161,** 940-949.

Kuromi, H. and Kidokoro, Y. (2003) Two synaptic vesicle pools, vesicle recruitment and replenishment of pools at the Drosophila neuromuscular junction. *J Neurocytol,* **32,** 551-565.

Lape, R. and Dani, J. A. (2004) Complex response to afferent excitatory bursts by nucleus accumbens medium spiny projection neurons. *J Neurophysiol,* **92,** 1276-1284.

Li, H., Wyman, T., Yu, Z. X., Li, S. H. and Li, X. J. (2003) Abnormal association of mutant huntingtin with synaptic vesicles inhibits glutamate release. *Hum Mol Genet,* **12,** 2021-2030.

Liang, N. Y. and Rutledge, C. O. (1982) Evidence for carrier-mediated efflux of dopamine from corpus striatum. *Biochem Pharmacol,* **31,** 2479-2484.

Meade, C. A., Deng, Y. P., Fusco, F. R., Del Mar, N., Hersch, S., Goldowitz, D. and Reiner, A. (2002) Cellular localization and development of neuronal intranuclear inclusions in

striatal and cortical neurons in R6/2 transgenic mice. *The Journal of comparative neurology,* **449,** 241-269.

Morton, A. J., Faull, R. L. and Edwardson, J. M. (2001) Abnormalities in the synaptic vesicle fusion machinery in Huntington's disease. *Brain Res Bull,* **56,** 111-117.

Neves, G. and Lagnado, L. (1999) The kinetics of exocytosis and endocytosis in the synaptic terminal of goldfish retinal bipolar cells. *The Journal of physiology,* **515 (Pt 1),** 181-202.

Petersén, A., Puschban, Z., Lotharius, J., NicNiocaill, B., Wiekop, P., O'Connor, W. T. and Brundin, P. (2002) Evidence for dysfunction of the nigrostriatal pathway in the R6/1 line of transgenic Huntington's disease mice. *Neurobiol Dis,* **11,** 134-146.

Richards, D. A., Guatimosim, C. and Betz, W. J. (2000) Two endocytic recycling routes selectively fill two vesicle pools in frog motor nerve terminals. *Neuron,* **27,** 551-559.

Richards, D. A., Guatimosim, C., Rizzoli, S. O. and Betz, W. J. (2003) Synaptic vesicle pools at the frog neuromuscular junction. *Neuron,* **39,** 529-541.

Rizzoli, S. O. and Betz, W. J. (2005) Synaptic vesicle pools. *Nat Rev Neurosci,* **6,** 57-69.

Schwartz, K., Weizman, A. and Rehavi, M. (2005) The effect of psychostimulants on [(3)H]dopamine uptake and release in rat brain synaptic vesicles. *J Neural Transm.*

Sulzer, D., Chen, T. K., Lau, Y. Y., Kristensen, H., Rayport, S. and Ewing, A. (1995) Amphetamine redistributes dopamine from synaptic vesicles to the cytosol and promotes reverse transport. *J Neurosci,* **15,** 4102-4108.

Venton, B. J., Seipel, A. T., Phillips, P. E., Wetsel, W. C., Gitler, D., Greengard, P., Augustine, G. J. and Wightman, R. M. (2006) Cocaine increases dopamine release by mobilization of a synapsin-dependent reserve pool. *J Neurosci,* **26,** 3206-3209.

Watanabe, S., Aono, Y., Fusa, K., Takada, K., Saigusa, T., Koshikawa, N. and Cools, A. R. (2005) Contribution of vesicular and cytosolic dopamine to the increased striatal dopamine efflux elicited by intrastriatal injection of dexamphetamine. *Neuroscience,* **136,** 251-257.

Wu, L. G. and Borst, J. G. (1999) The reduced release probability of releasable vesicles during recovery from short-term synaptic depression. *Neuron,* **23,** 821-832.

Yavich, L. and MacDonald, E. (2000) Dopamine release from pharmacologically distinct storage pools in rat striatum following stimulation at frequency of neuronal bursting. *Brain Res,* **870,** 73-79.

Zucker, R. S. and Regehr, W. G. (2002) Short-term synaptic plasticity. *Annu Rev Physiol,* **64,** 355-405.

Chapter 4: MsrA

The study of oxidative stress and how it affects the DA system including the reserve pool veiscles and the D2 autoreceptors was conducted. The results are published in the following two papers.

A. Quantification of Reserve Pool DA in MsrA Null Mice

Methionine sulfoxide reductase A knockout (*MsrA*$^{-/-}$) mice, which serve as a potential model for neurodegeneration, suffer from increased oxidative stress and have previously been found to have chronically elevated brain dopamine content levels relative to control mice. Additionally, these high levels parallel increased presynaptic dopamine release. In this work, fast-scan cyclic voltammetry at carbon-fiber microelectrodes was used to quantify striatal reserve pool dopamine in knockout mice and wild-type control mice. Reserve pool dopamine efflux, induced by amphetamine, was measured in brain slices from knockout and wild type mice in the presence of α-methyl-p-tyrosine, a dopamine synthesis inhibitor. Additionally, the stimulated release of reserve pool dopamine, mobilized by cocaine, was measured. Both efflux and stimulated release measurements were enhanced in slices from knockout mice, suggesting that these mice have greater reserve pool dopamine stores than wild-type and that these stores are effectively mobilized. Moreover, dopamine transporter labeling data indicate that the difference in measured dopamine efflux was likely not caused by altered dopamine transporter protein expression. Additionally, slices from MsrA$^{-/-}$ and wild-type mice were equally responsive to increasing extracellular calcium concentrations, suggesting that potential differences in either calcium entry or intracellular calcium handling are not responsible for increased reserve pool dopamine release. Collectively, these results demonstrate that *MsrA*$^{-/-}$ knockout mice maintain a larger dopamine reserve pool than wild-type control mice, and that this pool is readily mobilized.

Introduction

The abnormal regulation of dopamine (DA) has been associated with multiple neurodegenerative disease states (Bird and Iversen, 1974, Morgan et al., 1987), yet the role of DA reserve pool storage and mobilization in the pathophysiology of these conditions is now just being revealed. Many of these conditions, such as Parkinson's disease, Huntington's disease, and Lou Gehrig's disease, have been associated with the increased production or reactive oxygen species, thereby enhancing the degree of cell oxidative stress in the brain (Patten et al., 2010, Cohen, 1983, Perez-Severiano et al., 2004).

Interestingly, elevated DA levels have also been associated with enhanced oxidative stress (Oien et al., 2008b). Indeed, one model of oxidative stress, methionine sulfoxide reductase A knockout (*MsrA*$^{-/-}$) mice, have been reported to have chronically high brain DA levels (Oien et al., 2008b). These mice lack the antioxidant enzyme MsrA, which is part of the Msr system. Methionine sulfoxide posttranslational modifications can be reversed by the Msr system, which consists of MsrA (reduces *S* methionine sulfoxide enantiomer) and MsrB (reduces *R* methionine sulfoxide enantiomer) (Moskovitz, 2005). The *MsrA*$^{-/-}$ mouse is hypersensitive to oxidative stress, accumulates higher levels of carbonylated protein, and expresses brain pathologies associated with neurodegenerative diseases (Moskovitz et al., 2001, Pal et al., 2007). Recent studies have shown that these mice have abnormally high DA levels in the brain at the ages of 6 and 12 months, compared to wild type (WT) control mice. Additionally, these high levels parallel an increased presynaptic DA release when stimulated *in vitro* without drug treatments.

A possible mechanism for an increase in stimulated DA release in *MsrA*$^{-\backslash-}$ mice involves the mobilization of reserve pool DA. In general, DA-containing vesicles are believed to be

separated into three pools: the readily releasable pool (RRP), the recycling pool, and the reserve pool (Neves and Lagnado, 1999, Rizzoli and Betz, 2005). The RRP undergoes exocytosis upon mild stimulation and is replenished by the mobilization of the recycling pool vesicles. The reserve pool, mobilized upon prolonged periods of synaptic activity (Neves and Lagnado, 1999), is the largest pool consisting of 80-90% of the total vesicles (Rizzoli and Betz, 2005). Pharmacological manipulations, using a combination of alpha-methyl-p-tyrosine (aMPT) and either cocaine (COC) or amphetamine (AMPH) (Venton et al., 2006, Ortiz et al., 2010), have been used to quantitatively measure reserve pool dopamine.

Other factors, such as calcium transport, may also influence the amplitude of stimulated dopamine release plots. Transient increases in intracellular calcium concentration trigger vesicular exocytosis (Nachshen and Sanchez-Armass, 1987, Kume-Kick and Rice, 1998) as well as the movement of RRP and reserve pool vesicles (Rose et al., 2002). Moreover, the increase in oxidative stress may result in calcium dysregulation. For example, the activity of calmodulin, a calcium regulatory protein that activates the plasma membrane calcium ATPase (PMCA), diminishes due to oxidative post-translational modifications as tissues age (Michaelis et al., 1996). The oxidation of specific methionines in calmodulin results in about a 50% reduction of PMCA activation (Bartlett et al., 2003), thereby impairing the ability of cells to clear calcium from the cell (Palacios et al., 2004). Oxidized calmodulin can accumulate in brain tissues as a result of low antioxidant levels and it is speculated that oxidation of methionines on calmodulin may be acting as a molecular switch in calcium regulation, oxidative stress, and DA release (Chen et al., 2001, Bigelow and Squier, 2005).

To investigate possible mechanisms underlying elevated DA content and release found in $MsrA^{-/-}$ mice, fast-scan cyclic voltammetry (FSCV) at carbon-fiber microelectrodes was used to

measure the mobilization and efflux of reserve pool DA in striatal brain slices from *MsrA*$^{-/-}$ mice and WT control mice (Oien et al., 2008b). We hypothesized that the DA reserve pool is enhanced in MsrA$^{-/-}$ mice compared to WT control mice. In order to measure reserve pool DA, slices were pre-treated with αMPT and then treated with either AMPH, to measure the efflux of reserve pool DA, or with COC, to measure the stimulated release of mobilized DA reserve pool vesicles. Collectively, our results suggest that reserve pool DA is more abundant in the *MsrA*$^{-/-}$ striatum and that the number of vesicles is greater compared to WT controls.

Experimental Procedures

Animals. The *MsrA*$^{-/-}$ and WT control mice have been described previously (Moskovitz et al., 2001). All mice used in these experiments were fed *ad libitum*, housed with 12 h of light per day, and caged individually. All procedures and conditions of live mice, including euthanasia, were approved by the University of Kansas Institutional Animal Care and Use Committee. Every effort was made to minimize the number of animals used and animal suffering.

Brain Slice Preparation. Brain slices of 12-month-old *MsrA*$^{-/-}$ mice and age-matched WT mice were prepared as previously described (Johnson et al., 2006). Mice were anesthetized by isoflurane inhalation and then decapitated. The brain was immediately removed and placed in ice cold artificial cerebrospinal fluid (aCSF) consisting of (mM): NaCl 126, KCl 2.5, NaH_2PO_4 1.2, $CaCl_2$ 2.4, $MgCl_2$ 1.2, $NaHCO_3$ 25, HEPES 20, and D-Glucose 11. The pH of the aCSF was adjusted to 7.4. The cerebellum was removed from the brain using a razor blade and the brain was then mounted on an aluminum block. A vibratome slicer (Leica, Wetzlar, Germany) was used to make 300 µm thick coronal slices. Each brain slice was equilibrated in the superfusion

chamber which was maintained at 34°C, through which aCSF flowed at a continuous rate of 2 mL/min, prior to obtaining measurements.

DA Release in Brain Slices. Carbon-fiber microelectrodes were fabricated using a single 7 μm diameter carbon-fiber (Goodfellow Cambridge Ltd, Huntingdon, U.K.) that was aspirated through a glass capillary tube (1.2 mm outer diameter, 0.68 mm inner diameter, 20 mm long, A-M Systems, Inc. Carlsborg, WA), and was pulled using a heated coil puller (Narishige International USA, Inc., East Meadow, NY) (Kraft et al., 2009). The carbon-fiber was trimmed to about 25 μM and further insulated using with epoxy resin (EPON resin 815C, EPIKURE 3234 curing agent, Miller-Stephenson, Danbury, CT, USA), and then cured at 100°C for 1 h. The electrodes were backfilled with 0.5 M potassium acetate to provide an electrical connection between the carbon fiber and an inserted silver wire.

A triangular waveform was applied to the carbon-fiber electrode starting at -0.4 V, increasing to +1.0 V, and then scanning back down to -0.4 V. For stimulated release measurements, a scan rate of 300 V/s and an update rate of 60 cyclic voltammograms (CVs) per second were used. For measurements of AMPH-induced DA efflux, an update rate of 5 CVs was used to limit the memory space occupied by the file. A headstage amplifier (UNC Chemistry Department Electronics Design Facility, Chapel Hill, NC) was interfaced with a computer via a breakout box and custom software provided by R.M. Wightman and M.L.A.V. Heien (University of North Carolina, Chapel Hill). A Ag/AgCl reference electrode consisted of a chorided silver wire. The carbon fiber microelectrode was inserted 100 μm into the dorsolateral caudate-putamen region of the striatum between the prongs of a bipolar stimulation electrode (Plastics One, Roanoke, VA), which was separated by a distance of 200 μm. A single pulse at 60 Hz was applied to the brain slice and the current was then measured at the peak oxidation potential for DA (about +0.6 V

versus Ag/AgCl reference electrode). Working electrodes were calibrated with DA standards of known concentration in a flow cell before and after each use. The average of pre- and post-calibration measurements was used as the calibration factor. Drugs were introduced into the brain slice superfusion chamber by opening a three-way valve that allowed the desired solution to flow by gravity feed.

For AMPH-induced DA efflux experiments, brain slices were stimulated with single electrical stimulus pulses until the magnitude of evoked DA release was consistent between measurements. Brain slices were then treated with 50 µM aMPT. During this treatment, stimulated DA release was measured every 5 min. Once DA release diminished, 20 µM AMPH was added to the aCSF/aMPT solution and a 25 min duration file was collected.

To measure electrically evoked DA release from mobilized reserve pool vesicles, the same procedure for pre-treatment with aMPT was used. However, slices were treated with 20 µM COC after stimulated release was diminished. During this treatment, electrically-evoked release was measured every 5 minutes.

Sensitivity of DA release to extracellular calcium. To measure changes in the sensitivity to calcium in *MsrA*$^{-/-}$ mice DA release evoked by a single electrical stimulus pulse was first measured in slices with aCSF that contained 2.4 mM calcium. Next, aCSF containing 0 mM calcium was introduced into the superfusion chamber. Once DA release disappeared, brain slices were cumulatively treated with aCSF containing 0.6, 1.2, 1.8, and 2.4 mM calcium. Slices were treated with each concentration for 15 min, with files collected every five 5 min using a single pulse stimulation. Values obtained at the 15 min point were used in Fig. 4.

Immunoblotting. *MsrA*$^{-/-}$ and WT brains were dissected from post-mortem mice. Each striatal lysate was placed in a glass tube and homogenized with Teflon in 50 mM HEPES buffer pH 7.4 plus protease inhibitors (Roche) at 4°C. Homogenized extract was centrifuged for 20 min to separate the membrane fraction. Buffer containing 50 mM HEPES, 0.62% CHAPS, and 150 mM NaCl was added to each membrane fraction and agitated for 30 min. Each fraction was centrifuged for 20 min. Protein concentration of the supernatant was determined by BCA Protein Assay Kit (Pierce). Equal protein amounts (20 µg) of each soluble membrane fraction was loaded into a HEPES 4-20% Protein Gel (Pierce, Pittsburg, PA) and submitted to electrophoresis. Proteins were transferred to a nitrocellulose membrane and blocked overnight in 5% dry milk in buffer. Protein was detected using rabbit anti-DAT antibody (1:1000; Chemicon, Billerica, MA). Primary antibodies were detected by horseradish peroxide-conjugated goat-anti-rabbit secondary antibodies (1:2000; Bio-Rad, Hercules, CA). Protein bands were visualized by chemiluminescent substrate and exposure to autoradiography film. Densitometry analysis was done using ImageJ software (publicly available software obtained from the National Institutes of Health website).

Statistical Analyses. Data were analyzed by ANOVA or students t-test using GraphPad Prism 4.03 (GraphPad Software, Inc., La Jolla, CA). All numerical values are represented as mean ± SEM. A *p* value of 0.05 or less was considered significant.

Results

Reserve Pool DA Levels

It has been previously demonstrated that in *MsrA*$^{-/-}$ mice stimulated DA release, evoked by a single-pulse electrical stimulation, is significantly higher than that of WT controls (Oien et al., 2008b). To determine if reserve pool DA is similarly more abundant in *MsrA*$^{-/-}$ mice, striatal brain slices were subjected to treatment with aMPT and AMPH-induced efflux was measured. Each slice was treated with 50 µM aMPT to inhibit tyrosine hydroxylase, the rate limiting enzyme in DA synthesis. A stimulus pulse was then applied to the slice every 5 min until DA release was diminished. At this point, DA remaining in terminals consisted only of reserve pool DA. The slices were then treated with 20 µM AMPH, a competitive DAT inhibitor that induces the quantitative efflux of cytosolic and vesicular DA. AMPH enters the pre-synaptic terminals in one of two ways: either by lipophilic diffusion through membranes or by passage through DAT protein molecules (Fischer and Cho, 1979, Liang and Rutledge, 1982). AMPH also displaces vesicular DA into the cytoplasm where it can be released by reverse transport caused when AMPH enters through the DAT causing allosteric translocation of the transporters (Chiueh and Moore, 1975, Jones et al., 1998). The AMPH induced efflux of DA was measured over the course of 25 min and the amplitude of the DA peak ($[DA]_{AMPH}$) was used to determine the amount of DA released (Fig.1a). A CV shown at the peak current on this efflux curve indicates that the species released by AMPH treatment is DA. In *MsrA*$^{-/-}$ mice, AMPH-induced DA efflux was significantly greater than that observed in WT control mice, indicating that the striatal DA reserve pool is enhanced in *MsrA*$^{-/-}$ mice (Fig. 1b; $p = 0.022$; *MsrA*$^{-/-}$, 7.02 ± 1.42 µM, n = 5 mice; WT, 5.63 ± 0.33 µM, n = 4 mice).

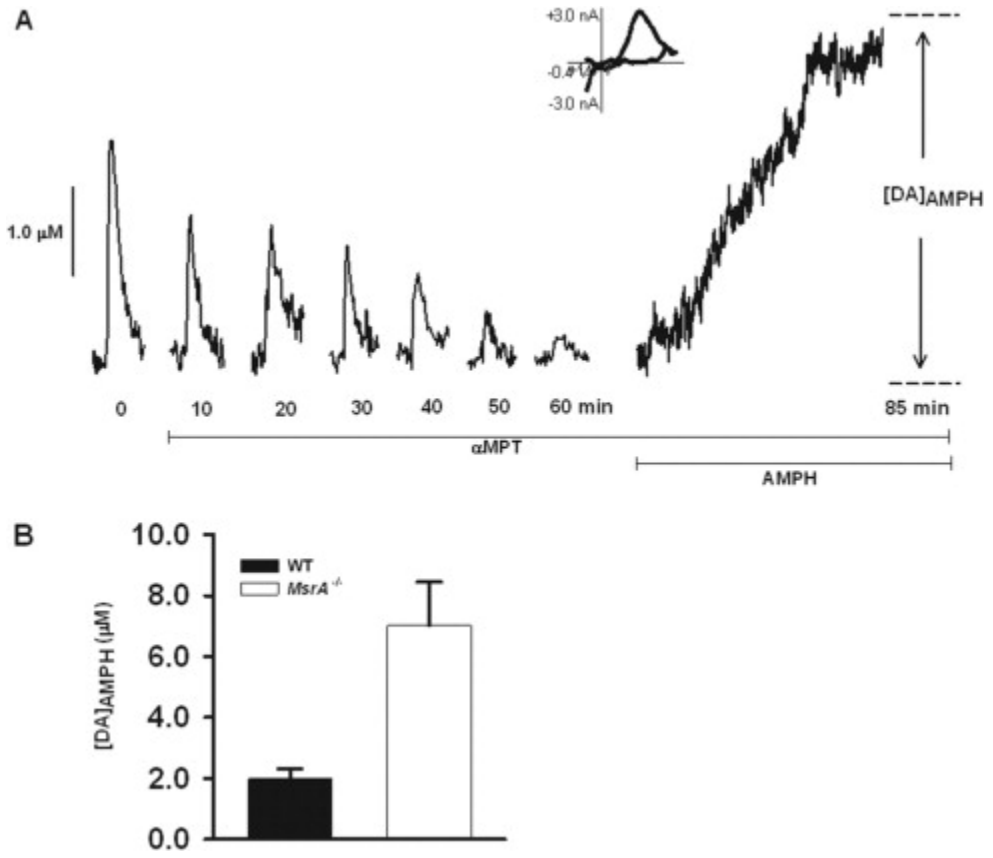

Figure 1. AMPH induced DA efflux is increased in *MsrA*$^{-/-}$ mice compared to WT mice. (A) Representative data in which a brain slice from a WT mouse was treated with 50 µM aMPT while single stimulus pulses were applied every 5 min until DA release was diminished. The slice was then treated with 20 µM AMPH for 25 min, and $[DA]_{AMPH}$ was measured. A CV is provided from the time of peak release, and confirms the release of DA. (B) In *MsrA*$^{-/-}$ mice, $[DA]_{AMPH}$ is significantly higher in MsrA$^{-/-}$ slices than in WT slices ($*p < 0.05$; *MsrA*$^{-/-}$, 7.02 ± 1.42 µM, n = 5 mice; WT, 5.63 ± 0.33 µM, n = 4).

Mobilization of Reserve Pool DA

To identify differences in the exocytotic release of mobilized DA reserve pool vesicles, DA release, electrically evoked in striatal brain slices from MsrA$^{-/-}$ and WT mice control mice, was measured with FSCV (Fig. 2a). Once DA release peak amplitude was the same between separate stimulations in the absence of drug, aMPT was added to the perfusate at a final concentration of 50 μM in order to stop DA synthesis. After DA release was diminished, COC was added to the aMPT/aCSF solution at a final concentration of 20 μM. COC has previously been shown to mobilize reserve pool DA (Venton et al., 2006). DA release was electrically evoked by the application of locally applied single stimulus pulses every 5 min throughout the entire process. The addition of COC caused stimulated DA release to grow in both *MsrA*$^{-/-}$ and WT control slices. Although COC treatment caused DA release to increase to similar levels in *MsrA*$^{-/-}$ and WT control slices, DA release reappeared for a longer amount of time in slices from *MsrA*$^{-/-}$ mice (~180 min) compared to slices from WT mice (~80 min)(Fig. 2b). The area under the curve generated using slices from WT mice was 40% of that generated using slices from MsrA$^{-/-}$ mice.

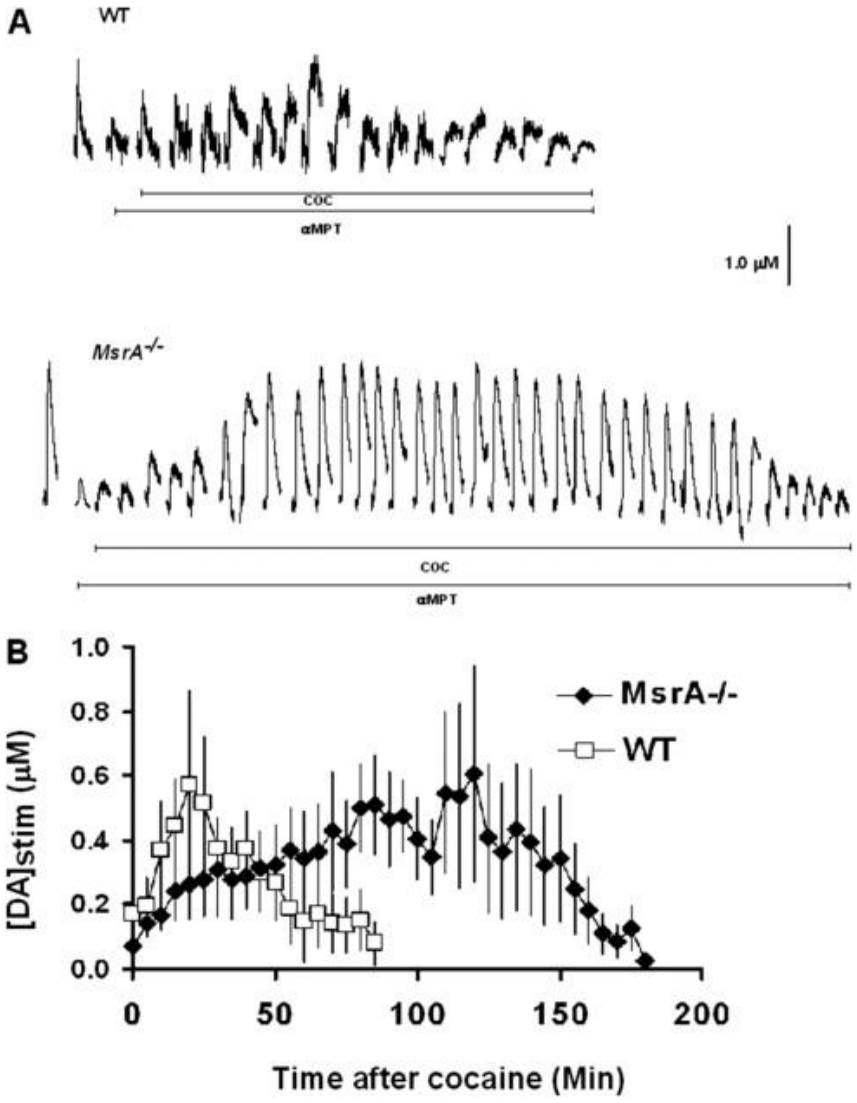

Figure 2. More reserve pool DA is mobilized in slices from *MsrA*$^{-/-}$ mice compared to those from WT mice. Brain slices from *MsrA*$^{-/-}$ and WT mice were exposed to 50 μM aMPT while single stimulus pulses were applied every 5 min. Once DA release disappeared, 20 μM COC was added to the slice. The application of stimulus pulses was continued during this time. (A) Representative data from *MsrA*$^{-/-}$ and WT slices. The addition of COC after pretreatment with aMPT resulted in an increase in stimulated DA release. Stimulated release plots taken immediately after the addition of aMPT have been omitted for clarity. (B) Pooled data from *MsrA*$^{-/-}$ and WT mice after the addition of COC. Each data point represents the average value (± SEM) of $[DA]_{stim}$ obtained from 5 *MsrA*$^{-/-}$ mice and 6 WT mice.

DAT Protein Levels

The DAT is a transmembrane protein that moves DA from the synaptic cleft into the presynaptic neuron. In membrane fractions of *MsrA*$^{-/-}$ and WT mice, no difference in DAT protein levels was detected (Fig. 3; $p = 0.65$; *MsrA*$^{-/-}$, 100.0 ± 19.8 %, n = 3 mice; WT, 115.6 ± 4.1 %, n = 3 mice). These data are consistent with a previous report that showed synaptic DA clearance was similar between *MsrA*$^{-/-}$ and WT mice (Oien et al., 2008).

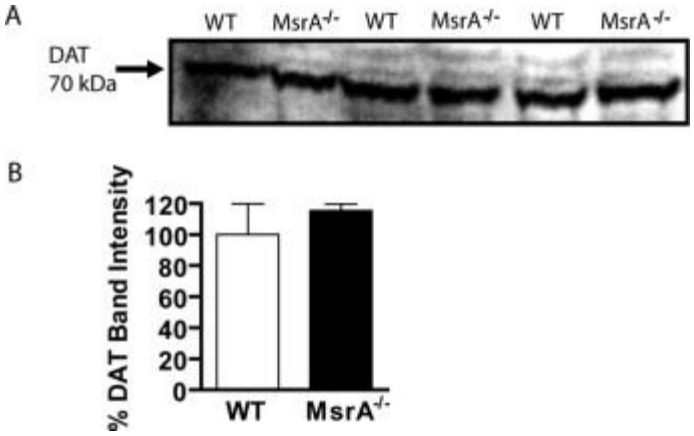

Figure 3. DAT protein levels are unchanged in *MsrA*$^{-/-}$ mice. *MsrA*$^{-/-}$ and WT cerebral membrane fractions were solubilized and equal amounts of protein were separated by gel electrophoresis. (A) Protein bands detected by anti-DAT antibodies indicate similar amounts of the protein at about 70 kDa. (B) Densitometry values of protein bands are shown as an average density from *MsrA*$^{-/-}$ (*black*) and WT (*white*) bands ($p = 0.69$; n = 3 MsrA$^{-/-}$ and 3 WT mice).

Extracellular Calcium Sensitivity

Vesicular DA exocytosis in the striatum is directly dependent on available extracellular calcium, which enters pre-synaptic terminals by voltage-gated calcium channels during membrane depolarization (Heuser and Reese, 1973; Cremona and De Camilli, 1997). In order to evaluate whether the calcium dependency of release was altered in *MsrA*$^{-/-}$ mice, brain slices were treated with various concentrations of extracellular calcium and stimulated DA release was measured (Fig. 4). A two-way ANOVA did not reveal an overall genotype effect on DA release throughout the entire range of extracellular calcium concentrations (Fig. 4; $p = 0.51$; $F_{1,21} = 0.48$; MsrA$^{-/-}$, n = 4 mice; WT, n = 6 mice).

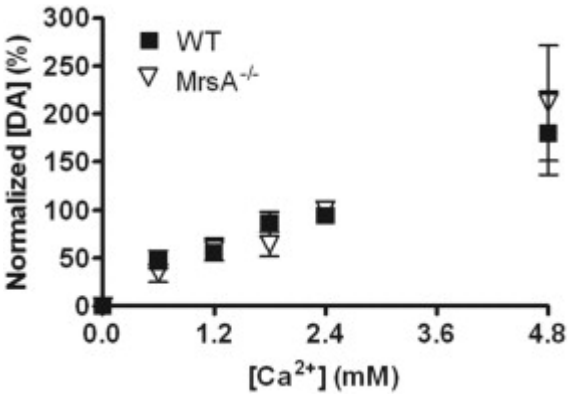

Figure 4. Calcium-dependent release was unchanged in 12-month-old *MsrA*$^{-/-}$ mice compared to age-matched WT mice. Brain slices were treated with 0, 0.6, 1.8, and 2.4 mM concentrations of extracellular calcium and electrically stimulated DA release was measured for 15 min at each concentration. DA release was normalized to maximum DA release within each data set. At 0 mM calcium no DA release was detected. Two-way ANOVA did not reveal an overall genotype effect on DA release throughout the entire range of extracellular calcium concentrations (Fig. 4; $p = 0.51$; $F_{1,21} = 0.48$; MsrA$^{-/-}$, n = 4 mice; WT, n = 6 mice).

Discussion

Previous studies using *MsrA*$^{-/-}$ mice have shown that DA release evoked using a single-pulse stimulation is increased (Oien et al., 2008b). In the present study, differences in DA reserve pool storage and mobilization in striatal brain slices from *MsrA*$^{-/-}$ mice and WT control mice were examined. AMPH-induced DA efflux, following pre-treatment with αMPT, was increased in striatal brain slices from *MsrA*$^{-/-}$ mice compared to those of WT littermates. Moreover, *MsrA*$^{-/-}$ slices showed an enhanced degree of COC-induced mobilization of DA reserve pool vesicles compared to WT. Furthermore, slices from MsrA$^{-/-}$ mice and WT control mice were equally sensitive to changes in extracellular calcium concentration.

Initial experiments were aimed at determining if alterations in either DAT or calcium regulation preferentially enhanced DA release in *MsrA*$^{-/-}$ mice. Our previous work has shown that the efficiency of DA reuptake by DAT is similar in *MsrA*$^{-/-}$ and WT mice (Oien et al., 2008b). Furthermore, here we show that DAT protein levels are similar in *MsrA*$^{-/-}$ and WT mice. This result further supports the concept that DAT function and protein levels are not altered in the absence of *MsrA*. Therefore, we expect that COC and AMPH effects on the DAT would be similar in both mice genotypes.

The exocytotic release of DA during synaptic transmission is mediated by calcium-dependent fusion with the active zone (Heuser and Reese, 1973; Cremona and De Camilli, 1997; Kavalali, 2006). Thus, the ability of extracellular calcium to enter through N- and P/Q-type voltage-gated calcium channels (VGCCs) located at the active zone exerts a strong influence over neurotransmitter release (Fox and Currie, 1997). We observed no difference in electrically evoked DA release between MsrA$^{-/-}$ and WT slices when extracellular calcium concentrations

were increased, suggesting that the VGCCs were functioning similarly. However, it is possible that other calcium handing mechanisms are altered in *MsrA*$^{-/-}$ mice, and that these alterations may somehow influence the ability of terminals to release DA, especially since intracellular calcium can influence the movement of vesicular DA between RRP and reserve pools (Rose et al., 2002).

One potential mechanism that could increase intracellular calcium levels is the oxidative inactivation of calcium regulatory proteins. In particular, methionine oxidation of calcium regulatory proteins, such as calmodulin (Michaelis et al., 1996) and calcium/calmodulin kinase II (Erickson et al., 2008), increases with age and is also increased in selenium deficient *MsrA*$^{-/-}$ mice compared to WT control mice (Moskovitz, 2007). An elevation in intracellular calcium associated with the lack of calcium chelating ability may be associated with increased reserve pool DA in *MsrA*$^{-/-}$ mice because calcium accelerates the mobilization of vesicles from the reserve pool stores (Kline et al., 2002).

To assess the content and mobilization of reserve pool DA in MsrA$^{-/-}$ and WT control mice, selected pharmacological agents were used. Treating brain slices with aMPT while electrically stimulating the brain slice depletes DA in RRP vesicles. Under these conditions, DA in the extracellular space will be packaged and also released, leaving only DA in reserve pool vesicles (Ortiz et al., 2010). Upon the addition of AMPH, DA in the reverse pool vesicles is released by reverse transport through the DAT and we are able to measure the resulting efflux. We found that, compared with WT littermate controls, AMPH-induced DA efflux is greater in *MsrA*$^{-/-}$ slices compared to WT slices, indicating that *MsrA*$^{-/-}$ mice have an increased supply of reserve pool dopamine. This increase parallels both the enhancement of stimulated DA release and the increase in striatal DA content found previously in *MsrA*$^{-/-}$ mice (Oien et al., 2008b). Because

equal levels of the DAT protein are found in *MsrA*$^{-/-}$ and WT mice, and DA uptake in the absence of pharmacological treatments appears to be similar between the two strains, it is unlikely that the enhancement of DA efflux found in the *MsrA*$^{-/-}$ striatum is the result of alterations in DAT expression or function. Thus, our results suggest that the overall amount of reserve pool DA is increased in the *MrsA*$^{-/-}$ striatum.

When DA reserve pool vesicles are mobilized by the application of COC, peak DA release evoked by single-pulse stimulation was the same between the *MsrA*$^{-/-}$ and WT mice, implying that there are the same number of DA molecules contained in each mobilized reserve pool vesicle. Because the peak dopamine release is attained earlier in WT mice than in MsrA$^{-/-}$ mice, impaired mobilization of reserve pool vesicles in the *MsrA*$^{-/-}$ cannot be ruled out. Area under the curve calculations suggest that the WT striatum possesses 40% the number of DA reserve pool vesicles found in the *MsrA*$^{-/-}$ striatum. This figure is in close agreement with the amount of DA released by electrical stimulation in the WT striatum (37% of *MsrA*$^{-/-}$; Oien et al., 2008b). Thus, a greater overall number of vesicles, albeit a similar proportion in relation to the reserve pool, are mobilized into the RRP in *MsrA*$^{-/-}$ mice than in WT mice. These vesicles then undergo exocytosis upon the application of a mild electrical stimulus pulse, which is intended to simulate the occurrence of a natural action potential. We speculate that this increase in the number of reserve pool vesicles enhances the magnitude of naturally occurring DA release events in *MsrA*$^{-/-}$ mice.

The mechanism of the chronically increased DA levels in *MsrA*$^{-/-}$ mice is still unknown. The abnormally high brain DA in *MsrA*$^{-/-}$ mice can be alleviated by caloric restriction (Oien et al., 2010), suggesting that metabolism and oxidative stress related mechanisms are involved in this phenomenon. Previous studies suggest an increase of the tyrosine hydroxylase activating protein

14-3-3zeta mRNA (Oien et al., 2008a) and protein (Oien et al., 2008b) may be associated with the increased levels of DA by enhanced DA synthesis. In addition, we have recently reported that methionine oxidation of the dopamine D2 receptor may participate in DA signaling in *MsrA*$^{-/-}$ mice (Oien et al., 2010), which may include the presynaptic D2 autoreceptor isoform. Another possible explanation for this abnormal DA regulation is increased methionine sulfoxide levels in alpha-synuclein that may interfere with its interaction with DA (Oien and Moskovitz, 2008, Oien et al., 2009, Outeiro et al., 2009). This theory is further supported by defective mobilization of DA from reserve pools in alpha-synuclein knockout mice and A30P mutated alpha-synuclein transgenic mice (Yavich et al., 2004, Yavich et al., 2005). In any case, it is apparent that dopaminergic neurons store this excess DA in reserve pool vesicles.

In summary, this work has identified an intracellular mechanism by which *MsrA*$^{-/-}$ mice store excess DA. To our knowledge, this is the first published study in which reserve pool DA levels have been directly measured in mice that are genetically altered to have increased oxidative stress. Moreover, this study offers a potential mechanism by which neurons cope with the excessive production of DA, and also provides a strategy for the study other DA-related pathologies.

B. References

Bartlett RK, Bieber Urbauer RJ, Anbanandam A, Smallwood HS, Urbauer JL, Squier TC (Oxidation of Met144 and Met145 in calmodulin blocks calmodulin dependent activation of the plasma membrane Ca-ATPase. Biochemistry 42:3231-3238.2003).

Bigelow DJ, Squier TC (Redox modulation of cellular signaling and metabolism through reversible oxidation of methionine sensors in calcium regulatory proteins. Biochim Biophys Acta 1703:121-134.2005).

Bird ED, Iversen LL (Huntington's chorea. Post-mortem measurement of glutamic acid decarboxylase, choline acetyltransferase and dopamine in basal ganglia. Brain 97:457-472.1974).

Bylund D. B. and Toews M. L. (1993) Radioligand binding methods: practical guide and tips. Am. J. Physiol. 265, L421–L429.

Carlsson T., Bjorklund T. and Kirik D. (2007) Restoration of the striatal dopamine synthesis for Parkinson’s disease: viral vector-mediated enzyme replacement strategy. Curr. Gene Ther. 7, 109–120.

Chen BT, Avshalumov MV, Rice ME (H(2)O(2) is a novel, endogenous modulator of synaptic dopamine release. J Neurophysiol 85:2468-2476.2001).

Chiueh CC, Moore KE (D-amphetamine-induced release of "newly synthesized" and "stored" dopamine from the caudate nucleus in vivo. J Pharmacol Exp Ther 192:642-653.1975).

Cohen G (The pathobiology of Parkinson's disease: biochemical aspects of dopamine neuron senescence. J Neural Transm Suppl 19:89-103.1983).

Eilam D., Clements K. V. and Szechtman H. (1991) Differential effects of D1 and D2 dopamine agonists on stereotyped locomotion in rats. Behav. Brain Res. 45, 117–124.

Emes M. J. (2009) Oxidation of methionine residues: the missing link between stress and signalling responses in plants. Biochem. J. 422, e1–e2.

Erickson JR, Joiner ML, Guan X, Kutschke W, Yang J, Oddis CV, Bartlett RK, Lowe JS, O'Donnell SE, Aykin-Burns N, Zimmerman MC, Zimmerman K, Ham AJ, Weiss RM, Spitz DR, Shea MA, Colbran RJ, Mohler PJ, Anderson ME (A dynamic pathway for calcium-independent activation of CaMKII by methionine oxidation. Cell 133:462-474.2008).

Fawaz C. S., Martel P., Leo D. and Trudeau L. E. (2009) Presynaptic action of neurotensin on dopamine release through inhibition of D(2) receptor function. BMC Neurosci. 10, 96.

Fischer JF, Cho AK (Chemical release of dopamine from striatal homogenates: evidence for an exchange diffusion model. J Pharmacol Exp Ther 208:203-209.1979).

Fowler S. C., Birkestrand B. R., Chen R., Moss S. J., Vorontsova E., Wang G. and Zarcone T. J. (2001) A force-plate actometer for quantitating rodent behaviors: illustrative data on locomotion, rotation, spatial patterning, stereotypies, and tremor. J. Neurosci. Methods 107, 107–124.

Fox AP, Currie KPM (Comparison of N- and P/Q-Type Voltage-Gated Calcium Channel Current Inhibition. J Neurosci 17:4570-4579.1997).

Geter-Douglass B., Katz J. L., Alling K., Acri J. B. and Witkin J. M. (1997) Characterization of unconditioned behavioral effects of dopamine D3/D2 receptor agonists. J. Pharmacol. Exp. Ther. 283, 7–15.

Hardin S. C., Larue C. T., Oh M. H., Jain V. and Huber S. C. (2009) Coupling oxidative signals to protein phosphorylation via methionine oxidation in Arabidopsis. Biochem. J. 422, 305–312.

Harrison C. and Traynor J. R. (2003) The [35S]GTPgammaS binding assay: approaches and applications in pharmacology. Life Sci. 74, 489–508.

Hickey M. A., Reynolds G. P. and Morton A. J. (2002) The role of dopamine in motor symptoms in the R6/2 transgenic mouse model of Huntington's disease. J. Neurochem. 81, 46–59.

Hornykiewicz O. (1962) Dopamine (3-hydroxytyramine) in the central nervous system and its relation to the Parkinson syndrome in man. Dtsch. Med. Wochenschr. 87, 1807–1810.

Ilani T., Fishburn C. S., Levavi-Sivan B., Carmon S., Raveh L. and Fuchs S. (2002) Coupling of dopamine receptors to G proteins: studies with chimeric D2/D3 dopamine receptors. Cell. Mol. Neurobiol. 22, 47–56.

Johnson MA, Rajan V, Miller CE, Wightman RM (Dopamine release is severely compromised in the R6/2 mouse model of Huntington's disease. J Neurochem 97:737-746.2006).

Jones SR, Gainetdinov RR, Wightman RM, Caron MG (Mechanisms of amphetamine action revealed in mice lacking the dopamine transporter. J Neurosci 18:1979-1986.1998).

Kline DD, Takacs KN, Ficker E, Kunze DL (Dopamine Modulates Synaptic Transmission in the Nucleus of the Solitary Tract. J Neurophysiol 88:2736-2744.2002).

Kraft JC, Osterhaus GL, Ortiz AN, Garris PA, Johnson MA (In vivo dopamine release and uptake impairments in rats treated with 3-nitropropionic acid. Neuroscience 161:940-949.2009).

Kume-Kick J, Rice ME (Dependence of dopamine calibration factors on media Ca2+ and Mg2+ at carbon-fiber microelectrodes used with fast-scan cyclic voltammetry. J Neurosci Methods 84:55-62.1998).

Lan H., Liu Y., Bell M. I., Gurevich V. V. and Neve K. A. (2009) A dopamine D2 receptor mutant capable of G protein-mediated signaling but deficient in arrestin binding. Mol. Pharmacol. 75, 113–123.

Levant B., Grigoriadis D. E. and DeSouza E. B. (1992) Characterization of [3H]quinpirole binding to D2-like dopamine receptors in rat brain. J. Pharmacol. Exp. Ther. 262, 929–935.

Lieberman J. A., Bymaster F. P., Meltzer H. Y. et al. (2008) Antipsychotic drugs: comparison in animal models of efficacy, neurotransmitter regulation, and neuroprotection. Pharmacol. Rev. 60, 358–403.

Liang NY, Rutledge CO (Evidence for carrier-mediated efflux of dopamine from corpus striatum. Biochem Pharmacol 31:2479-2484.1982).

Michaelis ML, Bigelow DJ, Schoneich C, Williams TD, Ramonda L, Yin D, Huhmer AF, Yao Y, Gao J, Squier TC (Decreased plasma membrane calcium transport activity in aging brain. Life Sci 59:405-412.1996).

Montmayeur J. P., Guiramand J. and Borrelli E. (1993) Preferential coupling between dopamine D2 receptors and G-proteins. Mol. Endocrinol. 7, 161–170.

Morgan DG, May PC, Finch CE (Dopamine and serotonin systems in human and rodent brain: effects of age and neurodegenerative disease. J Am Geriatr Soc 35:334-345.1987).

Moskovitz J (Methionine sulfoxide reductases: ubiquitous enzymes involved in antioxidant defense, protein regulation, and prevention of aging-associated diseases. Biochim Biophys Acta 1703:213-219.2005).

Moskovitz J (Prolonged selenium-deficient diet in MsrA knockout mice causes enhanced oxidative modification to proteins and affects the levels of antioxidant enzymes in a tissue-specific manner. Free Radic Res 41:162-171.2007).

Moskovitz J, Bar-Noy S, Williams WM, Requena J, Berlett BS, Stadtman ER (Methionine sulfoxide reductase (MsrA) is a regulator of antioxidant defense and lifespan in mammals. Proc Natl Acad Sci U S A 98:12920-12925.2001).

Moskovitz J., Rahman M. A., Strassman J., Yancey S. O., Kushner S. R., Brot N. and Weissbach H. (1995) Escherichia coli peptide methionine sulfoxide reductase gene: regulation of expression and role in protecting against oxidative damage. J. Bacteriol. 177, 502–507.

Moskovitz J., Berlett B. S., Poston J. M. and Stadtman E. R. (1997) The yeast peptide-methionine sulfoxide reductase functions as an antioxidant in vivo. Proc. Natl Acad. Sci. USA 94, 9585–9589.

Moskovitz J., Flescher E., Berlett B. S., Azare J., Poston J. M. and Stadtman E. R. (1998) Overexpression of peptide-methionine sulfoxide reductase in Saccharomyces cerevisiae and human T cells provides them with high resistance to oxidative stress. Proc. Natl Acad. Sci. USA 95, 14071–14075.

Nachshen DA, Sanchez-Armass S (Co-operative action of calcium ions in dopamine release from rat brain synaptosomes. J Physiol 387:415-423.1987).

Neves G, Lagnado L (The kinetics of exocytosis and endocytosis in the synaptic terminal of goldfish retinal bipolar cells. J Physiol 515 (Pt 1):181-202.1999).

Namkung Y., Dipace C., Javitch J. A. and Sibley D. R. (2009) G protein-coupled receptor kinase-mediated phosphorylation regulates post-endocytic trafficking of the D2 dopamine receptor. J. Biol. Chem. 284, 15038–15051.

Niimi K., Takahashi E. and Itakura C. (2009) Age dependence of motor activity and sensitivity to dopamine receptor 1 agonist, SKF82958, of inbred AKR/J, BALB/c, C57BL/6J, SAMR1, and SAMP6 strains. Brain Res. 1250, 175–182.

Nwaneshiudu C. A. and Unterwald E. M. (2009) Blockade of neurokinin-3 receptors modulates dopamine-mediated behavioral hyperactivity. Neuropharmacology 57, 295–301.

Oien D, Wang X, Moskovitz J (Genomic and Proteomic Analyses of the Methionine Sulfoxide Reductase A Knockout Mouse. Current Proteomics 5:96-103.2008a).

Oien DB, Moskovitz J (Substrates of the methionine sulfoxide reductase system and their physiological relevance. Curr Top Dev Biol 80:93-133.2008).

Oien DB, Ortiz AN, Rittel AG, Dobrowsky RT, Johnson MA, Levant B, Fowler SC, Moskovitz J (Dopamine D2 Receptor Function is Compromised in the Brain of the Methionine Sulfoxide Reductase A Knockout Mouse. J Neurochem 114(1):51-61.2010).

Oien DB, Osterhaus GL, Latif SA, Pinkston JW, Fulks J, Johnson M, Fowler SC, Moskovitz J (MsrA knockout mouse exhibits abnormal behavior and brain dopamine levels. Free Rad Biol Med 45:193-200.2008b).

Oien DB, Osterhaus GL, Lundquist BL, Fowler SC, Moskovitz J (Caloric restriction alleviates abnormal locomotor activity and dopamine levels in the brain of the methionine sulfoxide reductase A knockout mouse. Neurosci Lett 468:38-41.2010).

Oien DB, Shinogle HE, Moore DS, Moskovitz J (Clearance and phosphorylation of alpha-synuclein are inhibited in methionine sulfoxide reductase a null yeast cells. J Mol Neurosci 39:323-332.2009).

Ortiz AN, Kurth BJ, Osterhaus GL, Johnson MA (Dysregulation of intracellular dopamine stores revealed in the R6/2 mouse striatum. J Neurochem 112:755-761.2010).

Outeiro TF, Klucken J, Bercury K, Tetzlaff J, Putcha P, Oliveira LM, Quintas A, McLean PJ, Hyman BT (Dopamine-induced conformational changes in alpha-synuclein. PLoS One 4:e6906.2009).

Pahwa R., Lyons K. E. and Hauser R. A. (2004) Ropinirole therapy for Parkinson's disease. Expert Rev. Neurother. 4, 581–588.

Pal R, Oien DB, Ersen FY, Moskovitz J (Elevated levels of brain-pathologies associated with neurodegenerative diseases in the methionine sulfoxide reductase A knockout mouse. Exp Brain Res 180:765-774.2007).

Palacios J, Sepulveda MR, Lee AG, Mata AM (Ca2+ transport by the synaptosomal plasma membrane Ca2+-ATPase and the effect of thioridazine. Biochemistry 43:2353-2358.2004).

Patten DA, Germain M, Kelly MA, Slack RS (Reactive oxygen species: stuck in the middle of neurodegeneration. J Alzheimers Dis 20 Suppl 2:S357-367).

Perez-Severiano F, Santamaria A, Pedraza-Chaverri J, Medina-Campos ON, Rios C, Segovia J (Increased formation of reactive oxygen species, but no changes in glutathione peroxidase activity, in striata of mice transgenic for the Huntington's disease mutation. Neurochem Res 29:729-733.2004).

Rizzoli SO, Betz WJ (Synaptic vesicle pools. Nat Rev Neurosci 6:57-69.2005).

Romero H. M., Berlett B. S., Jensen P. J., Pell E. J. and Tien M. (2004) Investigations into the role of the plastidial peptide methionine sulfoxide reductase in response to oxidative stress in Arabidopsis. Plant Physiol. 136, 3784–3794.

Rose SD, Lejen T, Casaletti L, Larson RE, Pene TD, Trifaro JM (Molecular motors involved in chromaffin cell secretion. Ann N Y Acad Sci 971:222-231.2002).

Ruan H., Tang X. D., Chen M. L. et al. (2002) High-quality life extension by the enzyme peptide methionine sulfoxide reductase. Proc. Natl Acad. Sci. USA 99, 2748–2753.

Saxena S., Brody A. L., Schwartz J. M. and Baxter L. R. (1998) Neuroimaging and frontal-subcortical circuitry in obsessive-compulsive disorder. Br. J. Psychiatry Suppl. 35, 26–37.

Usiello A., Baik J. H., Rouge-Pont F., Picetti R., Dierich A., LeMeur M., Piazza P. V. and Borrelli E. (2000) Distinct functions of the two isoforms of dopamine D2 receptors. Nature 408, 199–203.

Venton BJ, Seipel AT, Phillips PE, Wetsel WC, Gitler D, Greengard P, Augustine GJ, Wightman RM (Cocaine increases dopamine release by mobilization of a synapsin-dependent reserve pool. J Neurosci 26:3206-3209.2006).

Walss-Bass C., Soto-Bernardini M. C., Johnson-Pais T. et al. (2009) Methionine sulfoxide reductase: a novel schizophrenia candidate gene. Am. J. Med. Genet. B Neuropsychiatr. Genet. 150B, 219–225.

Wang Y., Xu R., Sasaoka T., Tonegawa S., Kung M. P. and Sankoorikal E. B. (2000) Dopamine D2 long receptor-deficient mice display alterations in striatum-dependent functions. J. Neurosci. 20, 8305–8314.

Yavich L, Oksman M, Tanila H, Kerokoski P, Hiltunen M, van Groen T, Puolivali J, Mannisto PT, Garcia-Horsman A, MacDonald E, Beyreuther K, Hartmann T, Jakala P (Locomotor activity and evoked dopamine release are reduced in mice overexpressing A30P-mutated human alpha-synuclein. Neurobiol Dis 20:303-313.2005).

Yavich L, Tanila H, Vepsalainen S, Jakala P (Role of alpha-synuclein in presynaptic dopamine recruitment. J Neurosci 24:11165-11170.2004).

Zhang Y., D'Souza D., Raap D. K., Garcia F., Battaglia G., Muma N. A. and Van de Kar L. D. (2001) Characterization of the functional heterologous desensitization of hypothalamic 5-HT(1A) receptors after 5-HT(2A) receptor activation. J. Neurosci. 21, 7919–7927.

Zhang L., Yu C., Vasquez F. E., Galeva N., Onyango I., Swerdlow R. H. and Dobrowsky R. T. (2010) Hyperglycemia alters the schwann cell mitochondrial proteome and decreases coupled respiration in the absence of superoxide production. J. Proteome Res. 9, 458–471.

Chapter 5: Conclusion

The main focus of my research has been on the effects of neurodegentation and oxidative stress on the release of DA. In my studies of HD we have shown that the release of DA decreases in an age dependent manner in transgenic R6/1 and R6/2 mice (Ortiz et al., 2010, 2011a). This inhibition was not present in the chemically-induced 3NP treated rat model (Ortiz et al., submitted). Another difference between the two types of models was found when the number of DA reserve pool vesicles was measured. Using αMPT and AMPH to measure DA efflux the amount of DA release was decreased in 12 week old R6/2 mice and increased in 3NP-treated rats (Ortiz et al., 2010). Using a combination of αMPT and COC the DA reserve pool in R6/2 mice was once again measured and showed that the amount of DA in each vesicle was the same but the number of vesicles in the reserve pool was significantly decreased in the R6/2 mice (Ortiz et al., 2010). This has led us to believe that the chemically induced model may not be a good model of HD especially when compared to the genetically induced models.

Future studies for these projects include examining other chemically induced models of HD to determine if the discrepancies we found using the 3NP model are present in other chemically induced models. This would allow us to find a more reliable HD chemical model to use. The transgenic mouse models used were both from the R6 mouse germ line so it would be important to examine other mouse models such as the YAC model. Another aspect of this project that should be further studied is the reserve pool vesicles. By using fluorescence imaging it would be possible to quantify the number and location of reserve pool vesicles.

Neurodegenerative diseases and aging are both associated with oxidative stress and by studying the underlying mechanisms allows for potential future pharmaceutical approaches. Using the MsrA knockmouse we were able to study oxidative stress and the effects that it has on

DA release. The reserve pool DA was measured using αMPT and AMPH and also using αMPT and COC. We found that the reserve pool DA levels were increased in the MsrA$^{-/-}$ and that there was an increase in the number of vesicles present and each vesicle had the same amount of DA when compared to age matched wild type mice (Ortiz et al., 2011b). The DA release was also measured in brain slices in the presence of increasing calcium levels. There was no difference in DA release between the various calcium levels suggesting the calcium regulatory proteins, such as calmodulin and calcium/calmodulin kinase II in MsrA$^{-/-}$, are functioning properly (Oien et al., 2010). These results also suggest that DA release is not increasing or decreasing due to calcium levels as calcium levels also help to regulate vesicular mobilization and release. The increase of DA was thought to be due to an increase in DA synthesis which is due to a lack of autoreceptor signaling which is modulated by D2 receptors. The study of the D2 receptors in MsrA mice was done using D2 agonists and antagnosits, quinpirole and sulpiride. The MsrA$^{-/-}$ were less responsive to both quinpirole and sulpiride indicating poor D2 signaling (Oien et al., 2010).

Future studies for the MsrA project include looking further at the D2 autoreceptor as the current hypothesis is that the increase in DA synthesis found in these mice is due to poor D2 signaling. One possible way to further study the D2 autoreceptor is to purify the D2 protein and use mass spectrometry to look for possible changes in the oxidation of methionine residues. After the location of oxidation is found then these results can be compared to the oxidation that occurs in people with neurodegenerative disease.

References

Oien DB, Ortiz AN, Rittel AG, Dobrowsky RT, Johnson MA, Levant B, Fowler SC, Moskovitz J (Dopamine D(2) receptor function is compromised in the brain of the methionine sulfoxide reductase A knockout mouse. J Neurochem 114:51-61.2010).

Ortiz AN, Kurth BJ, Osterhaus GL, Johnson MA (Dysregulation of intracellular dopamine stores revealed in the R6/2 mouse striatum. J Neurochem 112:755-761.2010).

Ortiz AN, Kurth BJ, Osterhaus GL, Johnson MA (Impaired dopamine release and uptake in R6/1 Huntington's disease model mice. Neurosci Lett.2011a).

Ortiz AN, Oien DB, Moskovitz J, Johnson MA (Quantification of reserve pool dopamine in methionine sulfoxide reductase A null mice. Neuroscience 177:223-229.2011b).

Appendix

Dopamine D2 Function is Compromised in the Brain of MsrA$^{-/-}$ Mice

Work described in this appendix is based in part on work accomplished by Andrea Ortiz in collaboration with Dr. Derek Oien (then student of Prof. Jackob Moscovitz) and others. This work is published under the following reference:

Oien DB, Ortiz AN, Rittel AG, Dobrowsky RT, Johnson MA, Levant B, Fowler SC, Moskovitz J (Dopamine D2 Receptor Function is Compromised in the Brain of the Methionine Sulfoxide Reductase A Knockout Mouse. J Neurochem 114(1):51-61.2010).

Previous research suggests that brain oxidative stress and altered rodent locomotor behavior are linked. We observed bio-behavioral changes in methionine sulfoxide reductase A knockout mice associated with abnormal dopamine signaling. Compromised ability of these knockout mice to reduce methionine sulfoxide enhances accumulation of sulfoxides in proteins. We examined the dopamine D_2-receptor function and expression, which has an atypical arrangement and quantity of methionine residues. Indeed, protein expression levels of dopamine D_2-receptor were higher in knockout mice compared with wild-type. However, the binding of dopamine D_2-receptor agonist was compromised in the same fractions of knockout mice. Coupling efficiency of dopamine D_2-receptors to G-proteins was also significantly reduced in knockout mice, supporting the compromised agonist binding. Furthermore, pre-synaptic dopamine release in knockout striatal sections was less responsive than control sections to dopamine D_2-receptor ligands. Behaviorally, the locomotor activity of knockout mice was less responsive to the inhibitory effect of quinpirole than wild-type mice. Involvement of specific methionine residue oxidation in the dopamine D_2-receptor third intracellular loop is suggested by *in vitro* studies. We conclude that ablation of methionine sulfoxide reductase can affect

dopamine signaling through altering dopamine D_2-receptor physiology and may be related to symptoms associated with neurological disorders and diseases.

Introduction

Post-translational modifications resulting from reactive oxygen species can alter the functions of many proteins. While most protein modifications by reactive oxygen species are irreversible, methionine sulfoxide (MetO) modifications can be reversed by the methionine sulfoxide reductase (Msr) system, which consists of MsrA (reduces *S*-MetO) and MsrB (reduces *R*-MetO) (Moskovitz 2005). Reduction action of the Msr system may prevent irreversible protein damage, contribute to cellular antioxidant resistance, and regulate protein function. Evidence for a role of the Msr system in antioxidant defense is demonstrated by the adverse effects resulting from MsrA ablation (Moskovitz *et al.* 1995, 1997, 2001). Furthermore, over-expression of MsrA in various organisms and cells protects them from oxidative stress toxicity (Moskovitz *et al.* 1998; Ruan *et al.* 2002; Romero *et al.* 2004). The *MsrA* null mouse (*MsrA*−/−) is hypersensitive to oxidative stress, accumulates higher levels of carbonylated protein and expresses brain pathologies associated with neurodegenerative diseases (Moskovitz *et al.* 2001; Pal *et al.* 2007); this evidence suggests a major biological role of the Msr system. Furthermore, the Msr enzymes have been shown to switch several proteins between non-active and active forms by reducing specific MetO residues to methionine (Oien and Moskovitz 2008).

The *MsrA*−/− mouse exhibits age-dependent lower locomotor activity and abnormal gait indices (Oien *et al.* 2008) relative to control mice. Lower dopamine (DA) levels are associated with altered motor performance (Carlsson *et al.* 2007). Surprisingly, our recent observations showed that *MsrA*−/− brains in adult mice contained significantly higher levels of DA (Oien *et al.* 2008). Moreover, pre-synaptic neuronal DA in *MsrA*−/− striatal slices is released at higher DA pulses than wild-type (WT) slices as measured by fast scan cyclic voltammetry. These results raise the possibility that DA function is impaired in *MsrA*−/− mice. Moreover, *MsrA*−/− mice were less responsive to amphetamine treatment as assayed by locomotor activity and stereotypy, suggesting alteration of DA signaling. Dysfunctions of the corpus striatum and dopaminergic signaling are linked to a range of disorders including Parkinson's disease (Hornykiewicz 1962), Huntington's disease (Hickey *et al.* 2002), schizophrenia, and obsessive-compulsive disorder (Saxena *et al.* 1998).

The observed *MsrA*−/− locomotor deficits and DA abnormalities prompted us to further examine DA signaling events that are associated with striatal movement pathways. The dopamine D_1 receptor (D1DR) and dopamine D_2 receptor (D2DR) are closely associated with movement regulation, and theoretically are the DA receptors most related to the *MsrA*−/− locomotor phenotypes (Oien *et al.* 2008). In addition, D2DR is also expressed in its short form ($D2DR_S$) that serves as an autoreceptor for dopaminergic neurons. Thus, methionine oxidation in either the long form of D2DR or $D2DR_S$ or a combination of both may be related to the elevation in DA levels observed in *MsrA*−/− brains (Oien *et al.* 2008). In the current study we investigate the ligand-binding capabilities of DA receptors and their coupling efficiency to G-proteins in *MsrA*−/− versus WT mice. The presented data support the hypothesis that MetO modification to D2DRs participates in the *MsrA*−/− behavioral and biochemical phenotypes.

Materials

The radioligands [^{3}H]SCH23390 (85 Ci/mmol), [^{3}H]raclopride (84 Ci/mmol), [^{3}H]quinpirole (50 Ci/mmol), were purchased from Perkin Elmer (Waltham, MA, USA). Non-radioactive sulpiride, quinpirole, SKF82958, and GTPγS were purchased from Sigma, St Louis, MO, USA. Mouse and goat antibodies against D2DR were purchased from Abcam (Cambridge, MA, USA). Mouse β-actin antibodies were purchased from Molecular Probes, Eugene, OR, USA.

Mice

Mice used in these studies were WT (C57BL6/129 Sv) and *MsrA*−/− on the same genetic background at an age of 6–8 months unless otherwise noted. Both types of mice were littermates born to *MsrA*+/− heterozygous parents (Moskovitz *et al.* 2001). All procedures using mice were performed within guidelines of the NIH and KU Institutional Animal Care and Use Committee.

Immunohistochemistry analysis

Coronal brain sections from 12-month-old WT and *MsrA*−/− mice were processed as 20 μm-thick brain sections. Sections were treated with 3% H_2O_2 in methanol for 30 min. After blocking with 1% bovine serum albumin and 3% horse serum in phosphate-buffered saline, the sections were incubated for 24 h with primary goat antibodies against D2DR (1 : 500 dilution, stock concentration of 1.5 mg/mL). Sections were then incubated with biotinylated mouse anti-goat IgG antibodies (Santa Cruz Biotechnology, Santa Cruz, CA, USA), avidin–horseradish peroxide solution, 0.015% diaminobenzidine, 0.001% H_2O_2, and finally counter-stained with hematoxylin.

The brain slides were washed, dehydrated, mounted, and visualized using a brightfield microscope with a 100× objective lens.

Immunoblot analysis

Equal amounts of striatal membranal protein extracts or cytosolic brain proteins (extracted as described below for receptors fraction) were subjected to sodium dodecyl sulfate-gel electrophoresis. Immunoblot analyses with anti-goat D2DR antibodies (1 : 1000 dilution, stock concentration of 1.5 mg/mL) were performed according to common procedures. β-actin (loading control) was detected by primary anti-β-actin mouse antibodies.

Antagonists and agonists binding of D1DR and D2DR ligands

Saturation curves of receptor binding were determined by using the common membrane filtration assay (Bylund and Toews 1993). Briefly, brains (striatal region of each mouse type) were dissected and glass-Teflon homogenized in phosphate-buffered saline with protease inhibitor cocktail (Roche Molecular Biochemicals, Indianapolis, IN, USA). Following centrifugal precipitation at 20 000 *g* for 20 min, the supernatant was removed and saved (cytosolic fraction in immunoblots), and the membranal pellet was washed and precipitated again by centrifugation. Final pellet was homogenized in 1.0 mL of 50 mM Tris pH 7.4. Membranal protein fractions of 100 μg were used per assay, determined by BCA Protein Assay Kit (Thermo Scientific, Waltham, MA, USA). Total ligand binding was determined following incubation of membranal fractions with incrementing concentrations of radioligand for 2 h at 25°C. Non-specific ligand binding was determined using the same conditions with the addition of non-radioactive ligands, 1 mM DA for D1DR and 1 μM sulpiride for D2DR. Bound radioligand was

separated using a Brandel harvester (Brandel, Gaithersburg, MD, USA). Radioligand bound to the filter was measured by liquid scintillation counting. Specific ligand binding values were calculated by subtracting non-specific ligand binding from total ligand binding. The ligands used in the tests were: [^{3}H]SCH23390 and [^{3}H]raclopride as D1DR and D2DR antagonists, respectively, and [^{3}H]quinpirole as a D2DR agonist. The range for radioactive materials used was between 0.03 nM and 4.0 nM (increments by serial dilution).

GTPγS-induced inhibition of radiolabeled quinpirole binding to D2DR

The ability of agonists to stimulate the dissociation of GDP and association of GTP from G-protein was assessed using GTPγS, a non-hydrolyzable analogue of GTP (Zhang *et al.* 2001). When the agonist binds to the receptor, GDP is released from the G-protein and GTPγS binds (Harrison and Traynor 2003). The G-protein uncoupling on [^{3}H]quinpirole binding to the D2DR was investigated by measuring the inhibition of [^{3}H]quinpirole binding at incrementing GTPγS concentrations. The membrane portion of homogenized striatal regions were isolated and lysed in 5 mM Tris buffer by glass-Teflon homogenation. Membranal extracts (30 mg/mL; 80 μg per assay) were incubated with [^{3}H]quinpirole (1 nM) and GTPγS (0.1, 1, 10, 100, and 1000 nM) in 50 mM Tris buffer for 2 h at 25°C in a total volume of 1 mL. To determine non-specific binding, identical assays were performed in the presence of sulpiride (1 μM; racemic mixture). Unbound ligand was removed by Brandel filtration and the remaining bound ligand was quantified by liquid scintillation counting.

The effect of MsrA enzyme on quinpirole and raclopride binding was tested by using recombinant yeast MsrA (10 μg) (Moskovitz *et al.* 1997) with 15 mM dithiothreitol (DTT; this alone did not affect binding). D1DR binding to the agonist SKF82958 was determined using the

same conditions above, except for the addition of 2 nM [^{3}H]SCH23390 to quantify the competitive binding of non-radiolabeled SKF82958 ligand (performed because of limited sources of commercially available radiolabeled D1DR agonists).

Stimulated release of DA in striatal brain sections in the presence of quinpirole and sulpiride measured by fast scan cyclic voltammetry

Brain sections were prepared as previously described (Johnson *et al.* 2006). Mice were anesthetized by isoflurane inhalation. The brain was immediately removed and placed in ice cold artificial CSF. Artificial CSF consisted of 126 mM NaCl, 2.5 mM KCl, 1.2 mM NaH_2PO_4, 2.4 mM $CaCl_2$, 1.2 mM $MgCl_2$, 25 mM $NaHCO_3$, 20 mM HEPES, and 11 mM d-Glucose at pH 7.4 and was continuously saturated with 95% O_2/5% CO_2 throughout the experiment. Coronal sections of 300 μm in thickness were made using a vibratome slicer (Leica Microsystems, Bannockburn, IL, USA). A single section was placed in the superfusion chamber with artificial CSF flowing at 34°C and a continuous rate of 2 mL/min. Each brain section was equilibrated for 60 min prior to obtaining measurements. Quinpirole and sulpiride in artificial CSF were maintained in a separate reservoir and introduced through a three-way valve.

Carbon-fiber microelectrodes were fabricated as previously described (Kraft *et al.* 2009). A single carbon-fiber with a 7 μm diameter (Goodfellow Cambridge Ltd., Oakdale, PA, USA) was aspirated through a glass capillary tube (1.2 mm outer diameter, 0.68 mm inner diameter, 4 inches long, A-M Systems, Inc., Sequim, WA, USA) and pulled using a heated coil puller (Narishige International USA, Inc., East Meadow, NY, USA). Electrodes were trimmed to 20 μm from the glass seal, further insulated with epoxy resin (EPON resin 815C, EPIKURE 3234

curing agent, Miller-Stephenson, Morton Grove, IL, USA), and then cured at 100°C for 1 h. Prior to experimentation, electrodes were backfilled with 0.5 M potassium acetate.

A triangular waveform starting at −0.4 V, increasing to +1.0 V, and scanning back to −0.4 V was applied at the carbon-fiber working electrode. A scan rate of 300 V/s was used with an update rate of 10 Hz. A head-stage amplifier (UNC Chemistry Department Electronics Design) was interfaced with a computer via breakout box and custom software provided by R.M. Wightman and M.L.A.V. Heien. A choridated silver wire was used as an Ag/AgCl reference electrode. The carbon fiber was inserted 100 μm into the dorsolateral caudate-putamen region of the striatum. The fiber was between the prongs of a bipolar stimulation electrode (Plastics One, Roanoke, VA, USA), which were separated by 200 μm. Current was measured at 0.6 V, which is the oxidation potential for DA. DA release was measured in the presence of either 1 μM quinpirole or 5 μM sulpiride as previously described (Fawaz *et al.* 2009) using a 30-pulse stimulus train at a stimulation frequency of 60 Hz. During stimulation and DA release, stabilized scans of 15 s were collected every 2 min and averaged as 4-min time blocks.

Locomotor activity measured by force-plate actometer

The force-plate actometer and methods of data analysis have been previously described (Fowler *et al.* 2001). Briefly, the force-plate actometer consists of a low mass and highly stiff 5 mm thick plate (28 cm × 28 cm). This plate is supported by four Sensotec Model 31 load cells (0–250 g range). Each force plate is positioned below a Plexiglas cage that confines the mouse to the force-sensing plate and is encased in sound-attenuating cubicle. Horizontal movements of the mouse were recorded along the sensing surface with a spatial resolution of 1 mm and a temporal resolution of 0.01 s.

The duration of recording sessions was based upon preliminary experiments and relevant literature assessing spontaneous locomotor activity (Geter-Douglass *et al.* 1997; Usiello *et al.* 2000; Wang *et al.* 2000). The effects of the drugs used on locomotor activity were apparent within the initial period of 45 min following drug injection. Thus, 45-min periods were determined to be sufficient to monitor the locomotor response to the performed treatments. Total distance traveled per animal was measured and analyzed by 2-way anova (two mouse types) with repeated measures on the time block and session factors.

Administration of agonists of D1DR and D2DR for locomotor activity analyses

Prior to treating the mice with D1DR or D2DR agonists, the WT and *MsrA*−/− mice received intraperitoneal injection with 0.9% saline as a vehicle control and spontaneous locomotor activity was monitored for 45 min using force-plate actometers. After 4 days, the same mice were injected with either quinpirole (D2DR agonist, 0.1 and 0.5 mg/kg) or SKF82958 (D1DR agonist, 0.3 and 1.0 mg/kg) and locomotor activity was monitored for 45 min. A minimum of 4 days between trials was used to minimize potential carryover effects. Different sets of animals were used for each drug to prevent cross-reactivity and carryover effects between drugs. The drugs were administered at volume of 5 mL/kg.

MetO residues in recombinant long form of D2DR third intracellular loop

The long form of rat D2DR third intracellular loop ($D2DR_L$-IC_3) was expressed as a glutathione S-transferase (GST) fusion protein in bacteria (gift from Dr. Kim Neve, Oregon Health & Science University) and purified according to published procedures (Lan *et al.* 2009). The protein was oxidized overnight with 200 mM H_2O_2 and excess oxidants were removed by

catalase. In parallel, oxidized protein was reduced with recombinant poly-His-tagged yeast MsrA (10 μg) (Moskovitz *et al.* 1997) in the presence of 20 mM DTT for 1 h at 37°C (DTT alone does not reduce MetO residues under these conditions). After reduction, all proteins (non-treated, H_2O_2-treated, and MsrA-reduced) were subjected to gel-electrophoresis followed by Commassie blue staining for the isolation of the corresponding GST-D2DR$_L$-IC$_3$. Bands corresponding to the predicted weight of ~54 kDa were excised and protein was isolated. The protein was subjected to tryptic digestion prior to analysis by a LCT Premier electrospray ionization tandem mass spectrometer (Waters Corp., Milford, MA, USA). The mass spectrometry analyses of the peptides and their MetO content were performed according to previously published methods (Zhang *et al.* 2010).

Results

Expression levels and ligand binding capabilities of D2DR in MsrA−/− striatum

Postmortem brain sections from *MsrA*−/− and WT mice were immunostained with anti-D2DR antibodies. The *MsrA*−/− striatal region exhibited higher reaction levels with the antibodies compared with this region in WT mice (Fig. 1a). D2DR expression levels were quantified by immunoblot analysis on brain extracts followed by densitometry analysis (Fig. 1b). Similar to the increase of DA in *MsrA*−/− brains (Oien *et al.* 2008), the up-regulation of the D2DR may be part of compensatory response for the dysfunction of the DA system in the *MsrA*−/− brain.

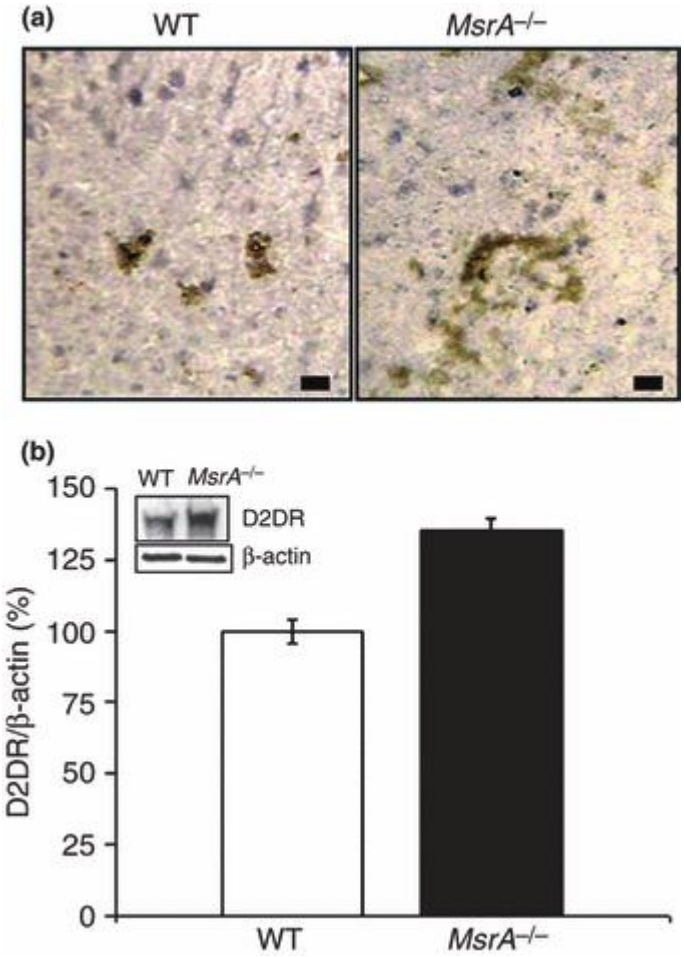

Figure 1. Immunohistochemistry and immunoblot analyses of D2DR in *MsrA*−/− and WT striatum. (a) Immunohistochemistry of coronal brain sections using primary antibodies against D2DR. Slides were visualized using light microscope with a 100× objective lens. Brownish structures correspond to the presence of D2DR. Scale bars represent 10 μm. (b) Immunoblot analysis using primary antibodies against D2DR. Representative bands are shown in the small

window followed by densitometry analysis for the corresponding D2DR band in each extract (relative density in WT represents 100%; $p < 0.01$, *t*-test). The densities of D2DR were corrected for the relative densities of β-actin.

The binding of the D2DR to appropriate ligands can reflect their expression levels and function in signaling. Binding of the D2DR antagonists are independent of G-protein coupling and more reflective of D2DR expression levels. Binding of the D2DR agonists are dependent on G-protein coupling and more reflective of D2DR function in signaling. Accordingly, the calculated B_{max} value of D2DR antagonist [^{3}H]raclopride was higher in *MsrA*−/− membranal fractions (250 ± 20 fmole/mg protein) compared with the value of WT (140 ± 4 fmole/mg protein) (Fig. 2a). In addition, the K_d value for [^{3}H]raclopride in both mouse types was similar (K_d of 0.70 ± 0.10 nM), suggesting no difference in the binding affinity of the bound antagonists to D2DR (it is noteworthy that the K_d values in these mice are different than rats, see 'Discussion'). The [^{3}H]raclopride B_{max} values also provide further supportive evidence to the observed elevated levels of the D2DR in *MsrA*−/− brain (Fig. 1). The calculated B_{max} value of D2DR agonist [^{3}H]quinpirole was lower in *MsrA*−/− membranal fractions (56 ± 7 fmole/mg protein) when compared with the value of the WT (140 ± 10 fmole/mg protein), while the K_d value for [^{3}H]quinpirole binding was similar in both mouse types (0.40 ± 0.05 nM) (Fig. 2a). These observations suggest that the coupling ability of the *MsrA*−/− D2DR to the respective G-proteins is compromised, in spite of the higher number of receptors in *MsrA*−/− mice (Fig. 1). In addition, adding recombinant MsrA to the binding reaction mixture caused significant recovery of the *MsrA*−/− [^{3}H]quinpirole B_{max} value to the WT B_{max} value (Fig. 2b). This latter result strengthens the hypothesis that lack of MsrA enhances MetO formation in D2DR, which affects D2DR function and expression. In contrast to relative D2DR agonist-to-antagonist B_{max} differences

between the two mouse types (Fig. 2a and b), no significant differences were found for D1DR ligand binding to the antagonist SCH23390 or agonist SKF82958 between these mouse types (Fig. 2c and d). At relatively high concentrations, [^{3}H]SCH23390 was bound to *MsrA*−/− and WT striatal fractions to a similar extent (Fig. 2c). Similar results were found when SKF82958 was used (Fig. 2d). The SKF82958 ligand was not radiolabeled, thus binding efficiency was determined by its competitive binding in the presence of 2 nM [^{3}H]SCH23390 as previously described (Nwaneshiudu and Unterwald 2009). The amounts of [^{3}H]SCH23390 bound to the striatal fractions were significantly decreased ($p < 0.05$) by the presence of 16 nM of SKF82958. This supports the hypothesis that *MsrA* ablation primarily impacts the D2DR.

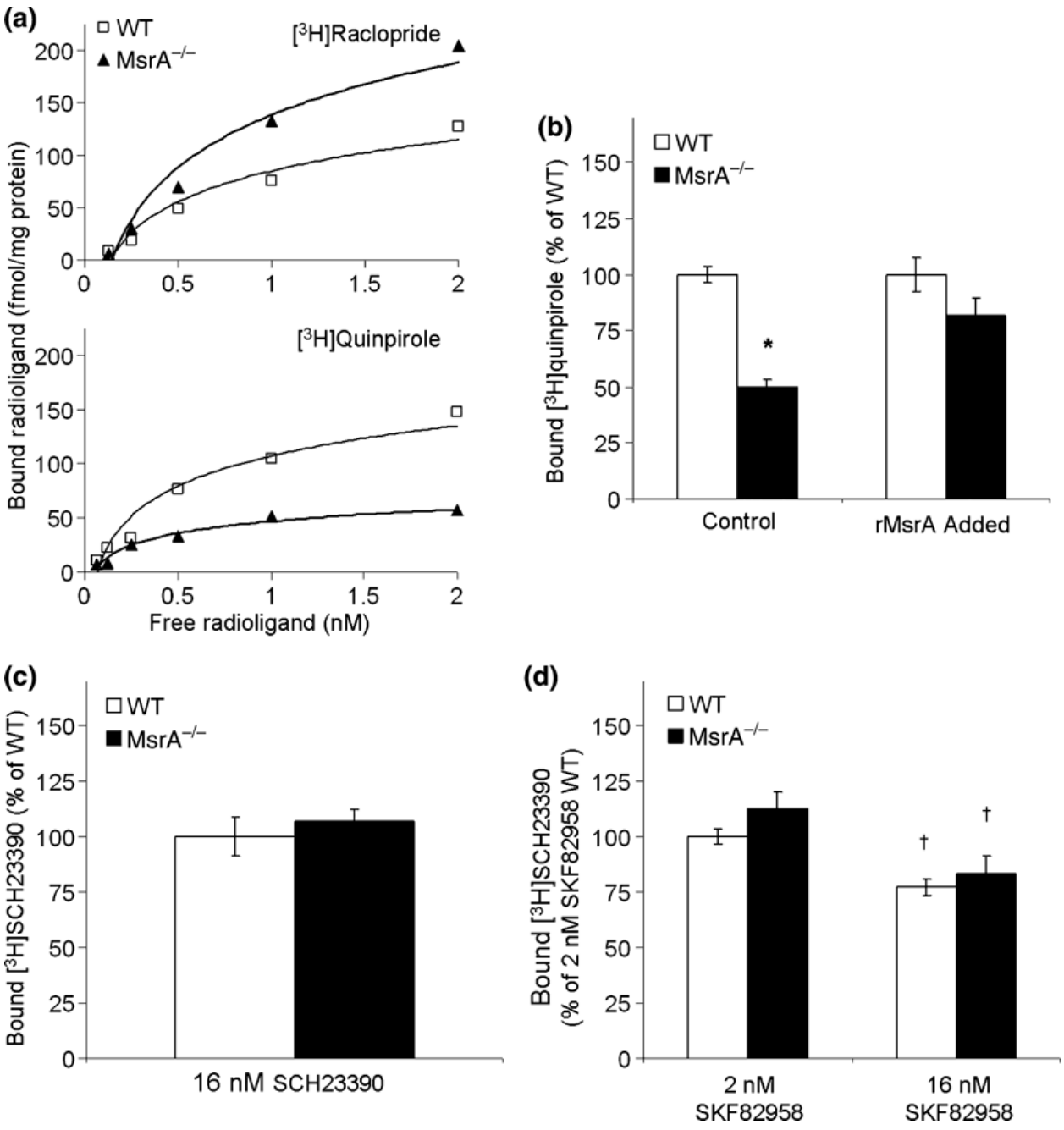

Figure 2. Binding efficiency of ligands to D2DR and D1DR in *MsrA*−/− and WT membranes. Specific ligand binding was calculated from subtracting non-specific ligand binding from total

ligand binding as described in 'Materials and Methods'. (a) Representative [^{3}H]raclopride and [^{3}H]quinpirole specific ligand binding curves of D2DR. (b) B_{max} of [^{3}H]quinpirole binding presented as percent of WT B_{max} value (represents 100% binding) in the absence (Control) and presence of recombinant yeast MsrA (rMsrA Added). (c) Binding of [^{3}H]SCH23390 at a saturating concentration (B_{max} value WT, under these conditions, represents 100% binding). (d) Relative binding of [^{3}H]SCH23390 at a concentration of 2 nM (as in panel c) in the presence of 2 nM and 16 nM SKF82958 concentrations. For all graphs, $n = 3$. Significance is denoted by * or † indicating $p < 0.05$ using *t*-test for difference by mouse type or by condition, respectively.

The non-hydrolyzable GTPγS analog will reduce the binding of [^{3}H]quinpirole to D2DR (quinpirole binds with lower affinity to uncoupled D2DR compared with coupled receptors). Consequently, competition curves were performed by inhibiting [^{3}H]quinpirole binding with increasing concentrations of GTPγS. Accordingly, the maximal inhibition from the competition curve reflects the number of D2DR coupled to G-proteins, while the 50% binding inhibition concentration (IC_{50}) from the curve reflects the potency of GTPγS to dissociate the D2DR and G-protein complex. The maximum binding of [^{3}H]quinpirole to D2DR in *MsrA*−/− was ~50% of the maximum binding of the agonist to the receptors in the WT brain (Fig. 3; WT = 50 ± 6 and *MsrA*−/− = 26 ± 3 fmole/mg protein in the presence of 1 μM [^{3}H]quinpirole). The IC_{50} was found to be similar for both mouse types (10 ± 1 nM), which is in agreement with current literature (Zhang *et al.* 2001). These data suggest reduced G-protein and D2DR coupling in the *MsrA*−/− brain. Moreover, the similar IC_{50} in both mouse types suggests that the dissociation rates of the receptors from the G-proteins are similar. The reduced interaction of G-proteins with D2DR in

MsrA−/− brains could be a consequence of either lower G-protein expression or interference in the initial binding of G-proteins to the third intracellular loop of D2DR. There was no significant difference in expression of $G\alpha_{i/o}$ proteins between the two mouse types (Figure S1), suggesting that the observed limitation in *MsrA*−/− D2DR agonist binding is probably not because of reduced $G\alpha_{i/o}$ levels. Since the expression levels of these G-proteins seem to be similar in the two mouse types (Figure S1), data in Fig. 3 are supportive of compromised D2DR agonist binding in *MsrA*−/− brains (Fig. 2a) and also may reflect interference in binding of *MsrA*−/− G-proteins to the third intracellular loop of D2DR.

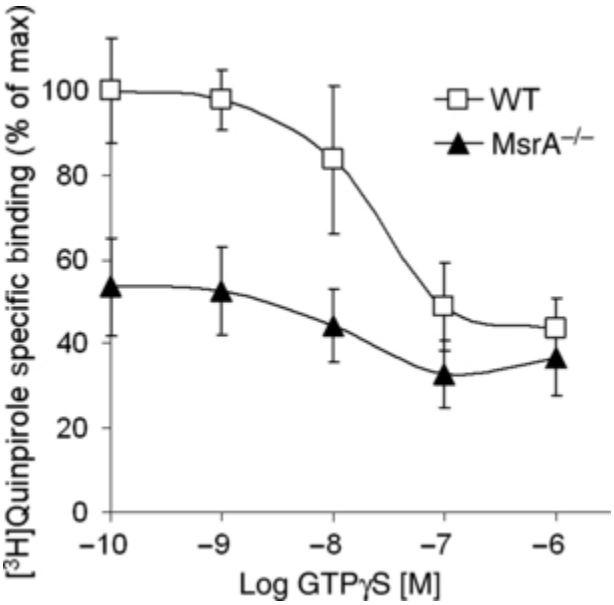

Figure 3. Inhibition of D2DR agonist binding in striatal membrane extracts of *MsrA*−/− and WT mice in the presence of GTPγS. The Y axis values of the graph represent the specific binding percentage of [^{3}H]quinpirole at GTPγS concentrations of 0.1, 1, 10, 100, and 1000 nM. The value at 100% specific binding represents maximum binding of WT D2DR to [^{3}H]quinpirole at 0.1 nM GTPγS. The maximum binding values were not significantly different from values obtained in the absence of GTPγS; data not shown, $n = 3$.

A shorter form of the D2DR, $D2DR_S$, serves as an autoreceptor on the pre-synaptic membrane of dopaminergic neurons. This receptor has a third intracellular loop that is truncated by 29 amino acids, but still retains four of the eight methionine residues. $D2DR_S$ has been previously demonstrated to respond to the D2DR agonist quinpirole and D2DR antagonist sulpiride by decreasing and increasing the pre-synaptic release of DA, respectively (Fawaz *et al.* 2009). Using a similar experimental design as Fawaz *et al.*, the pre-synaptic DA release in the striatal area from *MsrA*−/− and WT coronal sections was measured in the presence of quinpirole (Fig. 4a and b) and sulpiride (Fig. 4c and d). Pre-synaptic DA release was detected by fast scan cyclic voltammetry every 2 min, initially without any treatment and followed by treatment with a saturating dose of quinpirole. In the presence of quinpirole, *MsrA*−/− sections were less responsive than WT sections when both were compared to the respective initial stimulation and detection without the presence of drug. The DA release of the *MsrA*−/− pre-synaptic neurons was significantly higher than the decreased release of the WT pre-synaptic neurons ($p < 0.05$; two-way repeated measures anova). Moreover, the *MsrA*−/− pre-synaptic neurons were also less responsive to sulpiride than WT. After sulpiride treatment, the changes in DA concentration from the initial non-treated measurement of *MsrA*−/− slices were significantly lower than the increased DA concentration changes of the WT ($p < 0.05$). These results suggest that the $D2DR_S$ signaling is disrupted in *MsrA*−/− mice.

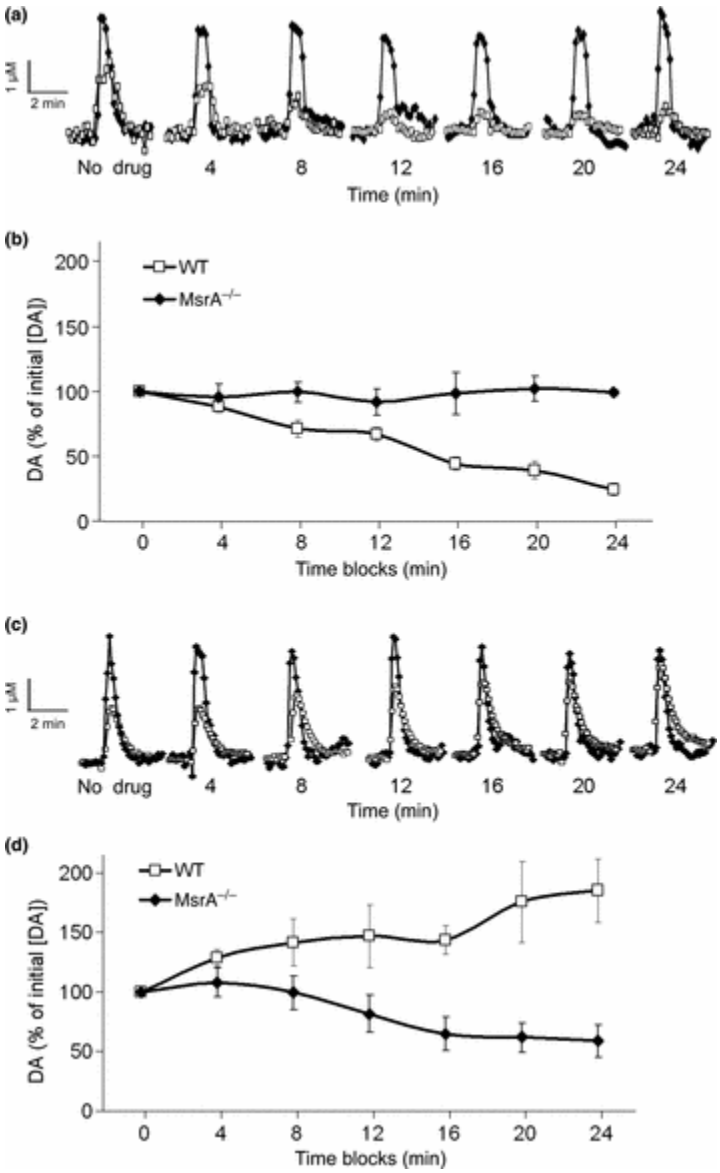

Figure 4. DA release in striatal sections from *MsrA*−/− and WT mice treated with D2DR agonist and antagonist. Coronal sections were stimulated using a 30 pulse-stimulus train and DA scans were collected by fast scan cyclic voltammetry. (a) A representative stimulated DA release plot generated from measurements in the presence and absence of quinpirole. WT, *open squares; MsrA*−/−, *filled diamonds*. (b) The DA release measured in 4-min time blocks of WT and *MsrA*−/− sections in the presence of quinpirole. The basal initial measurements without drug treatment (time block 0) were set to 100%. All subsequent measurements with quinpirole are

represented as a percentage of this value. (c) A representative stimulated DA release plot generated from measurements obtained in the presence and absence of sulpiride. WT, *open squares; MsrA*−/−, *filled diamonds*. (d) The DA release measured in 4-min time blocks of WT and *MsrA*−/− sections in the presence of sulpiride. The initial basal measurements without treatment (time block 0) were set to 100%. All subsequent measurements with sulpiride are represented as a percentage of the initial 100% values. For both experiments, $n = 3$ and $p < 0.05$ for genotype determined by two-way repeated measures anova. The basal DA concentrations in the absence of drug were WT = 1.63 ± 0.44 μM and *MsrA*−/− = 5.47 ± 0.36 μM.

The *in vitro* and brain section findings suggest functional changes in the DA system that should be expressed at the behavioral level. Consequently, we investigated the behavioral effects of D1DR and D2DR selective agonists on locomotor activity in *MsrA*−/− and WT mice. A significant difference in locomotor activity was observed between the mouse strains when injected with quinpirole. At a dose of 0.5 mg/kg, the *MsrA*−/− exhibited ∼40% more locomotor activity than WT, and at a dose of 0.1 mg/kg the *MsrA*−/− exhibited ∼35% more locomotor activity than WT (Fig. 5a; repeated measures anova for mouse type effect, $p < 0.02$). No significant difference in locomotor activity was observed between the two mouse types when injected with saline (Fig. 5), which is consistent with previous experiments (Oien *et al.* 2008). Given the higher expression level of the D2DR in *MsrA*−/− mice, these data suggest that the compromised responsiveness of the *MsrA*−/− D2DRs to the inhibitory effect of quinpirole may be because of irregularities in either DA binding or abnormal function of further downstream signaling events. Moreover, the lack of a significant dose effect in the quinpirole concentrations used is consistent with published data, illustrating by similar analyses that there was no dose effect in mice even at broader and higher dose ranges (Wang *et al.* 2000).

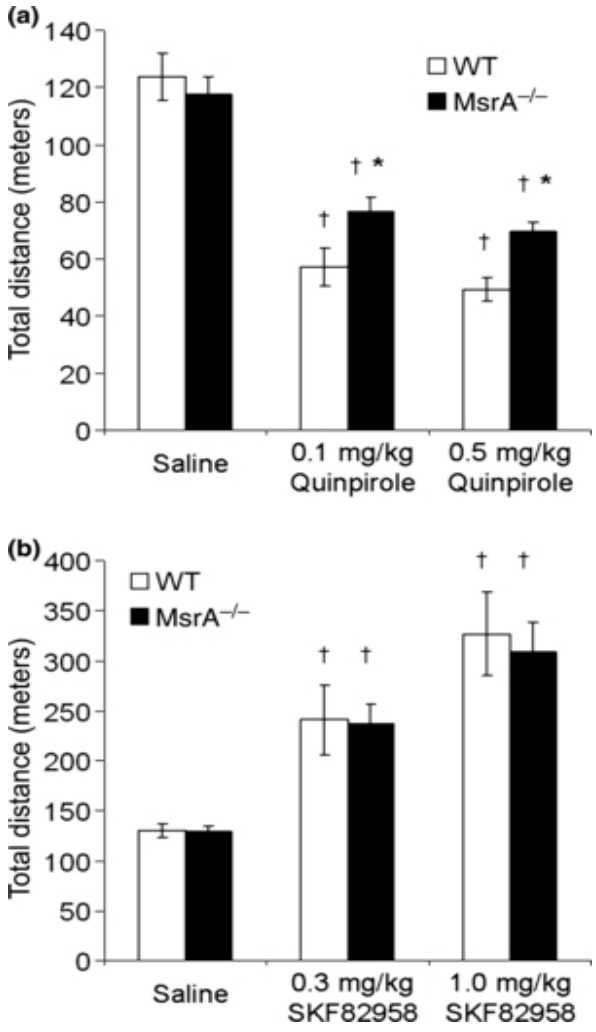

Figure 5. Locomotor activity after D2DR and D1DR agonist administration in *MsrA*−/− and WT mice. Total distance traveled was measured for 45 min after intraperitoneal injections of saline (vehicle) or indicated drug. (a) Quinpirole injection at doses of 0.5 mg/kg and 0.1 mg/kg. WT, $n = 7$; *MsrA*−/−, $n = 10$. $^{\dagger}p < 0.01$ for quinpirole effect and $*p < 0.02$ for the genotype effect, determined by anova. (b) SKF82958 injection at doses of 0.3 mg/kg and 1.0 mg/kg. WT, $n = 7$; *MsrA*−/−, $n = 10$. There was no significant effect of mouse type on SKF82958 effect, SKF82958 increased locomotor activity in the dose range used ($^{\dagger}p < 0.01$) and no dose-by-type interaction was detected; determined by anova.

In addition, *MsrA*−/− and WT mice were injected with two doses of the D1DR agonist SKF82958, and ensuing locomotor activity behavioral effects were assessed in 45-min sessions (Fig. 5b). The anova applied to these distance traveled data indicated no effect of mouse type, a significant effect of SKF82958 dose effect (repeated measures anova; $p < 0.01$), and no dose-by-type interaction. These data show that the D1DR agonist did not differentially affect the two types of mice (no type effect, no interaction effect). As expected from the literature for several types of inbred mice, SKF82958 substantially increased locomotor activity in the dose range used here (Niimi *et al.* 2009). These data strengthen the idea that methionine oxidation in the D2DR third cytoplasmic loop plays an important role in the *MsrA*−/− phenotype (the D2DR third intracellular loop contains eight methionines, and the D1DR C-terminus cytoplasmic region contains only one methionine; both of these regions are directly involved in signal transduction).

Oxidation vulnerability was examined with recombinant GST-D2DR$_L$-IC$_3$ and peroxide exposure. Non-H_2O_2 oxidized GST-D2DR$_L$-IC$_3$ protein, H_2O_2 oxidized GST-D2DR$_L$-IC$_3$ protein, and H_2O_2 oxidized GST-D2DR$_L$-IC$_3$ proteins treated with MsrA were all subjected to mass spectrometry analysis following gel-electrophoresis separation and tryptic digestion. The procedure used to detect peptides by this mass spectrometry analysis (Zhang *et al.* 2010) normally causes some methionine oxidation. To compensate for this, averaged MetO levels detected in the non-H_2O_2 oxidized GST-D2DR$_L$-IC$_3$ peptides were subtracted from the H_2O_2 oxidized forms of the protein (+/− MsrA and DTT). A 17-amino-acid peptide produced by collision-induced dissociation was found to contain the highest quantity of oxidized methionine (276-AQELEMEMLSSTSPPER-292; Fig. 6). Furthermore, the Met283 residue (present in daughter ion Y10) of the peptide was found to be relatively more oxidized in comparison with the Met281 residue (present in daughter ion Y12; data not shown). The net oxidation level of

Met283 treated with H_2O_2 *in vitro* was on average 2% (Fig. 6). This oxidation level resembles the basal physiological level of MetO in unpublished observations and in yeast cells without H_2O_2 in the growth media (Moskovitz *et al.* 1997). Accordingly, the current *in vitro* condition of oxidation may resemble physiological methionine oxidation. The addition of MsrA and DTT to oxidized GST-D2DR_L-IC_3 protein was able to reduce the sulfoxide of Met283 by 60% (Fig. 6). The MsrA enzyme can reduce only the *S*-form of MetO. Empirically, the distribution ratio of *S* to *R* forms of MetO is 1 : 1 (Oien and Moskovitz 2008). Typically, we observed that *in vitro* oxidation of methionine by H_2O_2 results in 60%*S*-MetO and 40%*R*-MetO (determined by amino acid analysis separation; unpublished results). Thus, the ability of the MsrA to reduce 60% of the total oxidized Met283 reflects the expected maximum reduction capability of the enzyme in an expected MetO racemic mixture of *R* and *S* forms following methionine oxidation by H_2O_2. In addition, the preferred oxidation of Met283 suggests this residue is more vulnerable to oxidation and also readily accessible to the reducing function of MsrA.

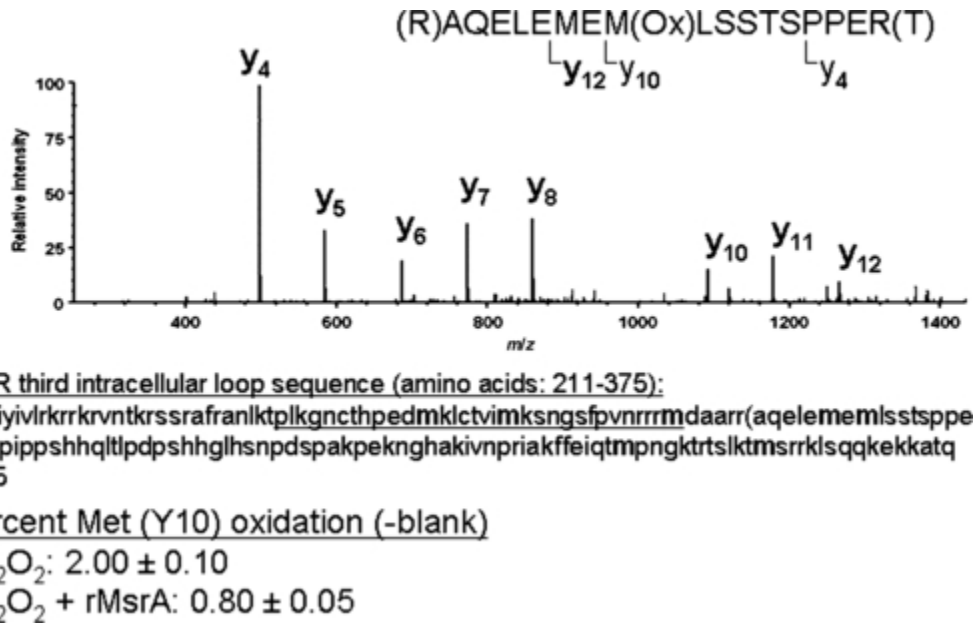

Figure 6. Oxidized methionine residues in $D2DR_L$-IC_3 recombinant protein. The short and long form D2DR differ by a 29-amino-acid region in the third cytoplasmic loop, which begins after amino acid 241 in the rat sequence (underlined). The methionines (m) are in bold. The corresponding recombinant fusion protein GST-$D2DR_L$-IC_3 was isolated and resulting peptides were subjected to tandem mass spectrometry after trypsin digestion. The sequence of the major oxidized peptide identified is shown and also indicated in the sequence by parenthesis. Representative relative signal levels for the daughter ions of the major peptide detected after collision-induced fragmentation are presented as relative intensity of each ion. The difference in percent methionine (Y10) oxidation between the presence and absence of rMsrA was found to be significant (three experiments, $p < 0.05$ by *t*-test).

Discussion

This study describes for the first time the possible effects of methionine oxidation on DA receptor function *in vivo* by using *MsrA*−/− mice. Previously, we observed an inverse relationship between abnormally high levels of DA accompanied by lowered locomotor activity in *MsrA*−/− mice (Oien *et al.* 2008). This is paradoxical because chronically low levels of brain DA are associated with Parkinson's disease-like motor effects including low levels of locomotor activity. These unexpected results led us to investigate that the alteration of DA receptor function and expression may be involved.

Both the D1DR and the D2DR modulate striatal information processing that is integral to the translation of cortical plans into actions by providing for the expression of selected motor responses with concurrent suppression of unwanted responses ('responses' may be cognitive or motor). The D2DR are of particular clinical interest because of their role in neuropsychiatric disorders, such as schizophrenia, where D2DR antagonists are therapeutic (Lieberman *et al.* 2008), or their role in the movement disorder, Parkinson's disease, where D2DR agonists are known to benefit patients (Pahwa *et al.* 2004). Thus, we predicted a reduced expression of striatal D2DR in *MsrA*−/− mice to explain the relative lower locomotor activity (Oien *et al.* 2008). Surprisingly, there was an increase of D2DR expression in *MsrA*−/− mice (Fig. 1). Higher levels of [^{3}H]raclopride binding to D2DR confirmed this increase (Fig. 2). The higher protein levels of the D2DR in *MsrA*−/− may be part of a compensatory mechanism for the accumulation of oxidized D2DR. In spite of the higher D2DR levels observed, the binding of [^{3}H]quinpirole suggests a compromised agonist binding of the D2DR in *MsrA*−/− brain (Fig. 2a). Supportive *in vivo* data to this phenomenon are demonstrated by the lesser D2DR agonist inhibitory effect on

locomotor function in *MsrA*−/− mice (Fig. 5a). Agonist occupation of G-protein coupled receptors leads to a cellular response that wanes, or desensitizes, with prolonged agonist exposure. MetO in the intracellular loops of the D2DR may cause a conformational change that may result in uncoupling of the receptor to G-protein subunits. The relative compromised binding of the D2DR to [^{3}H]quinpirole suggests lower efficiency in D2DR-G-protein coupling. Indeed, our data show that although the levels of $G\alpha_{i/o}$ are similar in both mouse types (Figure S1), the coupling of D2DR to G-proteins is reduced by ~50% in *MsrA*−/− relative to WT brain (Fig. 3). This suggests that the total $G\alpha_{i/o}$ coupling capacity is reduced in *MsrA*−/− brain rather than their coupling affinity to D2DR.

The ability of MsrA to restore D2DR agonist binding in *MsrA*−/− striatal extracts (Fig. 2b) supports the theory that methionine oxidation of D2DR occurs in the *MsrA*−/− brain. Accordingly, it may be beneficial to cause striatal over-expression of Msr to prevent MetO related abnormalities manifested by oxidized D2DR. Furthermore, the selectivity of the effect of methionine oxidation on D2DR (by MsrA ablation) was demonstrated by the similar binding of D1DR to striatal extracts in both mouse types (Fig. 2c and d). Data presented in Fig. 4 suggest the autoreceptor function of D2DR in *MsrA*−/− striatum is compromised in its functional response to quinpirole and sulpiride compared to WT $D2DR_S$. The *in vivo* observation that *MsrA*−/− mice are less responsive to the inhibitory effect of quinpirole on locomotor activity (Fig. 5a) supports the conclusion that there is a general malfunction of *MsrA*−/− D2DR. Furthermore, the *in vivo* specificity of the MsrA ablation effect to D2DR is strengthened by the similar response of both mouse types to D1DR agonist (Fig. 5b). According to the literature, the use of the administrated doses of 0.1 and 0.5 mg/kg quinpirole are within the common range used in mice. In mice, there is no increased locomotor response as the dose is increased; instead,

a suppression of locomotor activity is observed (Geter-Douglass *et al.* 1997; Usiello *et al.* 2000; Wang *et al.* 2000). Mice are different from rats in their response to quinpirole. In rats there is an increase of locomotor response with a higher quinpirole dose (Eilam *et al.* 1991; Koeltzow *et al.* 2003). This observation maybe is linked to observed difference in the ligand K_d values in rats (Levant *et al.* 1992) vs. mice (current study).

Taken together, it is suggested that lack of MsrA leads to methionine oxidation in both long and short forms of D2DR and diminishes their overall function efficacy. The general lowered *MsrA*−/− response to quinpirole, both *in vitro* and *in vivo* (Figs 2 and 5) implies that conserved regions of both D2DR subtypes are primarily affected in the *MsrA*−/− mouse (this does not exclude involvement of the 29 amino acid sequence that is not present in the $D2DR_S$). The compromised G-protein coupling in *MsrA*−/− may be a result of oxidative modification of specific methionine residues, especially in the cytoplasmic loops of the D2DR that are important for G-proteins coupling (i.e. $D2DR_L$-IC_3) (Montmayeur *et al.* 1993; Ilani *et al.* 2002). To assess the possibility of methionine oxidation in $D2DR_L$-IC_3 and reversal by MsrA *in vitro*, a recombinant GST-$D2DR_L$-IC_3 protein was oxidized and treated with recombinant MsrA. An oxidation of a specific methionine (Met283) in recombinant GST-$D2DR_L$-IC_3 protein occurred and was reduced to methionine by 60% with MsrA (Fig. 6). Met283 is present in both subtypes of D2DR and may be an important target for oxidation that affects the general function of this receptor. Future experiments are underway to monitor *in vivo* MetO levels and location in the D2DR of *MsrA*−/− mice. Overall, the collective evidence indicates that primarily D2DR related signaling is affected in *MsrA*−/− mice. However, the contributions of other signaling events to the observed abnormalities will still need further investigations.

Mechanistically, we suggest that oxidation of specific methionine residues may also affect phosphorylation of adjacent amino acids in $D2DR_L$-IC_3, thereby altering DA signal transduction pathways. For example, a regulatory role of MetO in protein phosphorylation was recently reported (Emes 2009; Hardin *et al.* 2009; Oien *et al.* 2009). Accordingly, it is possible that specific MetO residues in $D2DR_L$-IC_3 inhibit phosphorylation events that are important for proper coupling of the receptor to G-proteins as well (Namkung *et al.* 2009).

Our data can be interpreted to suggest that lack of MsrA in mouse brain causes D2DR malfunction via G-protein uncoupling leading to the production of higher DA levels (as a potential compensatory mechanism), reduced locomotor activity, and diminished behavioral responsiveness to D2DR agonists (Oien *et al.* 2008). Understanding the role of MsrA and MetO in DA physiology may result in identifying other proteins and neurotransmitter receptors that are altered by oxidative modification of methionine.

Recently, it was reported that mutations in the upstream region of *MsrA* may be potential markers for schizophrenia. If this proves true, research clearly supports the relevance of the *MsrA*−/− DA system to the occurrence of DA-related abnormal behavior (Walss-Bass *et al.* 2009).

A. References

Bartlett RK, Bieber Urbauer RJ, Anbanandam A, Smallwood HS, Urbauer JL, Squier TC (Oxidation of Met144 and Met145 in calmodulin blocks calmodulin dependent activation of the plasma membrane Ca-ATPase. Biochemistry 42:3231-3238.2003).

Bigelow DJ, Squier TC (Redox modulation of cellular signaling and metabolism through reversible oxidation of methionine sensors in calcium regulatory proteins. Biochim Biophys Acta 1703:121-134.2005).

Bird ED, Iversen LL (Huntington's chorea. Post-mortem measurement of glutamic acid decarboxylase, choline acetyltransferase and dopamine in basal ganglia. Brain 97:457-472.1974).

Bylund D. B. and Toews M. L. (1993) Radioligand binding methods: practical guide and tips. Am. J. Physiol. 265, L421–L429.

Carlsson T., Bjorklund T. and Kirik D. (2007) Restoration of the striatal dopamine synthesis for Parkinson’s disease: viral vector-mediated enzyme replacement strategy. Curr. Gene Ther. 7, 109–120.

Chen BT, Avshalumov MV, Rice ME (H(2)O(2) is a novel, endogenous modulator of synaptic dopamine release. J Neurophysiol 85:2468-2476.2001).

Chiueh CC, Moore KE (D-amphetamine-induced release of "newly synthesized" and "stored" dopamine from the caudate nucleus in vivo. J Pharmacol Exp Ther 192:642-653.1975).

Cohen G (The pathobiology of Parkinson's disease: biochemical aspects of dopamine neuron senescence. J Neural Transm Suppl 19:89-103.1983).

Eilam D., Clements K. V. and Szechtman H. (1991) Differential effects of D1 and D2 dopamine agonists on stereotyped locomotion in rats. Behav. Brain Res. 45, 117–124.

Emes M. J. (2009) Oxidation of methionine residues: the missing link between stress and signalling responses in plants. Biochem. J. 422, e1–e2.

Erickson JR, Joiner ML, Guan X, Kutschke W, Yang J, Oddis CV, Bartlett RK, Lowe JS, O'Donnell SE, Aykin-Burns N, Zimmerman MC, Zimmerman K, Ham AJ, Weiss RM, Spitz DR, Shea MA, Colbran RJ, Mohler PJ, Anderson ME (A dynamic pathway for calcium-independent activation of CaMKII by methionine oxidation. Cell 133:462-474.2008).

Fawaz C. S., Martel P., Leo D. and Trudeau L. E. (2009) Presynaptic action of neurotensin on dopamine release through inhibition of D(2) receptor function. BMC Neurosci. 10, 96.

Fischer JF, Cho AK (Chemical release of dopamine from striatal homogenates: evidence for an exchange diffusion model. J Pharmacol Exp Ther 208:203-209.1979).

Fowler S. C., Birkestrand B. R., Chen R., Moss S. J., Vorontsova E., Wang G. and Zarcone T. J. (2001) A force-plate actometer for quantitating rodent behaviors: illustrative data on locomotion, rotation, spatial patterning, stereotypies, and tremor. J. Neurosci. Methods 107, 107–124.

Fox AP, Currie KPM (Comparison of N- and P/Q-Type Voltage-Gated Calcium Channel Current Inhibition. J Neurosci 17:4570-4579.1997).

Geter-Douglass B., Katz J. L., Alling K., Acri J. B. and Witkin J. M. (1997) Characterization of unconditioned behavioral effects of dopamine D3/D2 receptor agonists. J. Pharmacol. Exp. Ther. 283, 7–15.

Hardin S. C., Larue C. T., Oh M. H., Jain V. and Huber S. C. (2009) Coupling oxidative signals to protein phosphorylation via methionine oxidation in Arabidopsis. Biochem. J. 422, 305–312.

Harrison C. and Traynor J. R. (2003) The [35S]GTPgammaS binding assay: approaches and applications in pharmacology. Life Sci. 74, 489–508.

Hickey M. A., Reynolds G. P. and Morton A. J. (2002) The role of dopamine in motor symptoms in the R6/2 transgenic mouse model of Huntington's disease. J. Neurochem. 81, 46–59.

Hornykiewicz O. (1962) Dopamine (3-hydroxytyramine) in the central nervous system and its relation to the Parkinson syndrome in man. Dtsch. Med. Wochenschr. 87, 1807–1810.

Ilani T., Fishburn C. S., Levavi-Sivan B., Carmon S., Raveh L. and Fuchs S. (2002) Coupling of dopamine receptors to G proteins: studies with chimeric D2/D3 dopamine receptors. Cell. Mol. Neurobiol. 22, 47–56.

Johnson MA, Rajan V, Miller CE, Wightman RM (Dopamine release is severely compromised in the R6/2 mouse model of Huntington's disease. J Neurochem 97:737-746.2006).

Jones SR, Gainetdinov RR, Wightman RM, Caron MG (Mechanisms of amphetamine action revealed in mice lacking the dopamine transporter. J Neurosci 18:1979-1986.1998).

Kline DD, Takacs KN, Ficker E, Kunze DL (Dopamine Modulates Synaptic Transmission in the Nucleus of the Solitary Tract. J Neurophysiol 88:2736-2744.2002).

Kraft JC, Osterhaus GL, Ortiz AN, Garris PA, Johnson MA (In vivo dopamine release and uptake impairments in rats treated with 3-nitropropionic acid. Neuroscience 161:940-949.2009).

Kume-Kick J, Rice ME (Dependence of dopamine calibration factors on media Ca2+ and Mg2+ at carbon-fiber microelectrodes used with fast-scan cyclic voltammetry. J Neurosci Methods 84:55-62.1998).

Lan H., Liu Y., Bell M. I., Gurevich V. V. and Neve K. A. (2009) A dopamine D2 receptor mutant capable of G protein-mediated signaling but deficient in arrestin binding. Mol. Pharmacol. 75, 113–123.

Levant B., Grigoriadis D. E. and DeSouza E. B. (1992) Characterization of [3H]quinpirole binding to D2-like dopamine receptors in rat brain. J. Pharmacol. Exp. Ther. 262, 929–935.

Lieberman J. A., Bymaster F. P., Meltzer H. Y. et al. (2008) Antipsychotic drugs: comparison in animal models of efficacy, neurotransmitter regulation, and neuroprotection. Pharmacol. Rev. 60, 358–403.

Liang NY, Rutledge CO (Evidence for carrier-mediated efflux of dopamine from corpus striatum. Biochem Pharmacol 31:2479-2484.1982).

Michaelis ML, Bigelow DJ, Schoneich C, Williams TD, Ramonda L, Yin D, Huhmer AF, Yao Y, Gao J, Squier TC (Decreased plasma membrane calcium transport activity in aging brain. Life Sci 59:405-412.1996).

Montmayeur J. P., Guiramand J. and Borrelli E. (1993) Preferential coupling between dopamine D2 receptors and G-proteins. Mol. Endocrinol. 7, 161–170.

Morgan DG, May PC, Finch CE (Dopamine and serotonin systems in human and rodent brain: effects of age and neurodegenerative disease. J Am Geriatr Soc 35:334-345.1987).

Moskovitz J (Methionine sulfoxide reductases: ubiquitous enzymes involved in antioxidant defense, protein regulation, and prevention of aging-associated diseases. Biochim Biophys Acta 1703:213-219.2005).

Moskovitz J (Prolonged selenium-deficient diet in MsrA knockout mice causes enhanced oxidative modification to proteins and affects the levels of antioxidant enzymes in a tissue-specific manner. Free Radic Res 41:162-171.2007).

Moskovitz J, Bar-Noy S, Williams WM, Requena J, Berlett BS, Stadtman ER (Methionine sulfoxide reductase (MsrA) is a regulator of antioxidant defense and lifespan in mammals. Proc Natl Acad Sci U S A 98:12920-12925.2001).

Moskovitz J., Rahman M. A., Strassman J., Yancey S. O., Kushner S. R., Brot N. and Weissbach H. (1995) Escherichia coli peptide methionine sulfoxide reductase gene: regulation of expression and role in protecting against oxidative damage. J. Bacteriol. 177, 502–507.

Moskovitz J., Berlett B. S., Poston J. M. and Stadtman E. R. (1997) The yeast peptide-methionine sulfoxide reductase functions as an antioxidant in vivo. Proc. Natl Acad. Sci. USA 94, 9585–9589.

Moskovitz J., Flescher E., Berlett B. S., Azare J., Poston J. M. and Stadtman E. R. (1998) Overexpression of peptide-methionine sulfoxide reductase in Saccharomyces cerevisiae and human T cells provides them with high resistance to oxidative stress. Proc. Natl Acad. Sci. USA 95, 14071–14075.

Nachshen DA, Sanchez-Armass S (Co-operative action of calcium ions in dopamine release from rat brain synaptosomes. J Physiol 387:415-423.1987).

Neves G, Lagnado L (The kinetics of exocytosis and endocytosis in the synaptic terminal of goldfish retinal bipolar cells. J Physiol 515 (Pt 1):181-202.1999).

Namkung Y., Dipace C., Javitch J. A. and Sibley D. R. (2009) G protein-coupled receptor kinase-mediated phosphorylation regulates post-endocytic trafficking of the D2 dopamine receptor. J. Biol. Chem. 284, 15038–15051.

Niimi K., Takahashi E. and Itakura C. (2009) Age dependence of motor activity and sensitivity to dopamine receptor 1 agonist, SKF82958, of inbred AKR/J, BALB/c, C57BL/6J, SAMR1, and SAMP6 strains. Brain Res. 1250, 175–182.

Nwaneshiudu C. A. and Unterwald E. M. (2009) Blockade of neurokinin-3 receptors modulates dopamine-mediated behavioral hyperactivity. Neuropharmacology 57, 295–301.

Oien D, Wang X, Moskovitz J (Genomic and Proteomic Analyses of the Methionine Sulfoxide Reductase A Knockout Mouse. Current Proteomics 5:96-103.2008a).

Oien DB, Moskovitz J (Substrates of the methionine sulfoxide reductase system and their physiological relevance. Curr Top Dev Biol 80:93-133.2008).

Oien DB, Ortiz AN, Rittel AG, Dobrowsky RT, Johnson MA, Levant B, Fowler SC, Moskovitz J (Dopamine D2 Receptor Function is Compromised in the Brain of the Methionine Sulfoxide Reductase A Knockout Mouse. J Neurochem 114(1):51-61.2010).

Oien DB, Osterhaus GL, Latif SA, Pinkston JW, Fulks J, Johnson M, Fowler SC, Moskovitz J (MsrA knockout mouse exhibits abnormal behavior and brain dopamine levels. Free Rad Biol Med 45:193-200.2008b).

Oien DB, Osterhaus GL, Lundquist BL, Fowler SC, Moskovitz J (Caloric restriction alleviates abnormal locomotor activity and dopamine levels in the brain of the methionine sulfoxide reductase A knockout mouse. Neurosci Lett 468:38-41.2010).

Oien DB, Shinogle HE, Moore DS, Moskovitz J (Clearance and phosphorylation of alpha-synuclein are inhibited in methionine sulfoxide reductase a null yeast cells. J Mol Neurosci 39:323-332.2009).

Ortiz AN, Kurth BJ, Osterhaus GL, Johnson MA (Dysregulation of intracellular dopamine stores revealed in the R6/2 mouse striatum. J Neurochem 112:755-761.2010).

Outeiro TF, Klucken J, Bercury K, Tetzlaff J, Putcha P, Oliveira LM, Quintas A, McLean PJ, Hyman BT (Dopamine-induced conformational changes in alpha-synuclein. PLoS One 4:e6906.2009).

Pahwa R., Lyons K. E. and Hauser R. A. (2004) Ropinirole therapy for Parkinson's disease. Expert Rev. Neurother. 4, 581–588.

Pal R, Oien DB, Ersen FY, Moskovitz J (Elevated levels of brain-pathologies associated with neurodegenerative diseases in the methionine sulfoxide reductase A knockout mouse. Exp Brain Res 180:765-774.2007).

Palacios J, Sepulveda MR, Lee AG, Mata AM (Ca2+ transport by the synaptosomal plasma membrane Ca2+-ATPase and the effect of thioridazine. Biochemistry 43:2353-2358.2004).

Patten DA, Germain M, Kelly MA, Slack RS (Reactive oxygen species: stuck in the middle of neurodegeneration. J Alzheimers Dis 20 Suppl 2:S357-367).

Perez-Severiano F, Santamaria A, Pedraza-Chaverri J, Medina-Campos ON, Rios C, Segovia J (Increased formation of reactive oxygen species, but no changes in glutathione peroxidase activity, in striata of mice transgenic for the Huntington's disease mutation. Neurochem Res 29:729-733.2004).

Rizzoli SO, Betz WJ (Synaptic vesicle pools. Nat Rev Neurosci 6:57-69.2005).

Romero H. M., Berlett B. S., Jensen P. J., Pell E. J. and Tien M. (2004) Investigations into the role of the plastidial peptide methionine sulfoxide reductase in response to oxidative stress in Arabidopsis. Plant Physiol. 136, 3784–3794.

Rose SD, Lejen T, Casaletti L, Larson RE, Pene TD, Trifaro JM (Molecular motors involved in chromaffin cell secretion. Ann N Y Acad Sci 971:222-231.2002).

Ruan H., Tang X. D., Chen M. L. et al. (2002) High-quality life extension by the enzyme peptide methionine sulfoxide reductase. Proc. Natl Acad. Sci. USA 99, 2748–2753.

Saxena S., Brody A. L., Schwartz J. M. and Baxter L. R. (1998) Neuroimaging and frontal-subcortical circuitry in obsessive-compulsive disorder. Br. J. Psychiatry Suppl. 35, 26–37.

Usiello A., Baik J. H., Rouge-Pont F., Picetti R., Dierich A., LeMeur M., Piazza P. V. and Borrelli E. (2000) Distinct functions of the two isoforms of dopamine D2 receptors. Nature 408, 199–203.

Venton BJ, Seipel AT, Phillips PE, Wetsel WC, Gitler D, Greengard P, Augustine GJ, Wightman RM (Cocaine increases dopamine release by mobilization of a synapsin-dependent reserve pool. J Neurosci 26:3206-3209.2006).

Walss-Bass C., Soto-Bernardini M. C., Johnson-Pais T. et al. (2009) Methionine sulfoxide reductase: a novel schizophrenia candidate gene. Am. J. Med. Genet. B Neuropsychiatr. Genet. 150B, 219–225.

Wang Y., Xu R., Sasaoka T., Tonegawa S., Kung M. P. and Sankoorikal E. B. (2000) Dopamine D2 long receptor-deficient mice display alterations in striatum-dependent functions. J. Neurosci. 20, 8305–8314.

Yavich L, Oksman M, Tanila H, Kerokoski P, Hiltunen M, van Groen T, Puolivali J, Mannisto PT, Garcia-Horsman A, MacDonald E, Beyreuther K, Hartmann T, Jakala P (Locomotor activity and evoked dopamine release are reduced in mice overexpressing A30P-mutated human alpha-synuclein. Neurobiol Dis 20:303-313.2005).

Yavich L, Tanila H, Vepsalainen S, Jakala P (Role of alpha-synuclein in presynaptic dopamine recruitment. J Neurosci 24:11165-11170.2004).

Zhang Y., D'Souza D., Raap D. K., Garcia F., Battaglia G., Muma N. A. and Van de Kar L. D. (2001) Characterization of the functional heterologous desensitization of hypothalamic 5-HT(1A) receptors after 5-HT(2A) receptor activation. J. Neurosci. 21, 7919–7927.

Zhang L., Yu C., Vasquez F. E., Galeva N., Onyango I., Swerdlow R. H. and Dobrowsky R. T. (2010) Hyperglycemia alters the schwann cell mitochondrial proteome and decreases coupled respiration in the absence of superoxide production. J. Proteome Res. 9, 458–471.